Derivative Properties from Equations of State

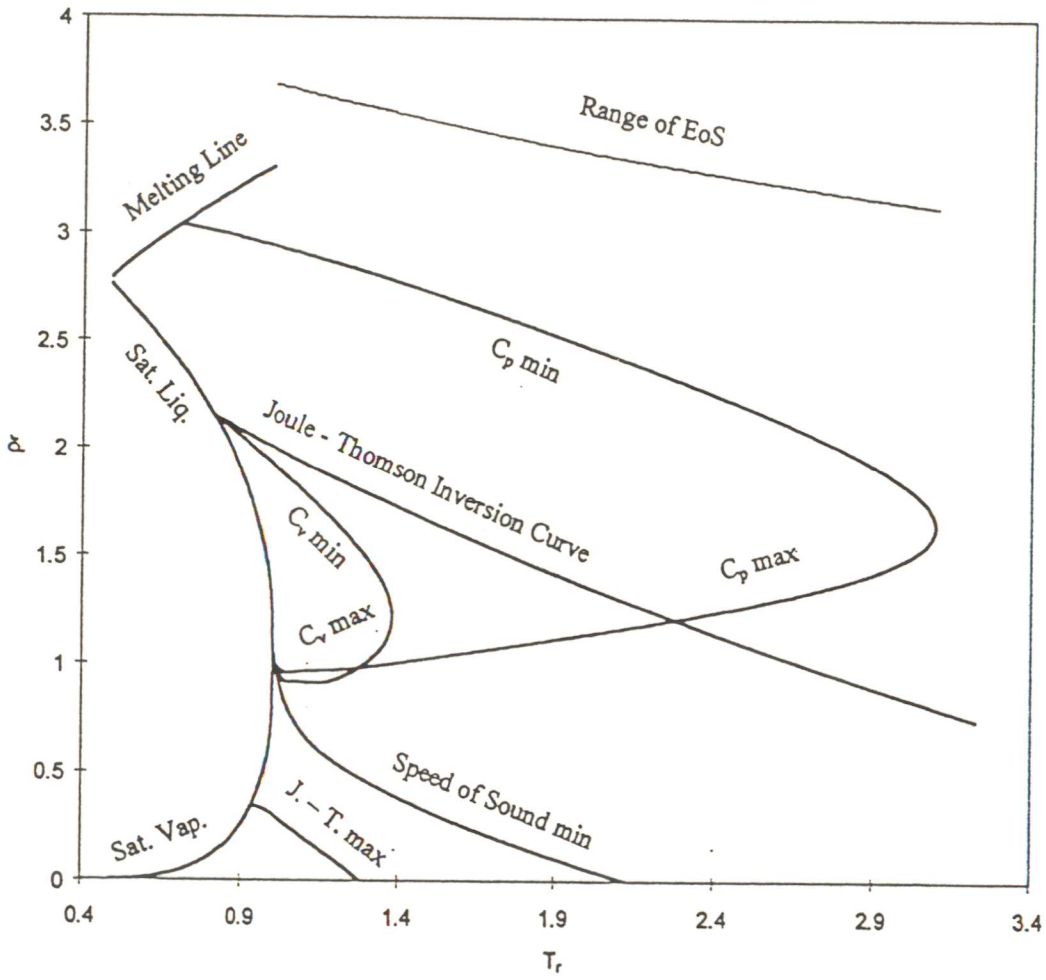

April 1998

M. Konttorp

TU Delft
Technische Universiteit Delft

Faculteit Technische Natuurwetenschappen
Scheikundige Technologie en Materiaalkunde

Derivative Properties from Equations of State

Master Thesis

Name : M. Konttorp

Supervisors :

J. P. O'Connell
University of Virginia
Department of Chemical Engineering

C. J. Peters
TU Delft
Sub Faculty of Chemical Technology and
Material Science
Section Applied Thermodynamics and
Phase Equilibria
The Netherlands

Summary

This thesis has been dedicated to the study of derivative properties obtained from equations of state. The derivative properties are dependent on first or second order temperature or density derivatives of the principal thermodynamic surface. This means that the inaccuracy of the principal surface is easily revealed by these properties. The derivative properties used in this study were :

- Isochoric heat capacity
- Isobaric heat capacity
- The Joule – Thomson
- The speed of sound
- The reduced bulk modulus

The real behavior of pure component properties derived from high accuracy multiparameter equations of state fitted to a large number of experimental data has been studied. The objective was to find general behavior among different substances. If there is a general behavior this would be helpful in the development of new and better functional structures for the description of thermodynamic properties. The isochoric heat capacity was found to have a regular behavior.

Another objective of the thesis has been to investigate the representation of derivative properties obtained from some model equations of state. Those equations were :

- Redlich - Kwong
- Soave - Redlich – Kwong
- Peng – Robinson
- SPHCT
- SAFT

The derived properties from the model equations for both pure substances and mixtures were compared to those from the high accuracy equations. All equations were found to give very poor representations of the isochoric heat capacity. In light of the poor estimation of the isochoric heat capacity obtained from model equations this behavior could serve as a tool in the further development of equations of state.

In order to obtain reference data for mixtures new thermodynamic relationships for derivative properties have been developed based on the Extended Corresponding States theory. The new relationships were found to give excellent descriptions of derivative properties for mixtures.

Acknowledgement

I would like to thank dr. C. J. Peters and dr. J. P. O'Connell for their continuos support and many helpful discussions during the project. I would also like to thank Daniel G. Friend at NIST in Boulder (Colorado) for providing heat capacity data on the methane/propane mixture.

Table of contents

List of figures

List of tables

Introduction

An equation of state (EOS) has proved to be a valuable tool in estimating fluid properties. The advantage of the EOS is the great number of fluid properties that can be derived from one equation. If the parameters can be described by mixing rules, the EOS in combination with the ideal gas isobaric heat capacity is able to describe virtually all thermodynamic properties of interest for an infinite number of mixtures. These advantages has triggered an intense research activity in the field of equations of state. (Sandler[27])
The different equations of state can be put into three classes :

- Elaborate multi parameter equations of state that are essentially within experimental error for all properties at nearly all conditions.
- Cubic or higher order polynomials in density with two to five parameters that are correlated with measurable quantities such as critical temperature and pressure.
- Equations based on the statistical mechanics of fluids.

It should also be noted that recently equations combining the critical scaling laws with the classical behavior have been established.
The multi parameter equations are used on systems where a great number of measured data are known. These equations are often used in applications where high accuracy is required. The high complexity of these equations prohibits their use when computational speed is required.
The cubic equations of state are the most widely used in industry. The strength of these relatively simple models are the computational speed and the low number of measurements required in order to estimate the parameters. These models are often valid only for a limited number of systems. The range of the models is also restricted.
The mechanical statistical based models represent efforts to link the microscopic structure of molecules to their macroscopic behavior. These equations are often more complex than the cubic equations, but due to the decreasing cost of computation the equations are becoming increasingly important in industry.

This thesis is a part of a joint project between the Laboratory of Applied Thermodynamics and Phase Equilibria at the Technical University of Delft and the Department of Chemical Engineering at the University of Virginia. The project is supported financially by the North Atlantic Technical Organization (NATO). The aim of the project is to study the behavior of derivative properties from different equations of state available in the literature outside the two - phase region, and to compare the predicted behavior of these equations to the real behavior of these properties. The information gained from this study will give us suggestions on how to improve the available models. The advantage of evaluating the derived properties are that they are measurable, and dependent on the first or second temperature and density derivative of the principal thermodynamic surface. If those properties can be modeled accurately the models can be transformed into a pressure surface and hopefully give more accurate equations of state.

In this thesis five derivative properties have been studied :

- The isochoric heat capacity
- The isobaric heat capacity
- The Joule - Thomson coefficient
- The speed of sound
- The reduced bulk modulus

These properties obtained from multi parameter equations of state has served as a reference of comparison for pure fluids. The Extended Corresponding States principle has been extended to predict these derived properties for mixtures. In this work the real behavior of pure components has been studied. Five equations of state has been tested on their ability to estimate derivative properties for pure components :

Cubic equations of state :

- The Peng - Robinson equation
- The Redlich - Kwong equation
- The Soave - Redlich - Kwong equation

Statistical mechanics based equations :

- The SPHCT equation
- The SAFT equation

The real behavior of mixtures predicted with the ECS theory has also been studied.

1. Derivative properties from high accuracy equations of state

1.1. Introduction

There are a great number of multi parameter equations of state available in the literature. The quality of those equations is largely dependent on the range and quality of measured data. In this project 10 substances has been chosen for evaluation. Those 10 substances have been chosen based upon the quality of the available equations, and their ability to represent different classes of substances. The classes and the chosen substances are listed below :

Non - polar hydrocarbons :

- Methane
- Ethane
- Propane
- i-Butane
- n-Butane

Non polar cyclic hydrocarbons :

- Cyclohexane

Refrigerants :

- R152a
- Sulphurhexafluoride

Polar substances :

- Methanol
- Water

For some of the substances listed above there has been published several equations of state. The equations used in this study are listed in Table 1.1 :

Table 1.1 Multiparameter equations of state

Substance	Type	Pressure to : (MPa)	Temperature range (K)	Reference
Cyclohexane	SWEOS	80	Melting line-700	Penoncello et. al[20] (1995)
Methane	SWEOS	1000	Melting line-625	Setzmann and Wagner[21] (1991)
Water	HILLEOS	1000	Triple point - 1273	Hill[22] (1990)
Water	SWEOS	25000	Melting line - 1273	Saul and Wagner[23] (1989)
Methanol	SWEOS	800	Melting line - 620	de Reuck and Craven[24] (1993)
Sulfurhexafluoride	SWEOS	55	222 - 525	Cole and de Reuck[25] (1990)
Methane	32MBWR	0-200	Melting line -600	Younglove et al.[4] (1987)
Ethane	32MBWR	0-70	Melting line -600	Younglove et al.[4] (1987)
Propane	32MBWR	0-100	Melting line - 600	Younglove et al.[4] (1987)
Isobutane	32MBWR	0-35	Melting line - 600	Younglove et al.[4] (1987)
N-butane	32MBWR	0-70	Melting line - 500	Younglove et al.[4] (1987)
1,1-Diflouroethane (R152a)	32MBWR	0-35	162-453	Outcalt and McLinden[5] (1986)

The abbreviation 32MBWR is short for the modified Benedict - Webb - Rubin equation with 32 parameters. The abbreviation SWEOS is short for the Schmidt - Wagner equation of state. The abbrevation HILLEOS is short for the Hill equation of state for water.

In order to test the behavior of the derivative properties obtained from model equations the ECS theory has been extended to analytically predict the derivative properties of mixtures. The advantage of the ECS procedure is the high accuracy of the predictions and the ability to predict the properties for an infinite number of mixtures.

1.2. Derivation of derivative properties for pure substances

If the thermodynamic surface is given in dimensionless Helmholtz free energy as a function of temperature and density the basic relations giving the derivative properties are as follows :

The following dimensionless variables are defined :

Ideal Helmholtz energy :

$$\Phi^0 = \frac{A^{id}}{RT}$$

Residual Helmholtz energy :

$$\Phi^r = \frac{A - A^{id}}{RT}$$

Dimensionless temperature :

$$\tau = \frac{T_c}{T}$$

Dimensionless density :

$$\delta = \frac{\rho}{\rho_c}$$

The derivatives of the Helmholtz energy are denoted as :

$$\Phi^r_\tau = \left(\frac{d\Phi^r}{d\tau}\right)_\delta, \quad \Phi^r_{\tau\tau} = \left(\frac{d^2\Phi^r}{d\tau^2}\right)_\delta$$

The subscripts are altered to give density derivatives. The superscript is altered to yield the definition of derivatives of the ideal Helmholtz energy.

- The isochoric heat capacity

$$\frac{C_v(\delta,\tau)}{R} = -\tau^2(\Phi^0_{\tau\tau} + \Phi^r_{\tau\tau}) \qquad (1.1)$$

- The isobaric heat capacity

$$\frac{C_p(\delta,\tau)}{R} = \frac{C_v(\delta,\tau)}{R} + \frac{\left(1+\delta\Phi^r_\delta - \delta\tau\Phi^r_{\delta\tau}\right)^2}{1+2\delta\Phi^r_\delta + \delta^2\Phi^r_{\delta\delta}} \tag{1.2}$$

- The speed of sound

$$\frac{w^2(\delta,\tau)}{RT} = 1+2\delta\Phi^r_\delta + \delta^2\Phi^r_{\delta\delta} - \frac{\left(1+\delta\Phi^r_\delta - \delta\tau\Phi^r_{\delta\tau}\right)^2}{\tau^2\left(\Phi^0_{\tau\tau} + \Phi^r_{\tau\tau}\right)} \tag{1.3}$$

- The Joule-Thomson coefficient

$$\mu(\delta,\tau)R\rho = \frac{-\left(\delta\Phi^r_\delta + \delta^2\Phi^r_{\delta\delta} + \delta\tau\Phi^r_{\delta\tau}\right)}{\left(1+\delta\Phi^r_\delta - \delta\tau\Phi^r_{\delta\tau}\right)^2 - \tau^2\left(\Phi^0_{\tau\tau} + \Phi^r_{\tau\tau}\right)\left(1+2\delta\Phi^r_\delta + \delta^2\Phi^r_{\delta\delta}\right)} \tag{1.4}$$

The SWEOS is always given in dimensionless Helmholtz energy. The SAFT EOS is given in dimensional Helmholtz energy, but can easily be manipulated to give the dimensionless Helmholtz energy defined here. All other equations discussed are given as a pressure surface as a function of temperature and density. If the thermodynamic surface is given in pressure as a function of density and temperature the basic thermodynamic relations are as follows :

- The isochoric heat capacity :

$$C_v(\rho,T) = C_v^0 - \int_0^\rho \left[\frac{T}{\rho^2}\left(\frac{\partial^2 P}{\partial T^2}\right)_\rho\right] d\rho \tag{1.5}$$

- The isobaric heat capacity :

$$C_p(\rho,T) = C_v(\rho,T) + \frac{T}{\rho^2}\left(\frac{\partial P}{\partial T}\right)^2_\rho \Big/ \left(\frac{\partial P}{\partial \rho}\right)_T \tag{1.6}$$

- The speed of sound :

$$w^2(\rho,T) = \left[\frac{C_p}{C_v}\left(\frac{\partial P}{\partial \rho}\right)_T \frac{10^6}{M_r}\right] \tag{1.7}$$

- The Joule-Thomson coefficient :

$$\mu(\rho,T)=\frac{1}{C_p}\left[\frac{T(\partial P/\partial T)_\rho}{\rho^2(\partial P/\partial \rho)_T}-\frac{1}{\rho}\right] \qquad (1.8)$$

These relationships are used in deriving thermodynamic properties from the 32MBWR equation of state.

1.3. Calculation of derivative properties for mixtures

1.3.1. The Extended Corresponding States procedure

In order to calculate the derivative properties for mixtures the ECS procedure is chosen. This ECS procedure allows an accurate calculation of all thermodynamic properties provided that there are accurate pure component surfaces available. The extended corresponding states method is based on the following relationships :

$$z_i(\rho,T)=z_0(\rho_i h_{i,o},T/f_{i,o}) \qquad (1.9)$$

and

$$a_i(\rho,T)=a_0(\rho h_{i,0},T/f_{i,0}) \qquad (1.10)$$

z is defined by z = Z-1 were Z is the compressibility factor. a is the dimensionless residual Helmholtz free energy.(a = [A-A^{id}]/RT) ρ and T are the density and temperature. The subscripts are denoting the reference fluid (0) and target fluid (i). The $f_{i,0}$ and $h_{i,0}$ are transformation parameters, defined by

$$f_{i,0}=(T_c^i/T_c^0)\theta(T_r,\rho_r) \qquad (1.11)$$

and

$$h_{i,0}=(\rho_c^0/\rho_c^i)\phi(T_r,\rho_r) \qquad (1.12)$$

where T_c and ρ_c are the critical temperature and volume for the fluids. T_r and ρ_r are defined as T^i/T^i_c and ρ^i/ρ^i_c, respectively. The functions $\phi(T_r,\rho_r)$ and $\theta(T_r,\rho_r)$ are shape factors. Given a state point defined by ρ and T plus the transformation variables $f_{i,0}$ and $h_{i,o}$ the equations (1.9) and (1.10) defines an exact transformation from one pure fluid

surface to another. The pressure P_i becomes $(f_{i,0}/h_{i,0})P_0$. The shape factors $\phi(T_r,\rho_r)$ and $\theta(T_r,\rho_r)$ can be approximated in a number of ways, but if the equation of state is known both for the reference fluid (0) and the target fluid (i) the exact calculation of $h_{i,0}$ and $f_{i,0}$ is possible for each state points. This eliminates the need to approximate the $\phi(T_r,\rho_r)$ and $\theta(T_r,\rho_r)$. In this work the transformation parameters $f_{i,0}$ and $h_{i,0}$ are calculated exact for every state point. The extension of this procedure to mixtures is accomplished by the following mixing rules :

$$f_{ij} = \varepsilon_{i,j}(f_{ii,0}f_{jj,0})^{1/2} \tag{1.13}$$

$$h_{ij} = \eta_{i,j}(\tfrac{1}{2}h_{ii,0}^{1/3} + \tfrac{1}{2}h_{jj,0}^{1/3})^3 \tag{1.14}$$

$$h_{x,0} = \sum_i \sum_j x_i x_j h_{ij,0} \tag{1.15}$$

$$f_{x,0}h_{x,0} = \sum_i \sum_j x_i x_j f_{ij,0} h_{ij,0} \tag{1.16}$$

where x_i and x_j are the mole fractions of the pure components. The η_{ij} and the ε_{ij} are binary interaction parameters. The previously defined $h_{i,0}$ and $f_{i,0}$ becomes $h_{ii,0}$ and $f_{ii,0}$. The only adjustable parameters are the binary interaction parameters η_{ij} and ε_{ij}.

3.3.2. Derivation of derivative properties using the ECS procedure

Starting with the dimensionless Helmholtz energy all thermodynamic properties can be derived using basic thermodynamic relationships. Equations (1.17) through (1.23) require only first derivatives of the Helmholtz energy a.

$$a_i = a_0 \tag{1.17}$$

$$z_i = (1 + H_\rho)z_0 + F_\rho u_0 \tag{1.18}$$

$$u_i = (1 - F_T)u_0 - H_T z_0 \tag{1.19}$$

$$s_i = s_0 - F_T u_0 - H_T z_0 \tag{1.20}$$

$$h_i = h_0 + (F_\rho - F_T)u_0 + (H_\rho - H_T)z_0 \quad (1.21)$$

$$g_i = g_0 + H_\rho z_0 + F_\rho u_0 \quad (1.22)$$

$$\ln \phi_i = g_0 + u_0 F_{n_i} + z_0 H_{n_i} \quad (1.23)$$

All energies are defined as : $x = \frac{X - X^{id}}{RT}$, where x = a,u,h,g

The entropy is defined as : $s = \frac{S - S^{id}}{R}$

Thermodynamic properties denoted with a subscript 0 are properties derived from the reference surface using basic thermodynamic relationships.

The factors H_x and F_x contains the derivatives of the transformation parameters $h_{i,0}$ and $f_{i,0}$.
Their definitions are :

$$F_T = \left(\frac{\partial f_{i,0}}{\partial T}\right)\frac{T}{f_{i,0}} \quad (1.24)$$

$$H_T = \left(\frac{\partial h_{i,0}}{\partial T}\right)\frac{T}{h_{i,0}} \quad (1.25)$$

$$F_\rho = \left(\frac{\partial f_{i,0}}{\partial \rho}\right)\frac{\rho}{f_{i,0}} \quad (1.26)$$

$$H_\rho = \left(\frac{\partial h_{i,0}}{\partial \rho}\right)\frac{\rho}{h_{i,0}} \quad (1.27)$$

$$H_{n_i} = \left(\frac{dh_x}{dn_i}\right)\frac{N^t}{h_x} \quad (1.28)$$

$$F_{n_i} = \left(\frac{df_x}{dn_i}\right)\frac{N^t}{f_x} \quad (1.29)$$

According to equation (1.9) the compressibility factor for the reference and the target fluid must be equal. As a result equation (1.18) imposes a constraint :

$$z_0 H_\rho = -u_0 F_\rho \tag{1.30}$$

In order to calculate the thermodynamic properties mentioned above the factors H_x and F_x
($x = T,\rho,n_i$) has to be known. The derivatives of the H factor are given by Ely[1] :

$$H_\rho = \frac{\left[(\kappa_i - \kappa_o)u_0\right]}{\left[(\kappa_0 - 1)u_0 + (\gamma_0 - 1)z_0\right]} \tag{1.31}$$

$$H_T = \frac{\left[(\gamma_i - \gamma_0)u_0 - (\gamma_0 - 1)(u_i - u_0)\right]}{\left[(\kappa_0 - 1)u_0 + (\gamma_0 - 1)z_0\right]} \tag{1.32}$$

with :

$$\gamma = \frac{T}{P}\left(\frac{\partial P}{\partial T}\right)_\rho \tag{1.33}$$

$$\kappa = \frac{\rho}{P}\left(\frac{\partial P}{\partial \rho}\right)_T \tag{1.34}$$

Making use of equation (1.19) and (1.30) allows calculation of the F factors. If the aim is to calculate the thermodynamic properties of a mixture mixing rules are utilized in order to calculate the factors H_x and F_x for the mixture. These mixing rules are derived from the equations (1.13-16) :

$$\frac{dh_{x,0}}{dT} = \sum_i \sum_j x_i x_j \left(\frac{dh_{ij,0}}{dT}\right) \tag{1.35}$$

with :

$$\frac{dh_{ij,0}}{dT} = \eta_{ij}\frac{1}{8}\left(h_{i,0}^{1/3} + h_{j,0}^{1/3}\right)^2\left(h_{i,0}^{-2/3}\frac{dh_{i,0}}{dT} + h_{j,0}^{-2/3}\frac{dh_{j,0}}{dT}\right) \tag{1.36}$$

$$\frac{df_{x,0}}{dT} = \frac{1}{h_{x,0}}\left(\sum_i\sum_j x_i x_j\left(\frac{df_{ij,0}}{dT}h_{ij,0} + f_{ij,0}\frac{dh_{ij,0}}{dT}\right) - f_{x,0}\frac{dh_{x,0}}{dT}\right) \tag{1.37}$$

with :

$$\frac{df_{ij,0}}{dT} = \varepsilon_{ij}\frac{f_{i,0}\dfrac{df_{j,0}}{dT} + f_{j,0}\dfrac{df_{i,0}}{dT}}{2\sqrt{f_{i,0}f_{j,0}}} \tag{1.38}$$

The calculation of caloric properties is more complicated. In order to calculate the isochoric heat capacity the second order temperature derivative of the Helmholtz energy is needed. Relationships for derivative thermodynamic properties are listed below :

$$c_{v,i} = -u_0 F_{TT} - z_0 H_{TT} - z_0 H_T + (1-F_T)^2 c_{v,0} - 2H_T(1-F_T)(z_0 - F_T)(\gamma_0 - 1) - H_T^2(z_0+1)(\kappa_0 - 1) - z_0 H_T(1-H_T) \tag{1.39}$$

$$c_{p,i} = c_{v,i} - 1 + (z_0+1)\frac{\left(F_T(1-\gamma_0) + H_T(\kappa_0 - 1) + \gamma_0\right)^2}{F_\rho(1-\gamma_0) + H_\rho(\kappa_0 - 1) + \kappa_0} \tag{1.40}$$

$$w(\rho,T) = \left[\frac{C_p}{C_v}RT(z_0+1)\left(F_\rho(1-\gamma_0) + H_\rho(\kappa_0-1) + \kappa_0\right)\frac{10^6}{M_r}\right]^{1/2} \tag{1.41}$$

$$\mu(\rho,T) = \frac{1}{C_p}\left[\frac{\left(F_T(1-\gamma_0) + H_T(\kappa_0-1) + \gamma_0\right)}{\rho\left(F_\rho(1-\gamma_0) + H_\rho(\kappa_0-1) + \kappa_0\right)} - \frac{1}{\rho}\right] \tag{1.42}$$

The dimensionless residual isochoric and isobaric heat capacities are defined as :

$$c_v = \frac{C_v - C_v^{id}}{R} \qquad c_p = \frac{C_p - C_p^{id}}{R}$$

The factors H_{TT} and F_{TT} are defined as follows :

$$H_{TT} = \left(\frac{d^2 h_{i,0}}{dT^2}\right)\frac{T^2}{h_{i,0}} \tag{1.43}$$

$$F_{TT} = \left(\frac{d^2 f_{i,0}}{dT^2}\right)\frac{T^2}{f_{i,0}} \tag{1.44}$$

In order to calculate the isochoric heat capacity second temperature derivatives of the transformation parameters $f_{i,0}$ and $h_{i,0}$ are needed. Expressions for these derivatives are obtained by using the equation for the isochoric heat capacity (1.39) and the expression given below :

$$\frac{d^2 z_i}{dT^2} = \frac{d^2 z_0}{dT^2} \tag{1.45}$$

These two equations can be solved with respect to F_{TT} and H_{TT}, resulting in the following expressions :

$$H_{TT} = \frac{(\gamma_0 - 1)A - u_0 B}{(\gamma_0 - 1)z_0 + (\kappa_0 - 1)u_0} \tag{1.46}$$

$$F_{TT} = \frac{(\kappa_0 - 1)A + z_0 B}{(\gamma_0 - 1)z_0 + (\kappa_0 - 1)u_0} \tag{1.47}$$

with :

$$A = -c_{v,j} + c_{v,0}(1 - F_T)^2 - z_0 H_T - z_0 H_T (1 - H_T) - (z_0 + 1)(\kappa_0 - 1)H_T^2 - 2(z_0 + 1)(\gamma_o - 1)(1 - F_T)H_T$$

$$B = \gamma_{T,0}(1 - F_T)^2 - \gamma_{T,j} + 2(\gamma_j - 1) - 2(\gamma_0 - 1)(1 - F_T) + (\kappa_{\rho,0} - 2(\kappa_0 - 1))H_T^2 + 2(\alpha_0 - \gamma_0 - \kappa_0 + 1)(1 - F_T)H_T$$

and

$$\alpha = \frac{\rho T}{P}\left(\frac{d^2 P}{dT d\rho}\right)$$

$$\gamma_T = \frac{T^2}{P}\left(\frac{d^2 P}{dT^2}\right)_\rho$$

$$\kappa_\rho = \frac{\rho^2}{P}\left(\frac{d^2 P}{d\rho^2}\right)_T$$

In order to calculate the caloric properties the factors H_{TT} and F_{TT} must be calculated for every component at the given state point. In order to obtain the factors for the mixture the following mixing rules can be used :

$$\frac{d^2 h_{x,0}}{dT^2} = \sum_i \sum_j x_i x_j \left(\frac{d^2 h_{ij,0}}{dT^2} \right) \tag{1.48}$$

with :

$$\begin{aligned} \frac{d^2 h_{ij,0}}{dT^2} = & \frac{\eta_{ij}}{12} \left(h_{i,0}^{1/3} + h_{j,0}^{1/3} \right) \left(h_{i,0}^{-2/3} \frac{dh_{i,0}}{dT} + h_{j,0}^{-2/3} \frac{dh_{j,0}}{dT} \right)^2 \\ & - \frac{\eta_{ij}}{12} \left(h_{i,0}^{1/3} + h_{j,0}^{1/3} \right)^2 \left(h_{i,0}^{-5/3} \left(\frac{dh_{i,0}}{dT} \right)^2 + h_{j,0}^{-5/3} \left(\frac{dh_{j,0}}{dT} \right)^2 \right) \\ & + \frac{\eta_{ij}}{8} \left(h_{i,0}^{1/3} + h_{j,0}^{1/3} \right)^2 \left(h_{i,0}^{-2/3} \frac{d^2 h_{i,0}}{dT^2} + h_{j,0}^{-2/3} \frac{d^2 h_{j,0}}{dT^2} \right) \end{aligned} \tag{1.49}$$

$$\begin{aligned} \frac{d^2 f_{x,0}}{dT^2} = & -\frac{2}{h_{x,0}} \frac{dh_{x,0}}{dT} \frac{df_{x,0}}{dT} - \frac{f_{x,0}}{h_{x,0}} \frac{d^2 h_{x,0}}{dT^2} \\ & + \frac{1}{h_{x,0}} \sum_i \sum_j x_i x_j \left(\frac{d^2 f_{ij,0}}{dT^2} h_{ij,0} + 2 \frac{df_{ij,0}}{dT} \frac{dh_{ij,0}}{dT} + f_{ij,0} \frac{d^2 h_{ij,0}}{dT^2} \right) \end{aligned} \tag{1.50}$$

with :

$$\begin{aligned} \frac{d^2 f_{ij,0}}{dT^2} = & \varepsilon_{ij} \frac{f_{i,0} \frac{d^2 f_{j,0}}{dT^2} + 2 \frac{df_{i,0}}{dT} \frac{df_{j,0}}{dT} + f_{j,0} \frac{d^2 f_{i,0}}{dT^2}}{2 \sqrt{f_{i,0} f_{j,0}}} \\ & - \frac{\varepsilon_{ij}}{4} (f_{i,0} f_{j,0})^{-3/2} \left(f_{i,0} \frac{df_{j,0}}{dT} + f_{j,0} \frac{df_{i,0}}{dT} \right)^2 \end{aligned} \tag{1.51}$$

The direct correlation function ($1-C_{ij}$) is a characteristic property of mixtures. The property can be calculated using the relationship below and the relationships given by the ECS theory.

$$1 - C_{ij} = N^t \left(\frac{d \ln \hat{\phi}_i}{dN_j^t} \right)_{T,V^t,N_{k \neq j}} + \left(\frac{d(N^t Z)}{dN_j^t} \right)_{T,V^t,N_{k \neq j}} \tag{1.52}$$

The ECS relationship for the direct correlation function is :

$$1-C_{ij} = (z_0+1)\left[1+(\kappa_0-1)\left(2H_{n_j}+H_{n_j}H_{n_i}\right)-(\gamma_0-1)\left(2F_{n_j}+F_{n_j}H_{n_i}+F_{n_i}H_{n_j}\right)\right]$$
$$+z_0\left(2H_{n_j}-H_{n_i}H_{n_j}+H_{n_in_j}\right)+u_0\left(2F_{n_j}+F_{n_in_j}\right)-c_{v,0}F_{n_i}F_{n_j} \qquad (1.53)$$

The cross derivatives of H and F are defined as follows :

$$H_{n_in_j} = \left(\frac{d^2h_x}{dn_idn_j}\right)\frac{N^{t^2}}{h_x}$$

$$F_{n_in_j} = \left(\frac{d^2f_x}{dn_idn_j}\right)\frac{N^{t^2}}{f_x}$$

If the van der Waals mixing rules are used the composition derivatives of the reducing parameters F and H are given by :

$$H_{n_i} = 2\left(\frac{\sum_k x_k h_{ki}}{h_x}-1\right) \qquad (1.54)$$

$$F_{n_i} = 2\left(\frac{\sum_k x_k f_{ki}h_{ki}}{f_xh_x}-1\right)-H_{n_i} \qquad (1.55)$$

$$H_{n_in_j} = 2\left(\frac{h_{ji}}{h_x}-1\right)-2H_{n_i}-2H_{n_j} \qquad (1.56)$$

$$F_{n_in_j} = 2\left(\frac{f_{ji}h_{ji}}{f_xh_x}-1\right)+\left(H_{n_j}+1\right)\left(H_{n_i}-F_{n_i}\right)+H_{n_i}\left(H_{n_j}-F_{n_j}\right)+H_{n_in_j} \qquad (1.57)$$

In order to calculate any of the above mentioned properties at a given state point the following steps should followed :

- Chose a thermodynamic surface representing the reference fluid
- Obtain thermodynamic surfaces for all components in the mixture
- Calculate the transformation parameters $f_{i,0}$ $h_{i,0}$ at a given state point.
- Calculate the derivatives of the transformation parameters. (H_T, F_T, H_{TT}, F_{TT}, ...)
- Calculate the transformation factors for the mixture, as well as their derivatives. ($f_{x,0}$, $h_{x,0}$, $H_{T,x}$, $F_{TT,x}$ ...)
- Using the mixture parameters and the reference fluid surface, calculation of any of the above mentioned properties is possible.

1.4. Analyses of the impact of the binary interaction parameters

In all ECS calculations performed in this report the van der Waals mixing rules given by the equations (1.13-16) were used. The thermodynamic properties are calculated for a mixture of methane and ethane. The molar fraction of methane is 0.5. The 32MBWR surfaces used where given by Younglove and Ely[4].Propane was used as the reference surface. The temperature was set to 330 K for all calculations. For each property two plots are given to illustrate the sensitivity to variations in the two binary interaction parameters. Note that the binary interaction parameter ε_{12} defined in equation (1.13) is denoted as K and the binary interaction parameter η_{12} defined in equation (1.14) is denoted by L. There were serious problems with convergence at densities lower than 3 mol/L. The erroneous points have been removed, and a straight line has been drawn to connect the ideal gas values (zero density) to the first acceptable points.

- Investigation of the influence of binary interaction parameters on the isochoric heat capacity

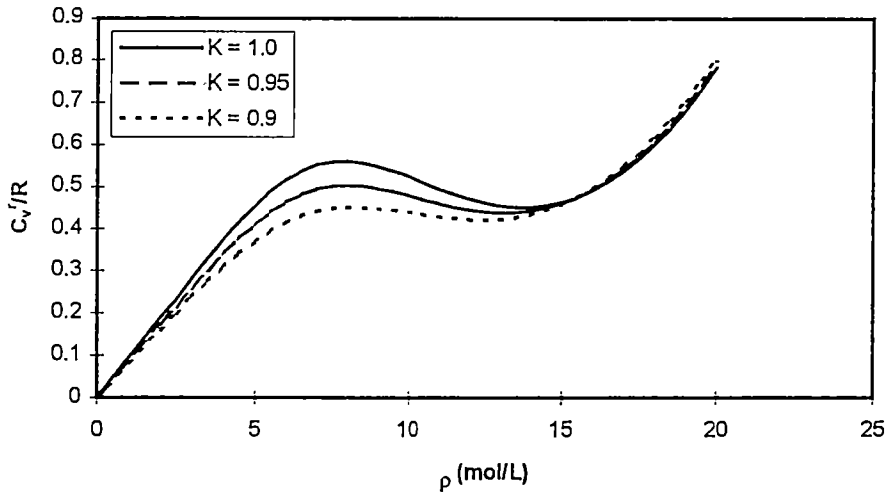

Figure 1.1 Effect of binary interaction parameters on C_v T = 330 K, $x_{methane} = x_{ethane} = 0.5$, L = 1.0

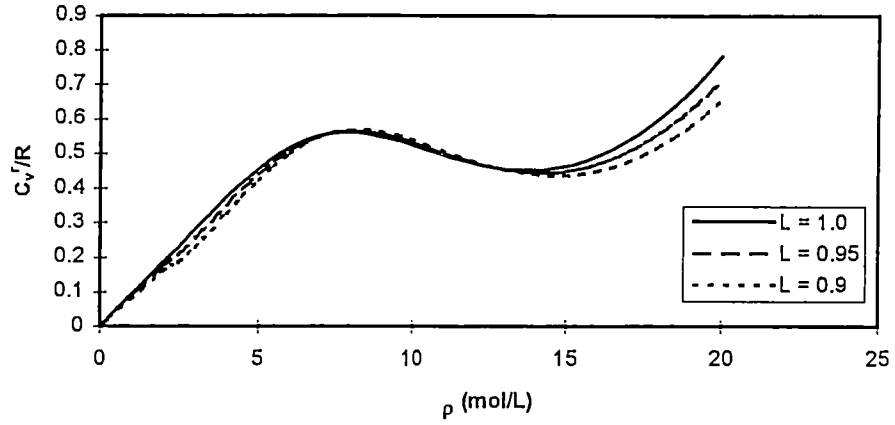

Figure 1.2 **Effect of binary interaction parameters on C_v T = 330 K, $x_{methane} = x_{ethane}$ =0.5, K = 1.0**

Variation in the interaction parameter K has the greatest effect in the neighborhood of the maximum in the isochoric heat capacity (Figure 1.1). Variations in the interaction parameter L has greatest effect at low and high densities (Figure 1.2). It seems that binary interaction parameters have little effect on the position of the maximum and minimum of the isochoric heat capacity.

- The influence of binary interaction parameters on isobaric heat capacity

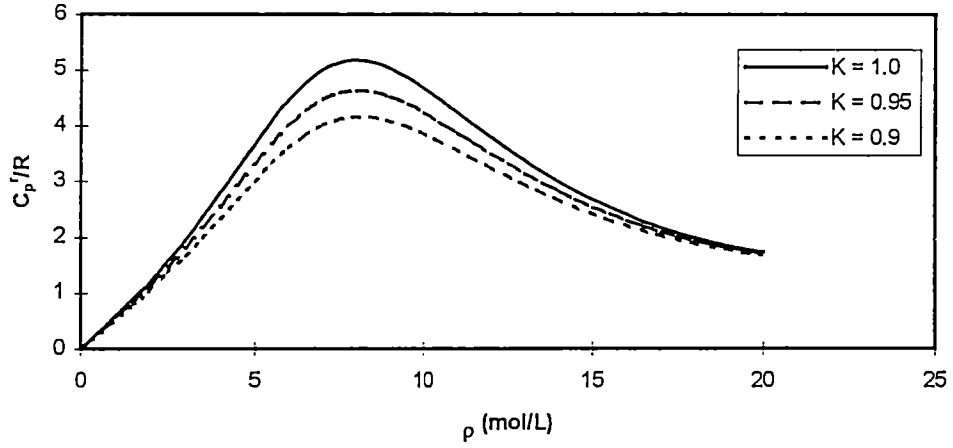

Figure 1.3 **Effect of binary interaction parameters on C_p T = 330 K, $x_{methane} = x_{ethane}$ =0.5, L = 1.0**

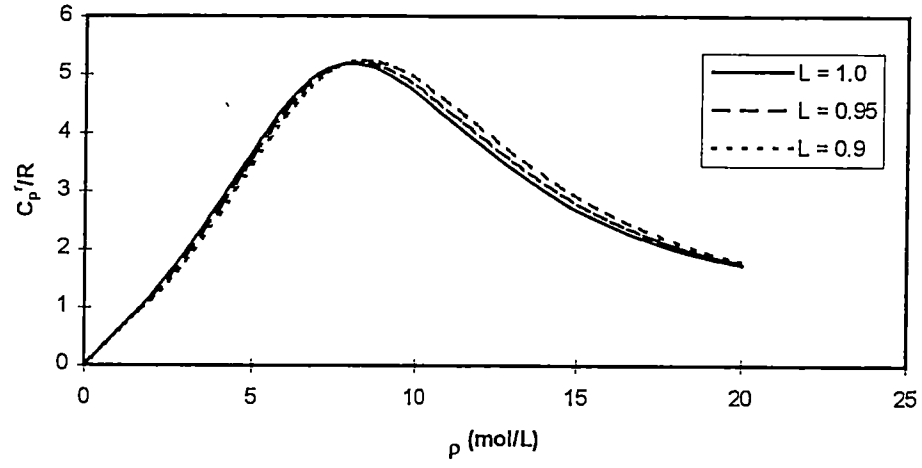

Figure 1.4 **Effect of binary interaction parameters on C_p T = 330 K, $x_{methane} = x_{ethane}$ =0.5, K = 1.0**

The interaction parameter K has significant effect on the value of the isobaric heat capacity at the maximum (Figure 1.3). The interaction parameter L has little effect on the isobaric heat capacity (Figure 1.4). The position of the maximum in the isobaric heat capacity is not affected by the varying the interaction parameters.

- The influence of binary interaction parameters on the Joule - Thomson coefficient

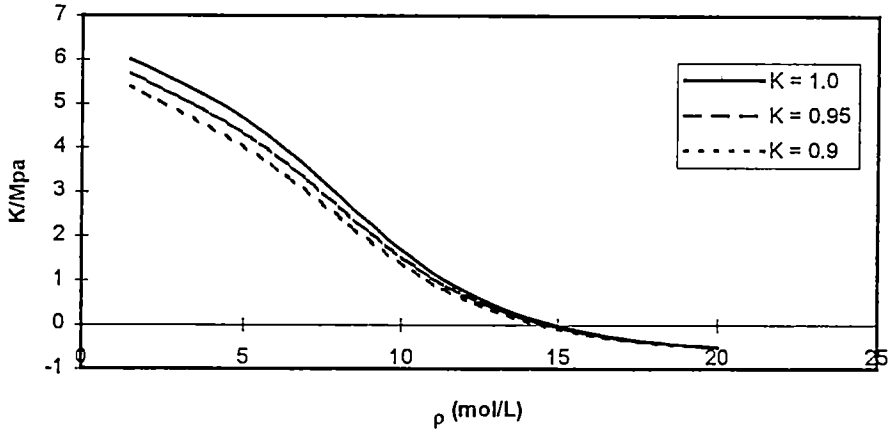

Figure 1.5 **Effect of binary interaction parameters on the Joule - Thomson coefficient T = 330 K, $x_{methane} = x_{ethane}$ =0.5, L = 1.0**

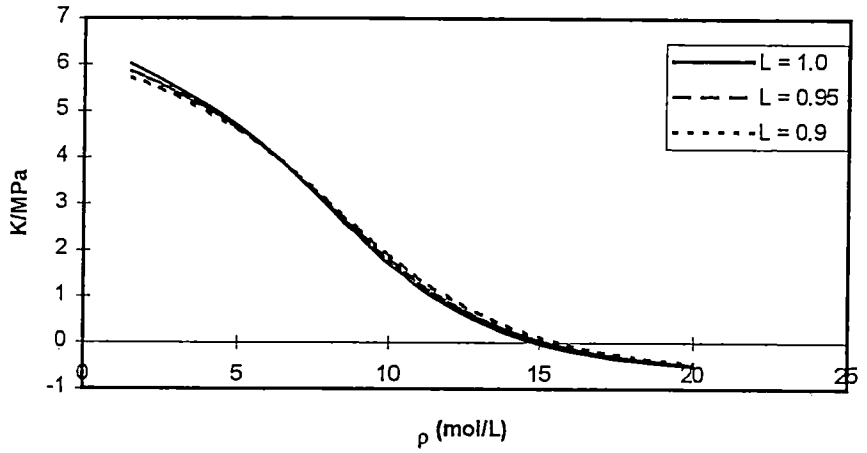

Figure 1.6 Effect of binary interaction parameters on the Joule - Thomson coefficient $T = 330$ K, $x_{methane} = x_{ethane} = 0.5$, $K = 1.0$

The limit of the Joule - Thomson coefficient as the density approaches zero has not been calculated because deriving the necessary formulas will be extremely time consuming. Variation in the interaction parameter K (Figure 1.5) has more effect than does the variation of the interaction parameter L (Figure 1.6). The Joule - Thomson inversion point seems not to be influenced by variations in either parameter.

- Influence of the binary interaction parameters on the speed of sound

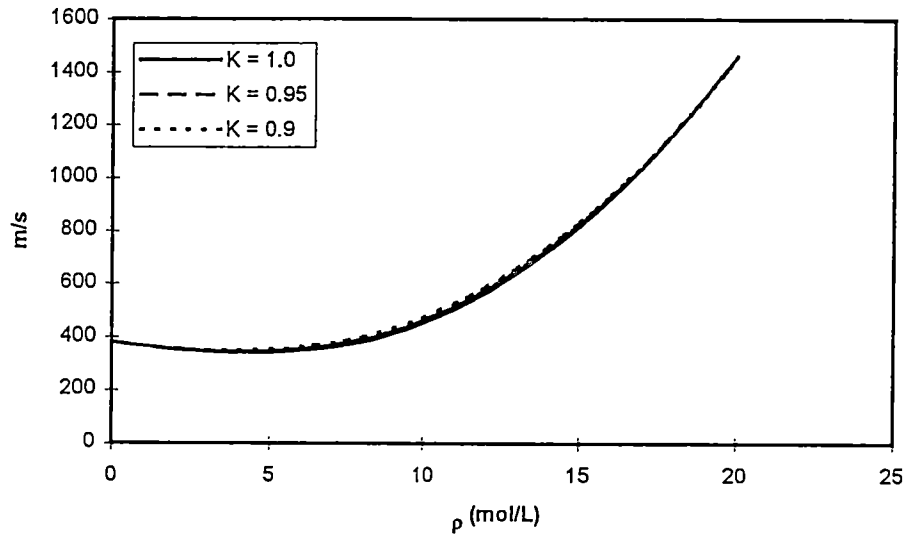

Figure 1.7 **Effect of binary interaction parameters on the speed of sound**
T = 330 K, $x_{methane} = x_{ethane} = 0.5$, L = 1.0

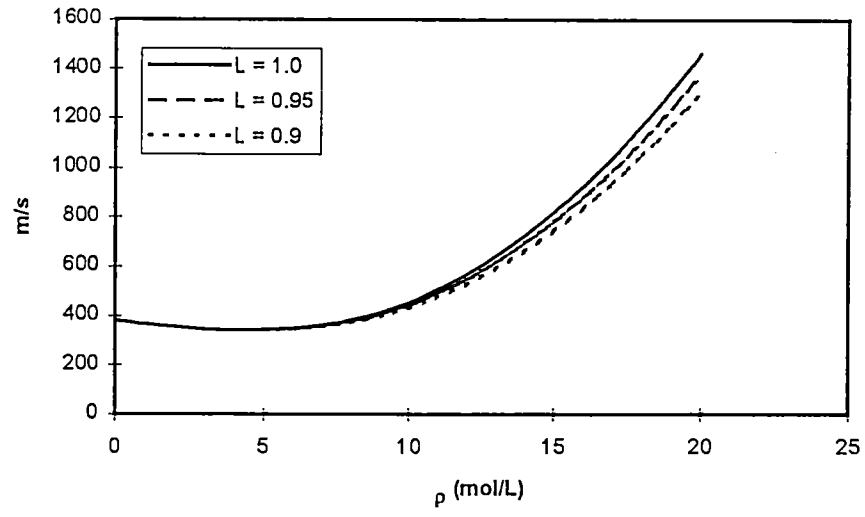

Figure 1.8 **Effect of binary interaction parameters on the speed of sound**
T = 330 K, $x_{methane} = x_{ethane}$ =0.5, K = 1.0

Variations of the interaction parameter K has little effect on the speed of sound (Figure 1.7). The effect of the interaction parameter L is seen only at high densities (Figure 1.8).

1.5. Evaluation of the accuracy of the ECS calculations

The results from the ECS calculation are compared to properties derived from a constant composition surface given by R. D. McCarty[6]. The mixture contains methane and ethane with molar fractions :

$x_{methane} = 0.68526$
$x_{ethane} = 0.31477$

All calculations are done by a temperature of 330 K. The critical density of the mixture is calculated as the mole fraction weighted sum of the pure component properties :

$$\rho_{c,x} = \frac{1}{\sum_i \frac{x_i}{\rho_{c,i}}} \qquad (1.58)$$

The critical density for the mixture is :

$\rho_c = 8.8263$ (mol/L)

The deviations are defined as

$$\Delta = (X_{reference} - X_{test})100 / X_{refernce}$$

where X is any of the properties. The interaction parameters are set to 1.0. The properties from the constant composition surface are also compared to those given by the principle of congruence. The principle of congruence states that for non polar ,approximately spherical molecules, the properties for the mixture are the molar fraction weighted sum of the pure component properties at the same density and temperature.

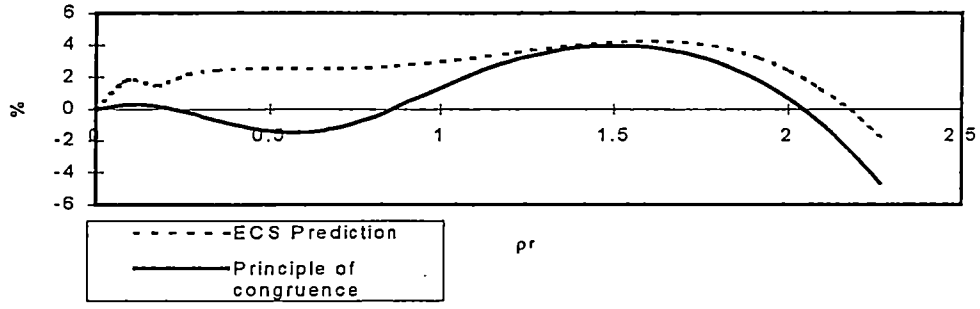

Figure 1.9 Residual plot C_v

The prediction given by the principle of congruence is generally better than that of the ECS calculation (Figure 1.9). This could be a result of a unsatisfactory refernce equation of state as well as of a failure of the ECS theory.

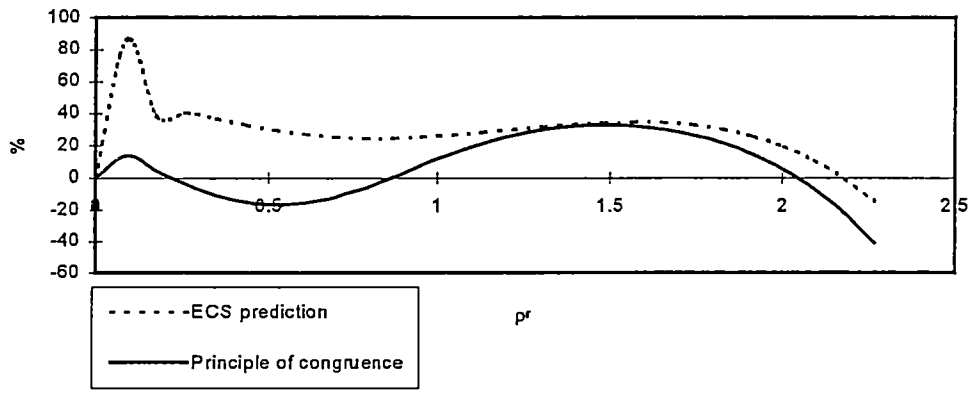

Figure 1.10 Residual plot C_v^r/R

This is basically the same comparison as the one given in Figure 1.9, but the ideal heat capacity is subtracted to give a comparison of the residual heat capacities. It is evident that deviations in the residual isochoric heat capacity are large.

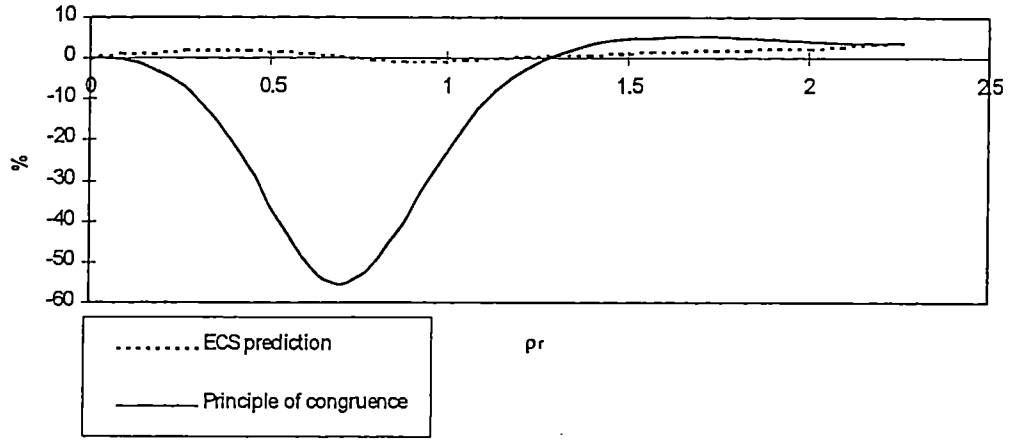

Figure 1.11 Residual plot C_p

In Figure 1.11 the comparison between the isobaric heat capacities is made. The principle of congruence gives huge deviations in the critical region. The ECS calculation gives a deviation less than 5 % in the whole range of densities.

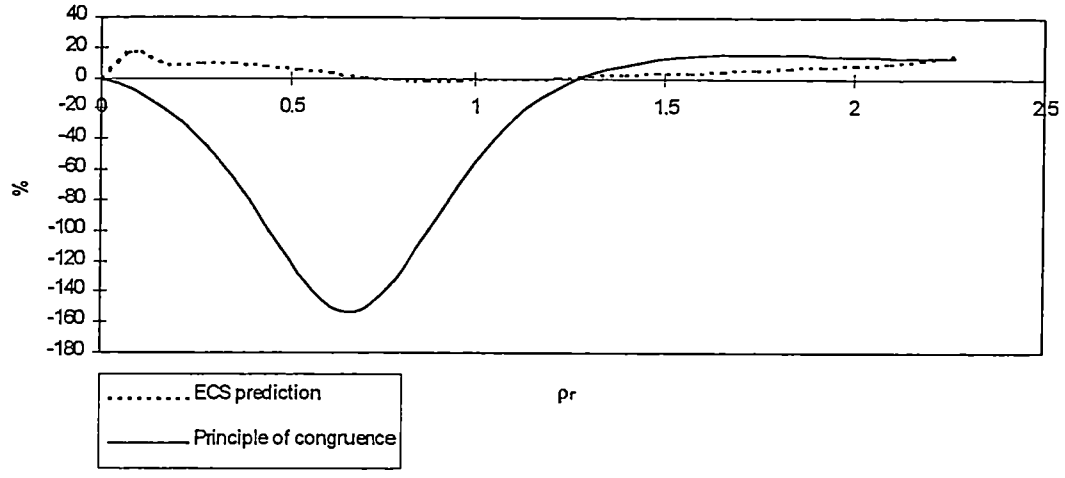

Figure 1.12 Residual plot C_p^r/R

In Figure 1.12 the residual isobaric heat capacities are compared. The predicted total isobaric heat capacity calculated with the ECS procedure resulted in deviation less than 5 % in the whole density range. If we compare the residual isobaric heat capacities it is evident that the deviation is much larger. Below the critical density it reaches almost 20 %.

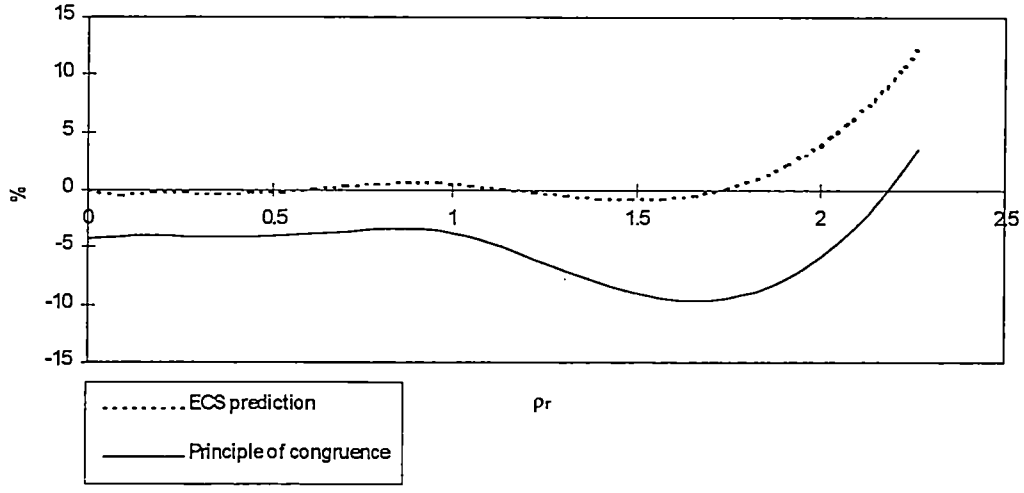

Figure 1.13 Residual plot speed of sound

In Figure 1.13 deviations in the speed of sound are given. The prediction given by the ECS calculation has a deviation of less than 5 % in the whole density range from 0 to 2. Above a reduced density of 2 the pure component surfaces used in the ECS calculation are probably not accurate.

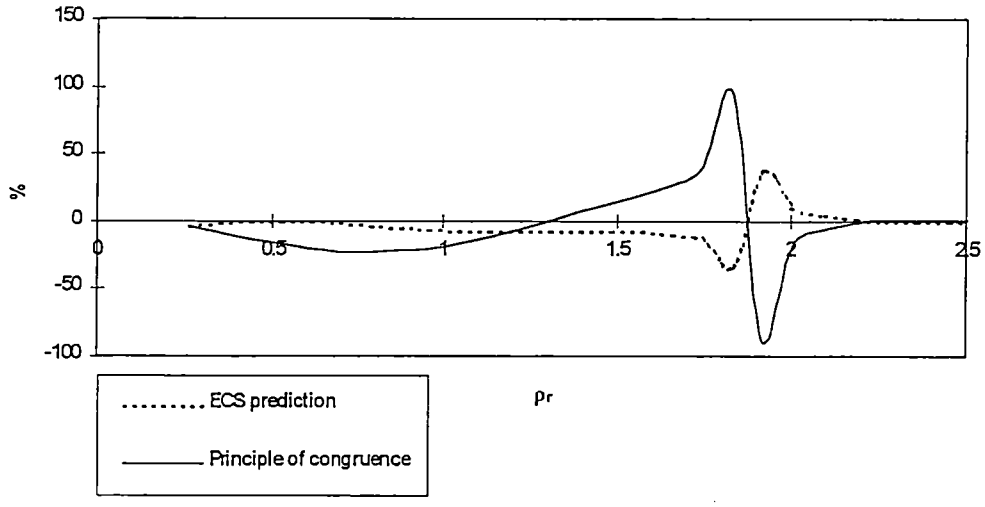

Figure 1.14 Deviation in the Joule - Thomson coefficient

In Figure 1.14 the deviations in the Joule - Thomson coefficient are given. Again the ECS prediction proves to be superior to the principle of congruence.

In order to give a more rigorous test of the ECS procedure measured isobaric heat capacities are compared to the ECS prediction in Figure 1.15 and Figure 1.16. The measured data are taken from Yesavage[7]. All calculations are done on the methane propane system. The measurements used here are at two pressures and two compositions.
The pseudo critical points for the mixtures are estimated by :

$x_{methane} = 0.23$: $P_c = 6.21$ MPa, $T_c = 353.40$ K, $\rho_c = 5.560$ mol/L
$x_{methane} = 0.49$: $P_c = 8.50$ MPa, $T_c = 325.17$ K, $\rho_c = 7.105$ mol/L

The volumetric interaction parameter L has been set to a value of one.

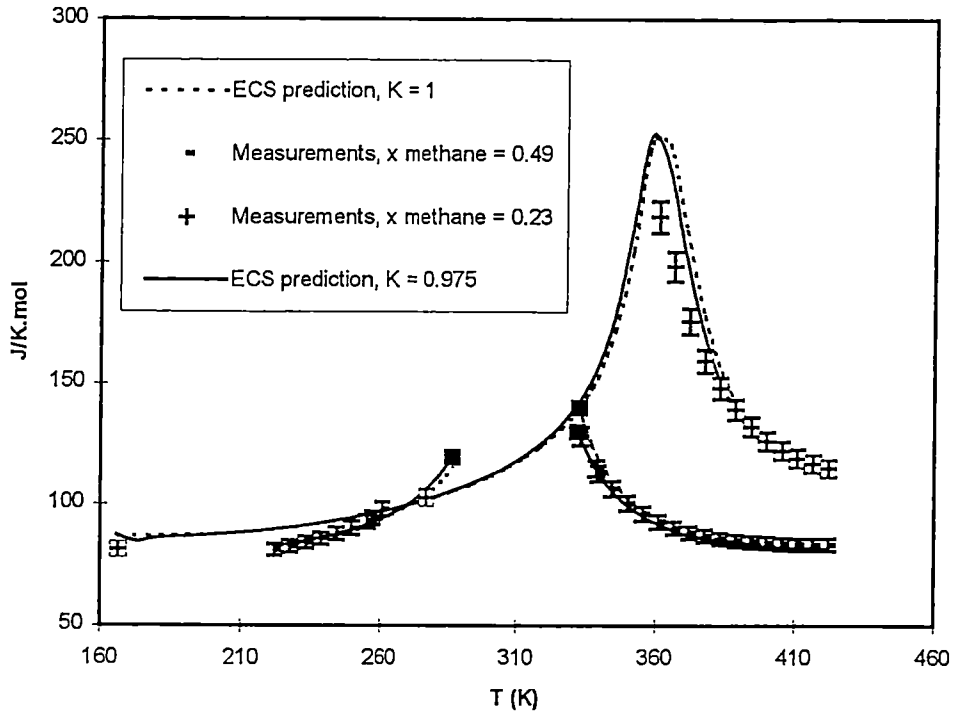

■ = saturation temperatures

Figure 1.15 Isobaric heat capacity for mixtures of methane and propane at P = 6.895 MPa

The estimated errors in the measurements are between 1.5 to 4 %. In Figure 1.15 error bars of 3 % are used. If we look at the values for the isobaric heat capacity obtained with the ECS procedure, setting all interaction parameters equal to one, it is evident that the predictions are good. There is however a systematical error in the critical region. An effort has been made to correct the deviations by changing the binary interaction parameter K. By setting this value to 0.975 we obtain a better representation of the data below the critical point. The systematical deviation above the critical point is not eliminated. This error may be due to the failure of the pure component surfaces to give a good representation of derived properties in the immediate vicinity of the critical point.

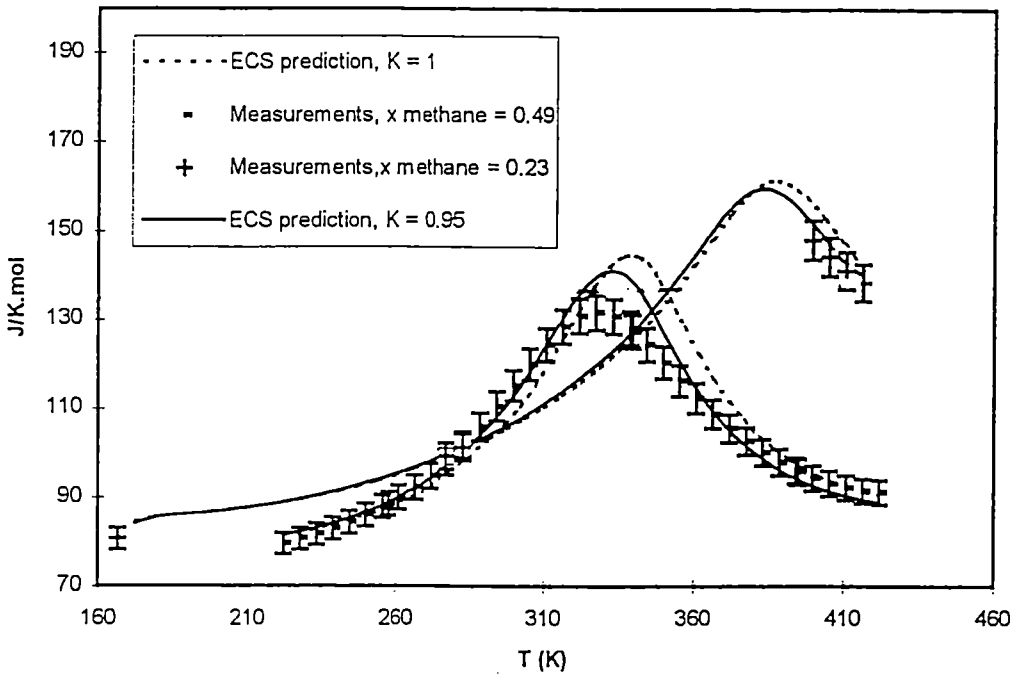

Figure 1.16 Isobaric heat capacity for mixtures of methane and propane at P = 10.342 MPa

In Figure 1.16 measured isobaric heat capacities at a 10.342 MPa are compared to those obtained from the ECS calculation. Again it's possible to obtain a good representation of the data away from the critical temperature by adjusting the binary interaction parameter K. In order to obtain a reasonable representation the interaction parameter has to be given a value of 0.95. This may seem a small adjustment, but even small differences in the interaction parameter are known to have profound effects on other properties such as phase equilibrium calculations.

1.6. Graphical representation of the derivative properties

In order to study the accuracy of equations of state some reference is needed. In this study, as already noted, multiparameter equations of state have been used in order to produce reference data. In studying the behavior of the different substances two types of behavior has been discovered. The behavior of the associating substances water and methanol is different from the behavior of non - associating substances. In order to point out the differences, water and methane have been chosen.

1.6.1. Properties of methane

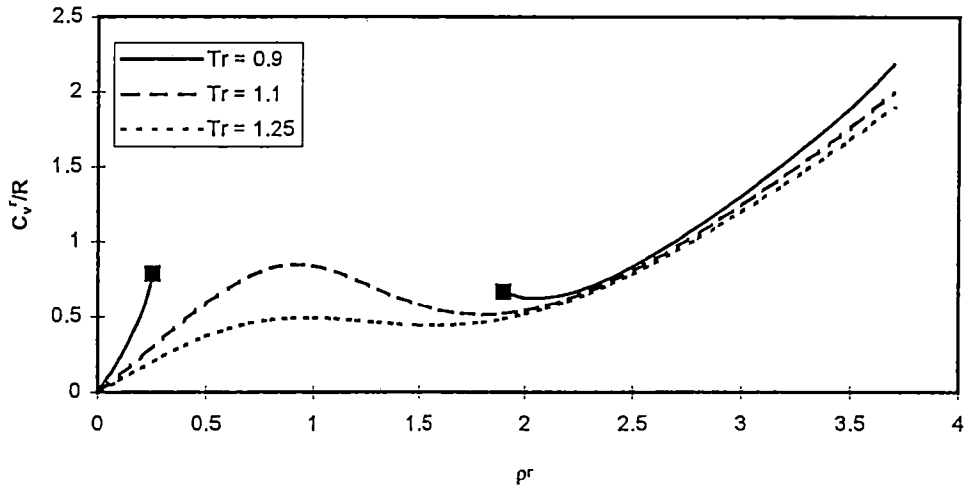

■ = saturated densities

Figure 1.17 C_v^r/R for methane from the SWEOS

In Figure 1.17 the residual isochoric heat capacity of methane is shown as a function of reduced density. The most apparent features of the curve are the maximum and the minimum that occur in the vicinity of the critical point. At high densities the value of the residual isochoric heat capacity seems to be a weak function of temperature.

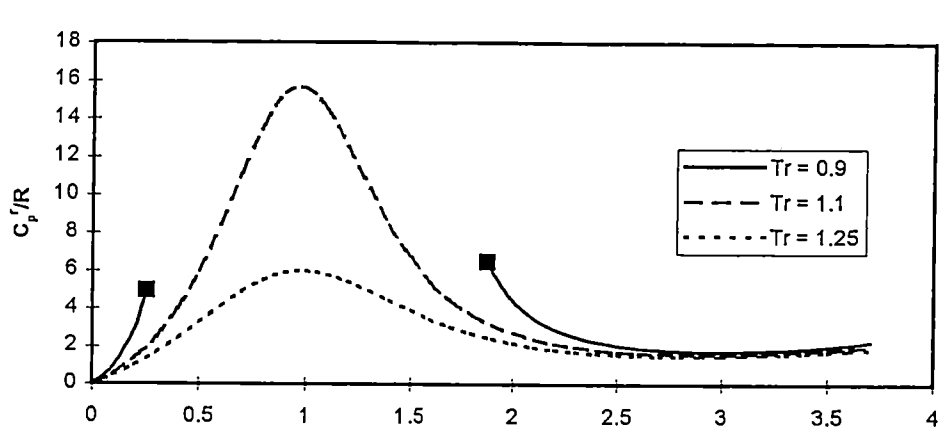

■ = saturated densities

Figure 1.18 C_p^r/R for methane from the SWEOS

In Figure 1.18 the residual isobaric heat capacity is plotted as a function of reduced density. The most apparent feature of the isobaric heat capacity is the strong maximum and the weak minimum that extends far from the critical region.

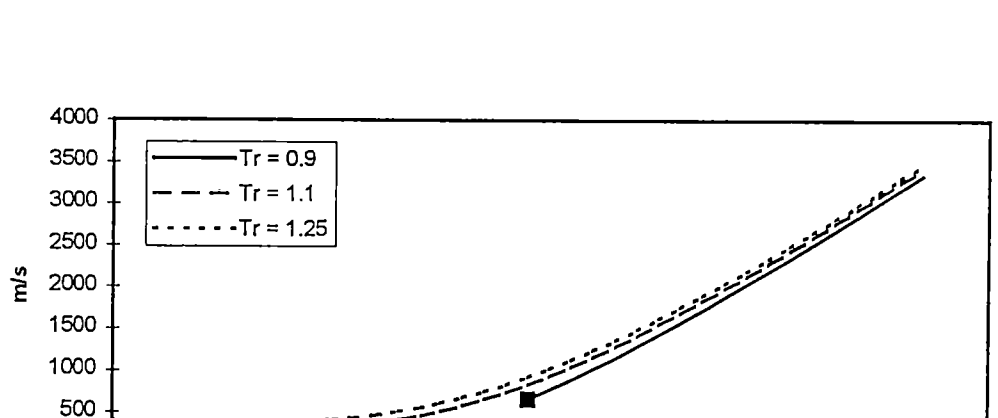

■ = saturated densities

Figure 1.19 Speed of Sound of methane from the SWEOS

In Figure 1.19 the speed of sound for methane is plotted as a function of reduced density. Compared to the heat capacities, the speed of sound is a weak function of temperature. The most characteristic feature of the curve is the minimum that slowly vanishes at high temperatures.

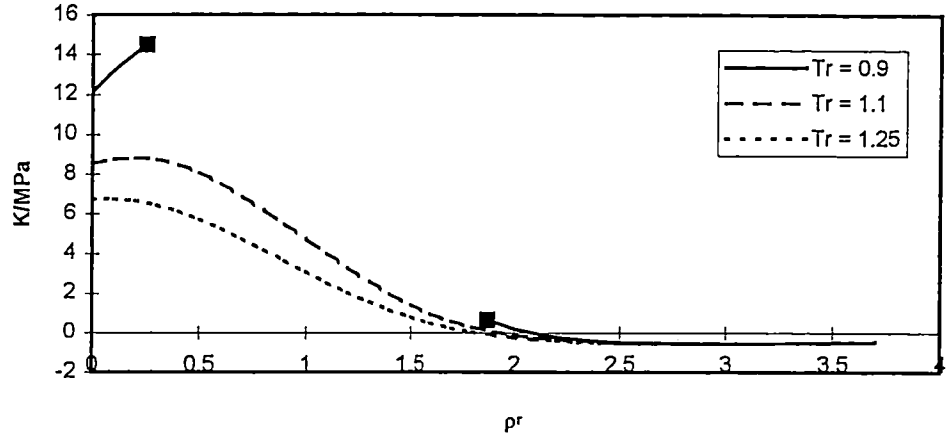

■ = saturated densities

Figure 1.20 The Joule - Thomson coefficient of methane from the SWEOS

In Figure 1.20 the Joule - Thomson coefficient for methane is plotted as a function of temperature. The most apparent feature of the curve is the maximum that occurs at low reduced densities. At reduced densities above 1 the curve also goes to a point where the value is zero. This is called the Joule - Thomson inversion point. At high densities, there is also a weak minimum in the curve.

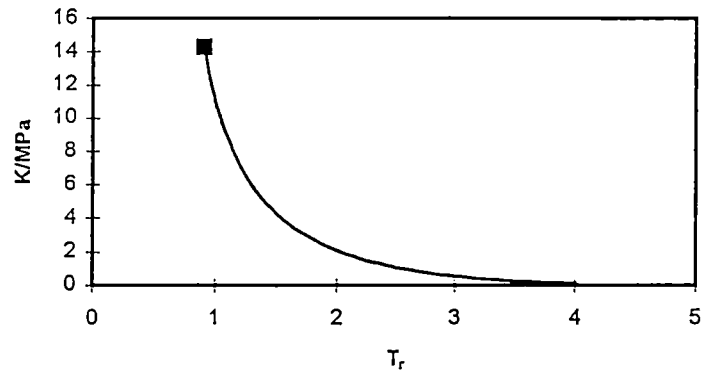

■ = saturated temperature

Figure 1.21 The Joule - Thomson coefficient methane with the SWEOS, $\rho_r = 0.27$

In Figure 1.21 one isochore of the Joule - Thomson coefficient is plotted as a function of reduced temperature. It shows how the value of the Joule - Thomson coefficient decreases as the temperature rises. That trend can also be observed for the other properties except for the speed of sound which increases with temperature.

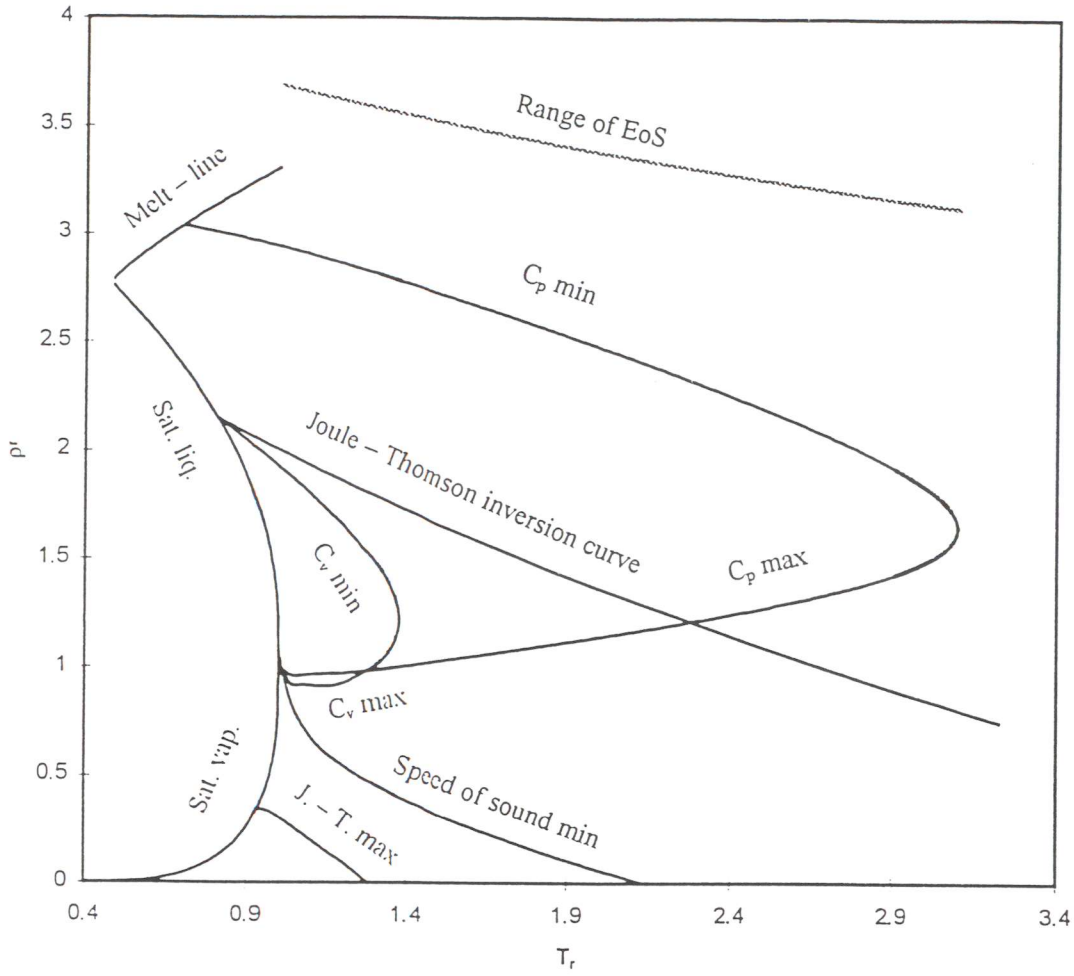

Figure 1.22 Property extrema and the Joule - Thomson inversion curve for methane

In Figure 1.22 the maxima and minima of the derivative properties as well as the Joule - Thomson inversion curve are plotted in reduced density reduced temperature space. The extreme points of the isochoric heat capacity are present only in the area close to the critical region. The maximum of the Joule - Thomson coefficient is only seen at reduced temperatures near unity. The extreme points of the isobaric heat capacity, the minimum of the speed of sound and the Joule - Thomson inversion curve are present over a much wider region.

1.6.2. Properties of water

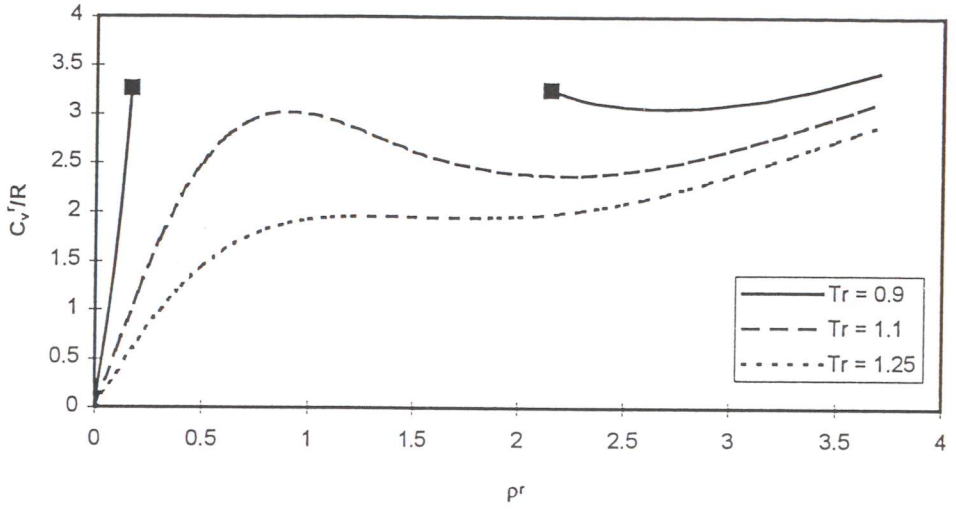

■ = saturated densities

Figure 1.23 C_v^r/R for water from the Hill EOS

The isochoric heat capacity for water (Figure 1.23) shows the same behavior as for methane (Figure 1.17) except there is a stronger temperature dependence at high reduced density.

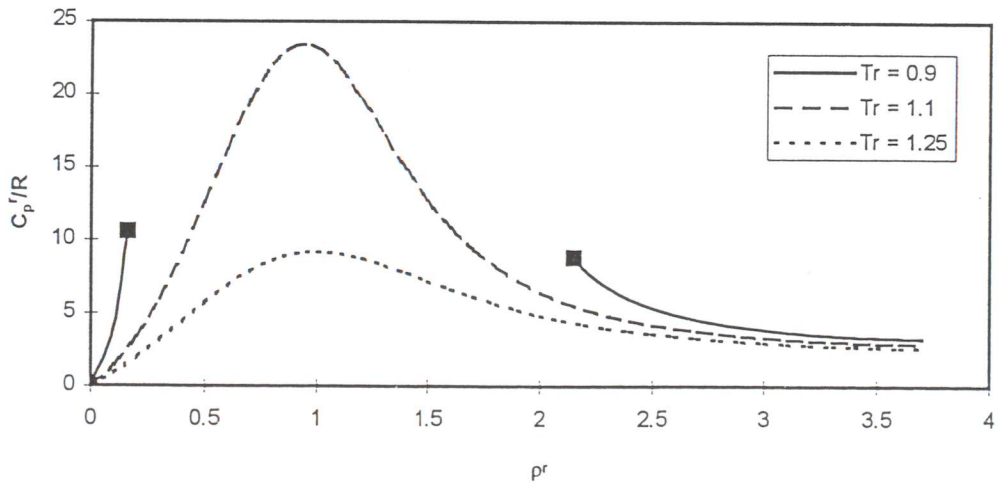

■ = saturated densities

Figure 1.24 C_p^r/R for water from the Hill EOS

The isobaric heat capacity for water (Figure 1.24) has no minimum at high reduced densities within the range of the EOS.

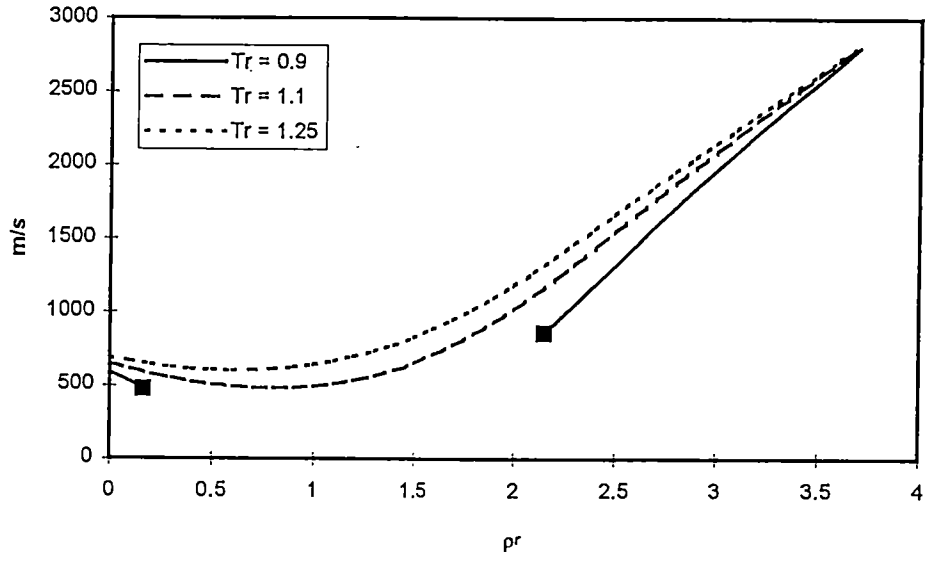

■ = saturated densities

Figure 1.25 Speed of Sound water with the Hill EOS

The speed of sound for water (Figure 1.25) has almost the same behavior as for methane except there is a decrease of the slope at high density that is absent in the case of methane (Figure 1.19).

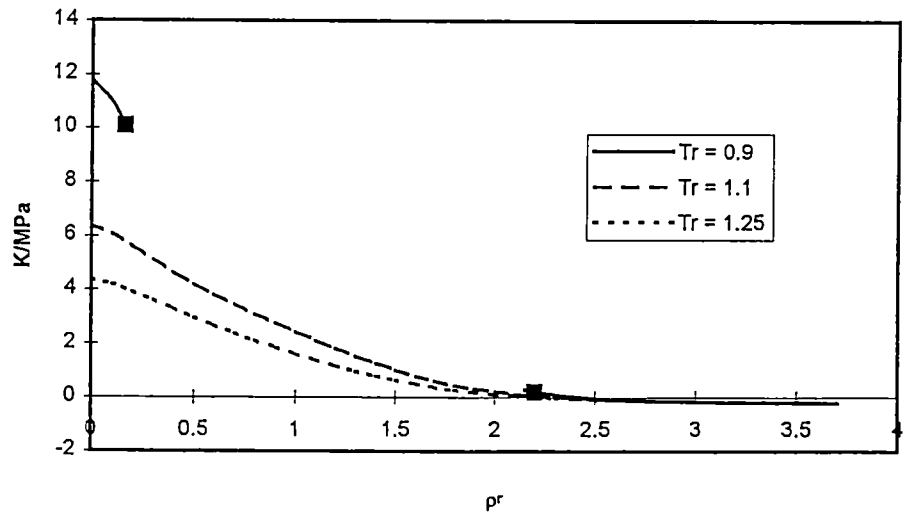

■ = saturated densities

Figure 1.26 The Joule - Thomson coefficient for water from the Hill EOS

In Figure 1.26 the Joule - Thomson curve for water is plotted as a function of reduced density. The most characteristic difference from methane (Figure 1.20) is the absence of a maximum at reduced densities below one.

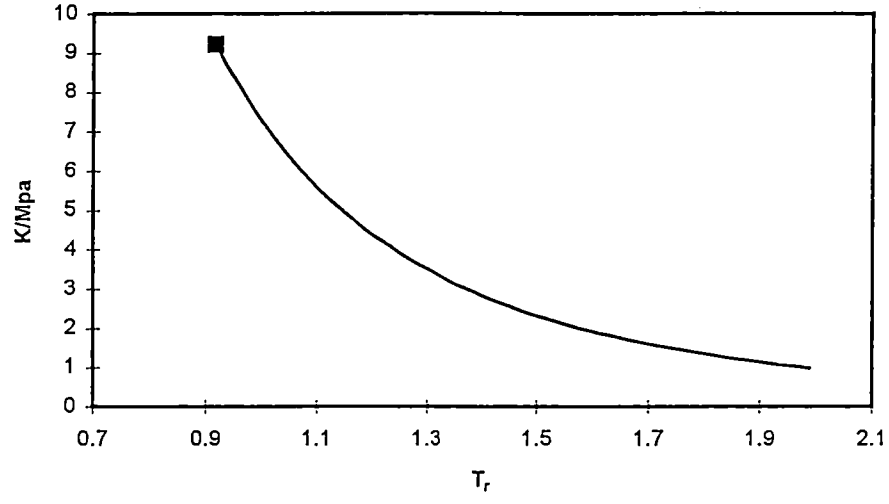

■ = saturation temperature

Figure 1.27 The Joule - Thomson coefficient for water from the Hill EOS

In Figure 1.27 one isochore of the Joule - Thomson coefficient is plotted as a function of temperature. The same decay with temperature as was the case for methane (Figure 1.21) is observed here.

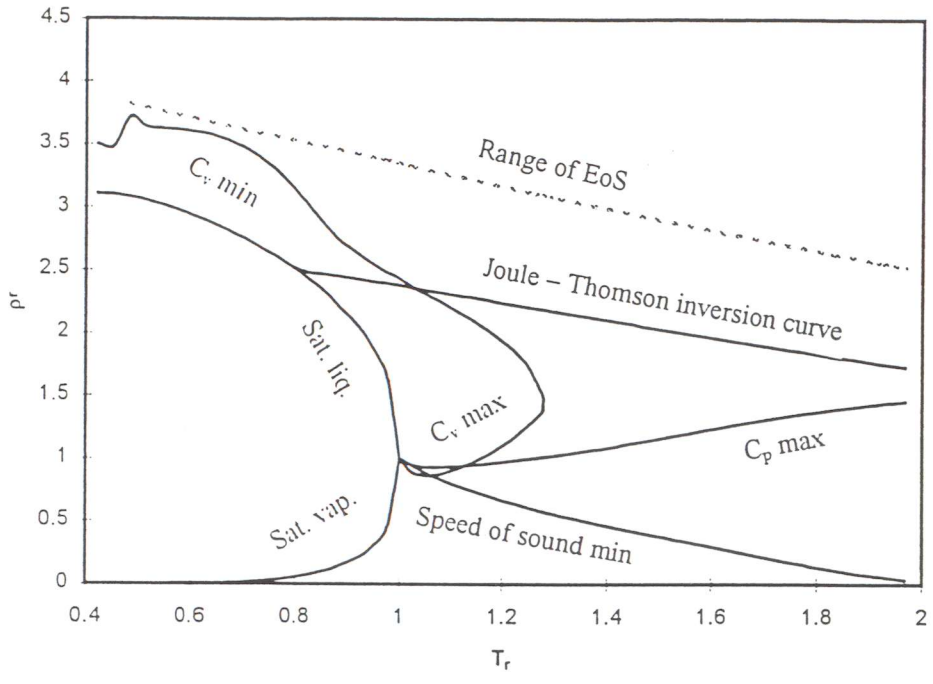

Figure 1.28 Property extrema and the Joule - Thomson inversion curve for water

In Figure 1.28 the minima, maxima and the Joule - Thomson curve for water are plotted in the reduced density reduced temperature space. The minimum in the isochoric heat capacity does not touch the saturated liquid line as it does for methane. It is not possible to conclude that there is no minimum in the isobaric heat capacity, since it may be outside the range of the EOS. If so, it is at a higher reduced density for water than for methane.

1.7 Discussion of results

In this chapter new analytical expressions for calculating the derivative properties with the ECS procedure have been developed. These derived properties were :

- The isochoric heat capacity
- The isobaric heat capacity
- The speed of sound
- The Joule - Thomson coefficient

All properties but the Joule - Thomson coefficient can be calculated in the whole range covered by the pure component equations of state. The Joule - Thomson coefficient can not be calculated in the limit where density approaches zero.

The sensitivity of the derived properties to variations of the binary energy and volume interaction parameters in the mixing rule was analyzed. The interaction parameter describing the energy interaction was found to have the larger influence on the values of the properties. The influence was strongest at densities close to the pseudo critical density for the mixture.

The accuracy of the results obtained with the ECS calculations has been analyzed. A comparison of ECS derived properties obtained with the principle of congruence, a pure component surface, and measured isobaric heat capacities shows that its results are of high quality. The biggest deviations were found in the region close to the pseudo critical point of the mixture.

The typical behavior of pure components has been studied. Differences in the behavior of associating and non - associating fluids have been found. Associating fluids does not show a maximum in the Joule - Thomson coefficient. The residual isochoric heat capacity of associating fluids tend to be a stronger function of temperature than the case is for non - associating fluids. The minimum in the isochoric heat capacity for associating fluids does not connect with the saturated liquid line.

2. Model equations of state

2.1. Introduction

All the derived properties for the model equations are given in this chapter. Their form is intended for non - associating substances. In their simplest form there are three parameters describing the intermolecular interaction energy, the volume of the molecules and the non - spherical character of the molecules.

2.2. Deriving derivative properties for pure fluids

2.2.1. The cubic equations

The first equation of state to give a qualitative description of the vapor and liquid phases and phase transitions was the famous cubic equation of van der Waals, proposed
in 1873 :

$$P = \frac{RT\rho}{(1-b\rho)} - a\rho^2 \qquad (2.1)$$

In this equation the constant b is the excluded volume, that is, that part of the molar volume which is not available to a molecule due to the presence of others. The first term to the right is the pressure resulting from the repulsion between the molecules. The second term to the right is the pressure resulting from the attraction between the molecules. In the van der Waals equation the energy parameter a is taken to be a constant. The constants in the van der Waals equation can be found using the critical - point conditions :

$$\left(\frac{dP}{d\rho}\right)_T = \left(\frac{d^2P}{d\rho^2}\right)_T = 0 \qquad (2.2)$$

For the van der Waals equation we find :

$$a = \frac{27R^2T_c^2}{64P_c} \quad b = \frac{RT_c}{8P_c} \qquad (2.3)$$

While the van der Waals equation is of historical interest, it is not quantitatively correct. For example, it predicts that the critical compressibility factor,

$$Z_c = \frac{P_c}{RT_c\rho_c} \tag{2.4}$$

is 0.375 for all fluids, while the value for different hydrocarbons varies from 0.24 to 0.29; the range is wider when non - hydrocarbons are considered. Also, the prediction of vapor pressures is inaccurate.

An important modification of the van der Waals equation was made by Redlich and Kwong[8], who introduced a temperature dependence and a slightly different volume dependence in the attractive term :

$$P = \frac{RT\rho}{1-b\rho} - a(T)\frac{\rho^2}{1+b\rho} \tag{2.5}$$

with :

$$a(T) = 0.42748\frac{R^2T_c^2}{P_c}\frac{1}{\sqrt{T_r}} \tag{2.6}$$

This equation is referred to as the Redlich Kwong equation or RK equation. The equation gives a somewhat better critical compressibility factor (Z_c=1/3), but it is still not very accurate for the phase boundary (vapor pressure) and the liquid density.

Soave[9] proposed a different temperature dependence for the energy parameter

$$a(T) = 0.42748\frac{R^2T_c^2}{P_c}\left[1+m(1-\sqrt{T_r})\right]^2 \tag{2.7}$$

and :

$$m = 0.480 + 1.57\omega - 0.176\omega^2 \tag{2.8}$$

resulting in more accurate vapor pressure predictions (especially above 1 bar) for light hydro carbons, leading to cubic equations of state becoming an important tool for the prediction of vapor - liquid equilibria at moderate to high pressures for non - polar fluids. This modification is referred to as the Soave - Redlich - Kwong equation or SRK equation.

Peng and Robinson[10] used a different volume dependence to give slightly improved liquid volumes (and, $Z_c = 0.307$) and changed the temperature dependence of a(T) to give :

$$P = \frac{RT\rho}{1-b\rho} - a(T)\frac{\rho^2}{1+2b\rho-b^2\rho^2} \tag{2.9}$$

with :

$$a(T) = 0.45724 \frac{R^2 T_c^2}{P_c} \left(1 + m(1 - \sqrt{T_r})\right)^2 \qquad (2.10)$$

and :

$$m = 0.37464 + 1.54226\omega - 0.26992\omega^2 \qquad (2.11)$$

This equation is referred to as the Peng - Robinson equation or the PR equation.

The PR and the SRK equations are widely used in industry, especially for refinery and reservoir simulation. The advantages of these equations are that they require little input information, little computer time, and, for hydrocarbons, lead to good results for process design. However, these equations do have some important shortcomings :

- Liquid densities are not well predicted
- The generalized parameters are not well predicted for non - hydrocarbons
- Predictions for long - chain molecules are inaccurate.
- Critical region properties are unreliable
- Vapor pressure predictions are not very accurate at low pressures

Using the equations ... in chapter 1 the derivative properties can be derived :

- Isochoric heat capacity with the RK and SRK equation :

$$\frac{C_v^r}{R} = \frac{T}{Rb} \frac{d^2 a}{dT^2} \ln(1 + b\rho) \qquad (2.12)$$

In the case of the RK equation the second temperature derivative of the energy parameter is given by :

$$\frac{d^2 a}{dT^2} = 0.42748 \frac{3R^2 T_c^2}{4P_c} \sqrt{T_c} T^{-5/2} \qquad (2.13)$$

For the SRK equation the relationship is :

$$\frac{d^2 a}{dT^2} = 0.42748 \frac{R^2 T_c^2}{P_c} m(1 + m) \frac{T^{-3/2}}{2\sqrt{T_c}} \qquad (2.14)$$

- Isochoric heat capacity with the PR equation

$$\frac{C_v^r}{R} = -\frac{T}{bR\sqrt{8}} \frac{d^2 a}{dT^2} \ln\left[\frac{(b\rho - 1 - \sqrt{2})(-1 + \sqrt{2})}{(b\rho - 1 + \sqrt{2})(-1 - \sqrt{2})}\right] \qquad (2.15)$$

with:

$$\frac{d^2a}{dT^2} = 0.45724\frac{R^2T_c^2}{P_c}m(1+m)\frac{T^{-3/2}}{2\sqrt{T_c}} \tag{2.16}$$

- Pressure derivative with regard to temperature from the RK and SRK equations :

$$\left(\frac{dP/R\rho}{dT}\right)_\rho = \frac{1}{1-b\rho} - \frac{1}{R}\frac{da}{dT}\frac{\rho}{1+b\rho} \tag{2.17}$$

For the RK equation the temperature derivative of the energy parameter a(T) is given by :

$$\frac{da}{dT} = -\frac{0.42748}{2}\frac{R^2T_c^2}{P_c}\sqrt{T_c}T^{-3/2} \tag{2.18}$$

In the case of the SRK equation the temperature derivative is given by :

$$\frac{da}{dT} = -0.42748\frac{R^2T_c^2}{P_c}m\frac{1}{\sqrt{TT_c}}\left(1+m(1-\sqrt{T_r})\right) \tag{2.19}$$

- Pressure derivative with regard to temperature from the PR equation :

$$\left(\frac{dP/R\rho}{dT}\right)_\rho = \frac{1}{1-b\rho} - \frac{1}{R}\frac{da}{dT}\frac{\rho}{1+2b\rho-b^2\rho^2} \tag{2.20}$$

with :

$$\frac{da}{dT} = -0.45724\frac{R^2T_c^2}{P_c}m\frac{1}{\sqrt{TT_c}}\left(1+m(1-\sqrt{T_r})\right) \tag{2.21}$$

- Pressure derivative with regard to density from the RK and SRK equations :

$$\left(\frac{dP/RT}{d\rho}\right)_T = \frac{1}{(1-b\rho)^2} - \frac{a(T)}{RT}\frac{\rho(2+b\rho)}{(1+b\rho)^2} \tag{2.22}$$

- Pressure derivative with regard to density from the PR equation :

$$\left(\frac{dP/RT}{d\rho}\right)_T = \frac{1}{(1-b\rho)^2} - \frac{a(T)}{RT}\frac{2\rho(1+b\rho)}{(1+2b\rho-b^2\rho^2)^2} \tag{2.23}$$

2.2.2. The SPHCT Eos

The SPHCT equation is a simplification of the PHCT equation. The PHCT equation is designed to give a description of polymeric fluids as originally proposed by Beret and Prausnitz[11]. The following assumptions were made :

1. The density dependence of all external degrees of freedom is the same as those of the translational degrees of freedom.
2. The density dependence of translational degrees of freedom is given by the Carnahan - Starling equation. (Carnahan and Starling[12])
3. A chain molecule behaves like a chain of spherical segments, each of which interacts with its neighbors with the square well potential.
4. An adjustable parameter c is defined so that 3c is the total number of external degrees of freedom of a molecule.

The PHCT theory defined three substancespecific parameters :

- The effective chain length c, describing the number of segments in chain like molecules.
- The closest packing volume (mv^0), describing the volume of the molecules.
- The segment energy εq, describing the interaction energy between two segments.

The basic form of both the SPHCT and the PHCT equation is :

$$Z = 1 + c(Z_{rep} - Z_{att}) \tag{2.24}$$

For both equations the repulsion term is given by :

$$Z_{rep} = \frac{4\eta - 2\eta^2}{(1-\eta)^3} \tag{2.25}$$

The density variable is given by :

$$\eta = \tau \rho m v^0 \tag{2.26}$$

τ has a constant value of 0.74048. The symbol m denotes the number of segments in one molecule. v^0 is given by :

$$v^0 = \frac{\pi N_{Av}}{6\tau}\sigma^3 \tag{2.27}$$

where σ is the temperature independent segment diameter and N_{av} is the avogadro number.

According to the PHCT theory the attraction forces are modeled using the double power series expansion of Alder et al.[13] :

$$Z_{att} = \sum_i \sum_j jD_{ij}\left[\frac{\varepsilon q}{ckT}\right]^i\left[\frac{\eta}{\tau}\right]^j \qquad (2.28)$$

where ε is the intermolecular potential per unit surface area and q is the surface area per molecule. The constants D_{ij} were adjusted to better fit data for alkanes. The quanteties ε and q always appears as a product εq so this equation has three parameters :

εq, mv^0 and c

A shortcoming of the original HPCT equation is the complexity caused by its attraction term. In order to reduce the complexity Lee et al.[14] suggested replacing the summation terms with one single term :

$$Z_{att} = \frac{Z_M \eta Y}{1+\eta Y} \qquad (2.29)$$

with :

$$Y = \exp\left[\frac{\varepsilon q}{2ckT}\right] - 1 \qquad (2.30)$$

The factor Z_M is the coordination number of one site on the chain, which has been determined empirically by Kim et al.[15]. This simplified equation is called the SPHCT equation.

The SPHCT equation has proved to give good liquid volumes, as well as accurate equilibrium properties for mixtures of molecules which differ greatly in size. (Peters et al.[16]) The SPHCT equation has two advantages over the cubic equations. First, its foundation in statistical thermodynamics makes the assumptions used in its development clear in terms of molecular behavior. Second, species are modeled as segment - segment type rather than the cruder molecule - molecule interactions of the cubic equations. However, the SPHCT equation has several limitations which hinder its use in engineering calculations. Although the parameters represent specific molecular behavior they are not related to macroscopic physical properties. This makes it necessary to use regression analyses in order to obtain their values. The values are dependent on the regression procedure and the experimental data. The equation is not constrained to give correct critical pressures and temperatures. Because of the fifth order dependence of density the equation requires more computational time than the cubic equations.
The derivative properties can be derived using equations (1.5-8) in chapter 1.

- The isochoric heat capacity is given by :

$$\frac{C_v^r}{R} = cTZ_{att}\left(2\frac{dY}{dT} + T\frac{d^2Y}{dT^2} - \frac{T}{Z_m}Z_{att}\left(\frac{dY}{dT}\right)^2\right) \tag{2.31}$$

- The temperature derivative of the pressure is given by :

$$\left(\frac{dP/R\rho}{dT}\right)_\rho = 1 + cZ_{rep} - cZ_{att} - cT\frac{Z_M\eta}{(1+\eta Y)^2}\frac{dY}{dT} \tag{2.32}$$

- The density derivative of the pressure is given by :

$$\left(\frac{dP/RT}{d\rho}\right)_T = 1 + cZ_{rep} + c\frac{4\eta}{(1-\eta)^2} + c\frac{3\eta(4\eta - 2\eta^2)}{(1-\eta)^4} - cZ_m\frac{\eta Y(2+\eta Y)}{(1+\eta Y)^2} \tag{2.33}$$

with :

$$\frac{dY}{dT} = -\frac{\varepsilon q}{2ckT^2}\exp\left(\frac{\varepsilon q}{2ckT}\right) \tag{2.34}$$

and :

$$\frac{d^2Y}{dT^2} = \left(\frac{\varepsilon q}{ckT^3} + \left(\frac{\varepsilon q}{2ckT^2}\right)^2\right)\exp\left(\frac{\varepsilon q}{2ckT}\right) \tag{2.35}$$

2.2.3. The SAFT equation of state

The SAFT equation is designed to model effects that come from association of molecules and shape effects from non - spherically molecules. For non - associating molecules the equation needs three substance specific parameters. Those are :

- The segment molar volume in a closest packed arrangement at zero temperature v^{00}, describing the volume of the molecules.
- The interaction energy of segments at infinite temperature u_0/k, describing the interaction energy between segments
- The effective chain length m, describing the number of segments in chain like molecules.

If the substance is self associating two additional parameters are defined :

- The associating energy ε^{AB}, describing the energy of the association bonding between two bonding segments.
- The associating volume κ^{AB}, describing the volume of the bonding segments.

The reduced fluid density η (segment packing fraction) is defined as

$$\eta = \tau \rho m \upsilon^0$$

where $\tau = 0.74048$, v^0 is the segment molar volume at the closest packing and m is the number of segments per molecule. The closest packing volume is related to temperature as follows :

$$\upsilon^0 = \upsilon^{00}\left[1 - C\exp\left(\frac{-3u^0}{kT}\right)\right]^3 \qquad (2.36)$$

The constant C has the value of 0.12. In this expression there are two compound specific parameters. Those are the closest packing volume at zero temperature υ^{00} and the interaction energy between segments at infinite temperature u^0. The interaction energy between segments is given by

$$\frac{u}{k} = \frac{u^0}{k}\left[1 + \frac{e}{kT}\right] \qquad (2.37)$$

The value for e/k is set to 10 with exception of some small molecules given in table 2.1 :

Table 2.1 Values of e/k

Substance	e/k (K)
Argon	1
Methane	1
Ammonia	1
Water	1
Nitrogen	3
CO	4.2
Cl_2	18
CS_2	38
CO_2	40
SO_2	88

The advantage of the SAFT equation is the ability to model specific molecular behavior. It also models association of molecules. The volume and interaction energy parameter are temperature dependent. The temperature dependence of the volume parameter is a special feature of the SAFT equation. The models's disadvantages are also many. The complexity of the equation prohibits its use in application where computational speed is needed. It also suffers from the same weaknesses as the SPHCT equation with regard to fitting procedure and the representation of thermodynamic properties in the near critical region.

The general form of the SAFT equation is the Helmholz energy given by :

$$A^{res} = A^{seg} + A^{chain} + mmA^{assoc} \qquad (2.38)$$

The segment Helmholz energy per mole of molecules A^{seg} can be calculated from

$$A^{seg} = mA_0^{seg} \qquad (2.39)$$

where A_0^{seg}, per mole of segments, is the residual Helmholz energy of nonassociating spherical segments and m is the segment number. It is composed of hard sphere and dispersion parts,

$$A_0^{seg} = A_0^{hs} + A_0^{disp} \qquad (2.40)$$

The hard sphere contribution can be calculated by as proposed by Carnahan and Starling[12] :

$$\frac{A_0^{hs}}{RT} = \frac{4\eta - 3\eta^2}{(1-\eta)^2} \tag{2.41}$$

The dispersion term is a power series fitted to molecular dynamics data for a square well fluid. The equation is given by Alder et al.[13] :

$$\frac{A_0^{disp}}{RT} = \sum_i \sum_j D_{ij} \left[\frac{u}{kT}\right]^i \left[\frac{\eta}{\tau}\right]^j \tag{2.42}$$

Rather than the parameters of Alder et al.[13] as in the PHCT model, the SAFT model uses D_{ij}'s fitted to experimental data for argon by Chen and Kreglewski[17].

The increment in the Helmholz energy due covalent bonding of several segments can be calculated from

$$\frac{A^{chain}}{RT} = (1-m)\ln\frac{1-\frac{1}{2}\eta}{(1-\eta)^3} \tag{2.43}$$

The increment in the Helmholz energy due to association is calculated for pure fluids from

$$\frac{A^{assoc}}{RT} = \sum_A \left[\ln X^A - \frac{X^A}{2}\right] + \frac{1}{2}M \tag{2.44}$$

where M is the number of associating sites on each molecule, X^A is the mole fraction of molecules not bonded at site A, and Σ_A represents a sum over all associating site on the molecule. The mole fraction of molecules not bonded can be determined as follows

$$X^A = \left[1 + N_{Av}\sum_B \rho X^B \Delta^{AB}\right]^{-1} \tag{2.45}$$

(Summation over all sites A,B,C, ...)

where N_{av} is the Avogadro's number and ρ is the molar density of molecules. The factor Δ^{AB} is the association strength that is approximated as

$$\Delta^{AB} = g(d)^{seg}\left[\exp(\varepsilon^{AB}/kT) - 1\right](\sigma^3\kappa^{AB}) \tag{2.46}$$

with :

$$\sigma = \left[\frac{6\tau}{\pi N_{Av}} \upsilon^{00} \right]^{1/3}$$

The segment radial distribution function $g(d)^{seg}$ is approximated as the hard sphere radial distribution function (Carnahan and Starling)

$$g(d)^{seg} \approx g(d)^{hs} = \frac{1 - \frac{1}{2}\eta}{(1-\eta)^3} \tag{2.47}$$

In order to avoid the great complexity introduced by the associating term in equation (2.38) only non - associating compounds will be studied. The derivative properties from the SAFT equation of state can be derived using the equations (1.1-4) in chapter 1. The compressibility factor is given by :

$$Z - 1 = Z^{seg} + Z^{chain} \tag{2.48}$$

$$Z^{seg} = m\left[\frac{4\eta - 2\eta^2}{(1-\eta)^3} + \sum_i \sum_j jD_{ij} \left[\frac{u}{kT} \right]^i \left[\frac{\eta}{\tau} \right]^j \right] \tag{2.49}$$

$$Z^{chain} = (1-m) \frac{\frac{5}{2}\eta - \eta^2}{(1-\eta)\left(1 - \frac{1}{2}\eta\right)} \tag{2.50}$$

The properties are given by :

- The isochoric heat capacity

$$\frac{C_v^r}{R} = \frac{C_v^{r,seg}}{R} + \frac{C_v^{r,chain}}{R} \tag{2.51}$$

$$\frac{C_v^{r,seg}}{R} = m\left(\left(\frac{C_v^{r,hs}}{R} \right)_0 + \left(\frac{C_v^{r,disp}}{R} \right)_0 \right) \tag{2.52}$$

$$\left(\frac{C_v^{r,hs}}{R}\right)_0 = -9\left(\frac{3u_0}{kT}\right)^2 F^2\left(\frac{4\eta^3 - 10\eta^2}{(1-\eta)^4}\right) - 3\left(\frac{3u_0}{kT}\right)^2 F(2F-1)\left(\frac{4\eta - 2\eta^2}{(1-\eta)^3}\right) \quad \textbf{(2.53)}$$

$$\left(\frac{C_v^{r,disp}}{R}\right)_0 = -\sum_i \sum_j D_{ij}\left(\frac{\eta}{\tau}\right)^j \left(\frac{u}{kT}\right)^i \left[(F1+F2)(2+F1+F2)+F3+F4\right] \quad \textbf{(2.54)}$$

with :

$$F = \frac{C\exp\left[\frac{-3u_0}{kT}\right]}{1 - C\exp\left[\frac{-3u_0}{kT}\right]}$$

and :

$$F1 = -i\frac{1+\frac{2e}{kT}}{1+\frac{e}{kT}}$$

,

$$F2 = -j3\left(\frac{3u_0}{kT}\right)F$$

,

$$F3 = i\left[\frac{1+\frac{4e}{kT}}{1+\frac{e}{kT}} - \frac{\frac{e}{kT}\left(1+\frac{2e}{kT}\right)}{\left(1+\frac{e}{kT}\right)^2}\right]$$

,

$$F4 = j6\left(\frac{3u_0}{kT}\right)F - j3\left(\frac{3u_0}{kT}\right)^2 F(1+F)$$

$$\left(\frac{C_v^{r,chain}}{R}\right)_0 = -(1-m)9\left(\frac{3u_0}{kT}\right)^2 F^2\left(\frac{3\eta^2}{(1-\eta)^2} - \frac{\eta^2}{4\left(1-\frac{1}{2}\eta\right)^2}\right)$$

$$-(1-m)3\left(\frac{3u_0}{kT}\right)^2 F(2F-1)\left(\frac{3\eta}{(1-\eta)} - \frac{\eta}{2\left(1-\frac{1}{2}\eta\right)}\right) \qquad (2.55)$$

- The pressure derivative with respect to density

$$\left(\frac{dP/RT}{d\rho}\right)_T = \left(\frac{dP/RT}{d\rho}\right)_T^{seg} + \left(\frac{dP/RT}{d\rho}\right)_T^{chain} \qquad (2.56)$$

$$\left(\frac{dP/RT}{d\rho}\right)_T^{seg} = Z^{seg} + m\left[\frac{4\eta+4\eta^2-2\eta^3}{(1-\eta)^4} + \sum_i\sum_j j^2 D_{ij}\left(\frac{u}{kT}\right)^i\left(\frac{\eta}{\tau}\right)^j\right] \qquad (2.57)$$

$$\left(\frac{dP/RT}{d\rho}\right)_T^{chain} = Z^{chain} + (1-m)\left[\frac{\frac{5}{2}\eta - 2\eta^2 + \frac{1}{4}\eta^3}{(1-\eta)^2\left(1-\frac{1}{2}\eta\right)^2}\right] \qquad (2.58)$$

- The pressure derivative with respect to temperature

$$\left(\frac{dP/R\rho}{dT}\right)_\rho = \left(\frac{dP/R\rho}{dT}\right)_\rho^{seg} + \left(\frac{dP/R\rho}{dT}\right)_\rho^{chain} \qquad (2.59)$$

$$\left(\frac{dP/R\rho}{dT}\right)_\rho^{seg} = \left(\frac{dP/R\rho}{dT}\right)_\rho^{hs} + \left(\frac{dP/R\rho}{dT}\right)_\rho^{disp} \qquad (2.60)$$

$$\left(\frac{dP/R\rho}{dT}\right)_\rho^{hs} = Z^{seg} - m3\left(\frac{3u_0}{kT}\right)F\left[\frac{4\eta+4\eta^2-2\eta^3}{(1-\eta)^4}\right] \qquad (2.61)$$

$$\left(\frac{dP/R\rho}{dT}\right)_{\rho}^{disp} = Z^{disp} - m\sum_i\sum_j D_{ij}\left(\frac{u}{kT}\right)^i\left(\frac{\eta}{\tau}\right)^j\left[i\frac{1+\frac{2e}{kT}}{1+\frac{e}{kT}} + j3\left(\frac{3u_0}{kT}\right)F\right] \qquad (2.62)$$

$$\left(\frac{dP/R\rho}{dT}\right)_{\rho}^{chain} = Z^{chain} - (1-m)3\left(\frac{3u_0}{kT}\right)F\left[\frac{\frac{5}{2}\eta - 2\eta^2 + \frac{1}{4}\eta^3}{(1-\eta)^2\left(1-\frac{1}{2}\eta\right)^2}\right] \qquad (2.63)$$

2.3. Derivative properties for mixtures

2.3.1. Mixing rules for cubic equations of state

All the cubic equations of state evaluated in this study uses the same mixing rules, called the van der Waals mixing rules. All the cubic equations have two parameters. One parameter b describes the covolume between the molecules. The mixing rule for this parameter is as follows :

$$b_x = \sum_i x_i b_i \qquad (2.64)$$

The second parameter is the interaction parameter a. This parameter describes the interaction forces between the molecules. The mixing rule for this parameter is as follows :

$$a_x = \sum_i\sum_j x_i x_j a_{ij}, \quad a_{ii} = a_i, \quad a_{jj} = a_j \qquad (2.65)$$

The cross terms are given by :

$$a_{ij} = \sqrt{a_i a_j}(1-k_{ij}) \qquad (2.66)$$

The factor k_{ij} is an empirical factor used to increase the quality of the results. It's usually fit to phase equilibrium data.

The third parameter is the acentric factor ω. This parameter describes the deviations from the behavior of spherical molecules. (Non - sphericity) This parameter is used only in the PR and the SRK EOS. Its mixing rule is given by :

$$\omega_x = \sum_i x_i \omega_i \tag{2.67}$$

2.3.2. Mixing rules for the SPHCT EOS

The mixing rules used with the SPHCT EOS are those proposed by Kim et al.[28] The SPHCT EOS has three mixturedependent parameters. The mixing rule for the close - packing volume mv^0 is :

$$(mv^0)_x = \sum_i x_i (mv^0)_i \tag{2.68}$$

The mixing rule for the c parameter is :

$$c_x = \sum_i x_i c_i \tag{2.69}$$

$$Y_x = \frac{\sum_i \sum_j x_i x_j c_i (mv^0)_{ji} Y_{ij}}{c_x (mv^0)_x} \tag{2.70}$$

where

$$Y_{ij} = \exp\left(\frac{\varepsilon_{ij} q_i}{2 c_i kT}\right) - 1 \tag{2.71}$$

and :

$$(mv^0)_{ji} = m_j v^0_{ji} \tag{2.72}$$

The cross terms v^0_{ij} and ε_{ij} are given by

$$v^0_{ij} = \frac{1}{8}\left(v_i^{0\,1/3} + v_j^{0\,1/3}\right)^3 \tag{2.73}$$

and

$$\varepsilon_{ij} = \sqrt{\varepsilon_i \varepsilon_j}\,(1 - k_{ij}) \tag{2.74}$$

The factor k_{ij} is an adjustable binary interaction parameter. Equation (2.70) may be cast in the form :

$$Y_{ij} = \exp\left\{\frac{q_i\sqrt{\varepsilon_i\varepsilon_j}(1-k_{ij})}{2c_i kT}\right\} - \qquad (2.75)$$

In the case of mixtures, besides the pure component parameters, one requires knowledge of m_i and q_i. Kim et al.[2] suggested that m_i and q_i may be obtained from the slopes of the graphs of mv^0 and $\varepsilon q/k$ versus the number of carbon atoms. As a result the volume of one segment, and the energy per surface unit can be estimated :

$$\frac{\varepsilon}{k} = 62.5 \quad [\mathrm{K/m^2}] \qquad (2.76)$$

$$v^0 = 0.008667 \quad [\mathrm{L/mol}] \qquad (2.77)$$

This allows calculation of the number of segments on basis of the knowledge of the pure component parameter $(mv^0)_i$. The surface area per segment can be calculated based on knowledge of the pure component parameter $(\varepsilon q/k)_i$.

2.3.3. Mixing rules for the SAFT equation

Mixing rules for the SAFT equation are given by Chapman et al.[18]. For the other equations of state mentioned in this chapter the pure component equations of state are transformed into equations for mixtures by combining the pure component parameters to obtain mixture parameters. In the case of the SAFT equation the functional structure changes from the one given in paragraph (2.2.3). The radial hard sphere distribution function $g(d)^{hs}$ for pure components changes into :

$$g_{ii}(d_{ii})^{hs} = \frac{1}{1-\zeta_3} + \frac{3d_{ii}}{2}\frac{\zeta_2}{(1-\zeta_3)^2} + 2\left(\frac{d_{ii}}{2}\right)^2\frac{\zeta_2^2}{(1-\zeta_3)^3} \qquad (2.78)$$

with

$$\zeta_k = \frac{\pi N_{Av}}{6}\rho\sum_i x_i m_i d_{ii}^k \qquad (2.79)$$

This expression was derived for mixtures of hard spheres by Reed and Gubbins[19].

The mixture parameters can be derived by combination of pure mixture parameters, as described earlier :

$$v_x^0 = \frac{\sum_i \sum_j x_i x_j m_i m_j v_{ij}^0}{\left(\sum_i x_i m_i\right)^2} \tag{2.80}$$

$$u_x v_x^0 = \frac{\sum_i \sum_j x_i x_j m_i m_j v_{ij}^0 u_{ij}}{\left(\sum_i x_i m_i\right)^2} \tag{2.81}$$

The cross terms are given by :

$$u_{ij} = \varepsilon_{ij}(u_{ii}u_{jj})^{1/2} \tag{2.82}$$

$$v_{ij}^0 = \frac{v_{ii}^0 + v_{jj}^0}{2} \tag{2.83}$$

The effective length of the molecules in the fluid can be approximated by :

$$m_x = \sum_i x_i m_i \tag{2.84}$$

Using the mixture parameters the different parts of the equation can be expressed as :

$$\frac{A^{chain}}{RT} = \sum_i x_i (1 - m_i) \ln(g_{ii}(d_{ii})^{hs}) \tag{2.85}$$

$$\frac{A^{assoc}}{RT} = \sum_i x_i \left[\sum_{A_i} \left(\ln\left(x^{A_i} - \frac{x^{A_i}}{2} \right) + \frac{1}{2} M_i \right) \right] \tag{2.86}$$

$$A^{seg} = m_x A_0^{seg} \tag{2.87}$$

2.4. Concluding comments

In this chapter we have briefly discussed some of the model equations available in literature. Only the most widely used equations, or equations presenting important concepts have been chosen. The cubic equations have been chosen because of their importance in reservoir simulation and process design for the oil industry. The SPHCT equation has been chosen because it represents an important concept. The molecules are seen as chains of segments rather than spherical balls as is the case for the cubic equations. The SPHCT equation also uses the more complex CS term to describe the inter segmental repulsion though the attraction term has a density dependence that is very similar to the RK and SRK equations of state. The SAFT equation of state also describes molecules as chains of segments. The SAFT equation also uses a CS term to describe segment - segment repulsion. In the SAFT equation there is an extra term for the increment of the residual Helmholz energy resulting from the chain character of molecules. Another difference from the other equations is the temperature dependence of the segment - segment energy and the effective segment volume. However, the attraction term used in the SAFT equation is similar to the one used in the original PHCT equation.

3. Evaluation of theoretical equations of state

3.1. Introduction

In order to reveal the weaknesses of equations of state they are compared with the multi parameter equations of state. The equations of state are of chapter 2 were considered :

Cubic equations :

- Redlich - Kwong
- Soave - Redlich - Kwong
- Peng Robinson

Statistical mechanics based equations :

- The SPHCT equation
- The SAFT equation

The cubic equations are well known and widely used in engineering practice. The advantage of the cubic equations are the simplicity and therefore low requirements of computational power. The parameters in those equations can be estimated solely on basis of the saturation pressure curve and critical properties.

The statistical mechanical based equations have a higher complexity and therefore are less valuable in applications requiring computational speed. The parameters of the equations are usually fitted to liquid density data and saturated pressures. This leads to an overestimation of critical pressures and temperatures. The SPHCT equation has been selected because of its simplicity.

The equations will be evaluated for methane and n-butane. All the equations are valid for methane. When it comes to n-butane different methods have been introduced in order to correct for the deviation from hard sphere behavior. The cubic equations use the acentric factor to account for the effects. The SPHCT equation uses the c parameter and the SAFT equation uses the m parameter for those purposes. Both the c and m parameters can be viewed as measures of effective chain length. The SAFT equation also has a specific increment in the Helmholz energy as function of the chain length. By evaluating the derived properties for both methane and n-butane the success or failure in describing chain - like behavior can be exposed.

3.2. Basis of evaluation

In order to analyze the deviations some special measures has been taken. The deviations in the isochoric heat capacity are revealed by comparing the residual heat capacity. The residual heat capacity is given by equation (3.1)

$$\frac{C_v^r}{R} = -\frac{1}{R}\int_0^{\rho} \frac{T}{\rho^2}\left(\frac{d^2P}{dT^2}\right)_{\rho} d\rho \qquad (3.1)$$

The advantage of comparing the residual heat capacities is that the dependence on the ideal heat capacity is removed.

In order to study the isobaric heat capacity without the influence of the isochoric heat capacity following property is used :

$$\frac{C_p^r - C_v^r}{R} = \frac{T}{R\rho^2}\left(\frac{dP}{dT}\right)_{\rho}^2 \Big/ \left(\frac{dP}{d\rho}\right)_T - 1 \qquad (3.2)$$

The advantage of comparing this property is that the deviations in the C_v and the ideal isobaric heat capacity is not influencing the comparison. In order to study the total isobaric heat capacity the residual isobaric heat capacity is included. Note that this quantity is not dependent on the ideal isobaric heat capacity.

$$\frac{C_p^r}{R} = \frac{C_v^r}{R} + \frac{T}{R\rho^2}\left(\frac{dP}{dT}\right)_{\rho}^2 \Big/ \left(\frac{dP}{d\rho}\right)_T - 1 \qquad (3.3)$$

In order to compare the Joule - Thomson coefficient the dependence on the isobaric heat capacity is discarded yielding the following expression :

$$\mu C_p \rho = \frac{T\left(\frac{dP}{dT}\right)_{\rho}}{\rho\left(\frac{dP}{d\rho}\right)_T} - 1 \qquad (3.4)$$

Instead of comparing the speed of sound the reduced bulk modulus will be used as a basis for comparison. The reduced bulk modulus is given by :

$$B_T = \frac{w^2}{RT}\frac{C_v M_r}{C_p 10^6} = \left(\frac{dP/RT}{d\rho}\right)_T \qquad (3.5)$$

3.3. Graphical evaluation of the equations of state for pure fluids

In order to expose the characteristic behavior of the derivative properties the all properties are evaluated at a reduced temperature of 1.1. At this temperature all the derivative properties are showing their characteristic minima and maxima.

3.3.1. The isochoric heat capacity

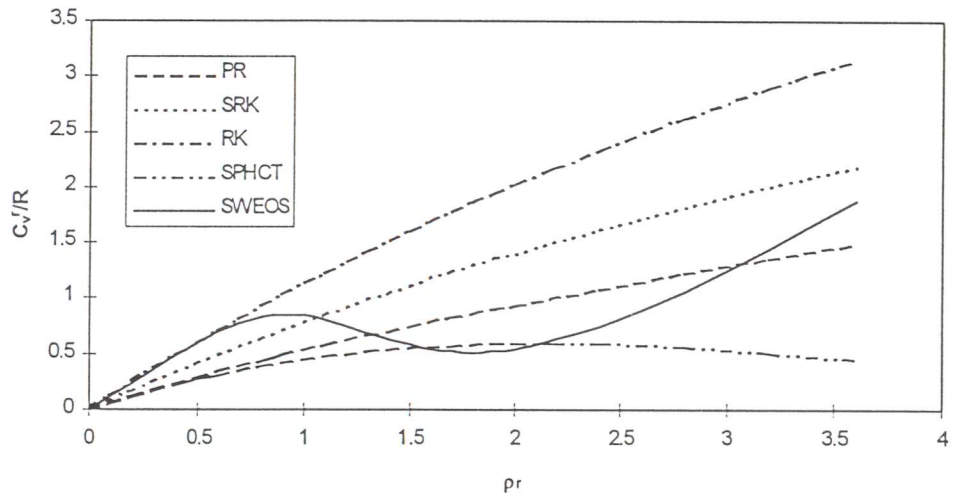

Figure 3.1 C_v^r/R methane with model equations of state at $T_r = 1.1$

In Figure 3.1 the isochoric heat capacity of methane is shown. None of the equations studied are able to give a qualitatively correct picture of the isochoric heat capacity. The SPHCT equation is the only one to give a maximum, but at a much to high reduced density. At low density only the RK equation is gives a good initial slope of the heat capacity.

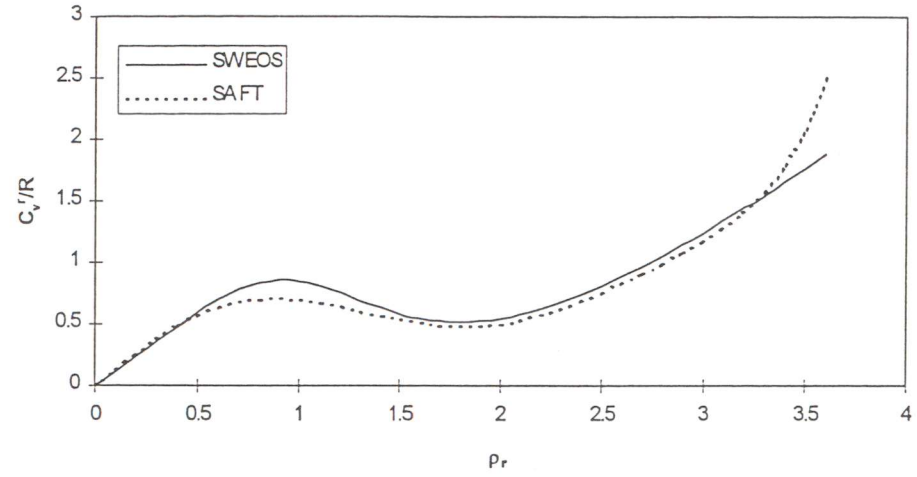

Figure 3.2 C_v^r/R methane with the SAFT equation at $T_r = 1.1$

In Figure 3.2 the isochoric heat capacity from the SAFT equation is compared to the heat capacity from the SWEOS. The SAFT equation is able to give a qualitatively correct picture of the isochoric heat capacity, with both a maximum and a minimum in the curve. At high densities the curve diverges. This happens because of the singularity in the denominator of the CS repulsion term in the SAFT equation.

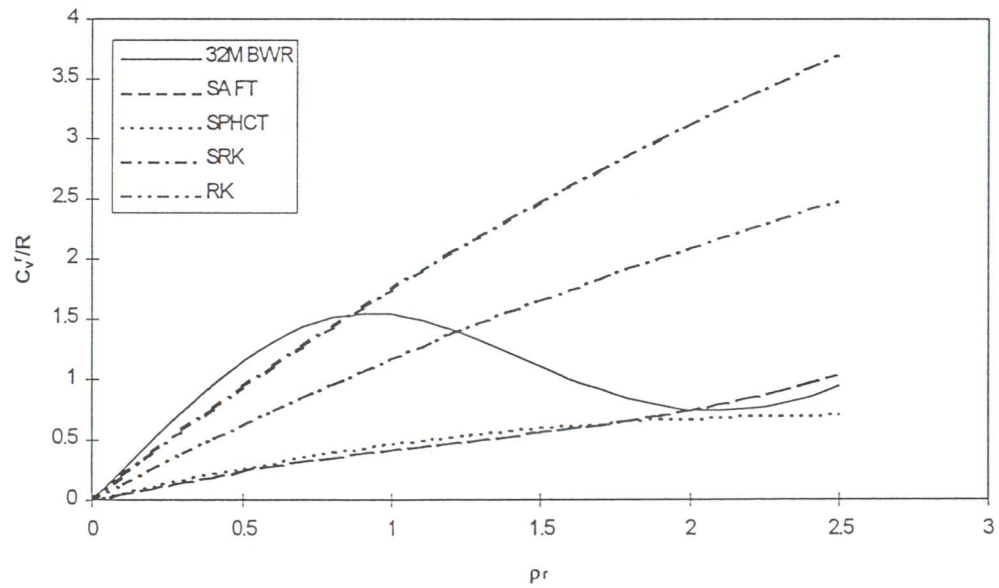

Figure 3.3 C_v^r/R n-butane with model equations

By examining Figure 3.3 it is evident that all the model equations are giving false values for the isochoric heat capacity for n-butane. The SAFT equation gave a good representation of the isochoric heat capacity for methane, but fails to give even qualitatively correct values for n-butane. This indicates that the equation is not able to handle the chainlike behavior of molecules, even though it works for molecules that can be approximated as hard spheres. The constants in the equation are fitted to energy

and PVT data for argon. According to the principle of corresponding states, transformation by critical parameters would give a good representation of the thermodynamic properties for small spherical non - polar molecules.

3.3.2. The isobaric heat capacity

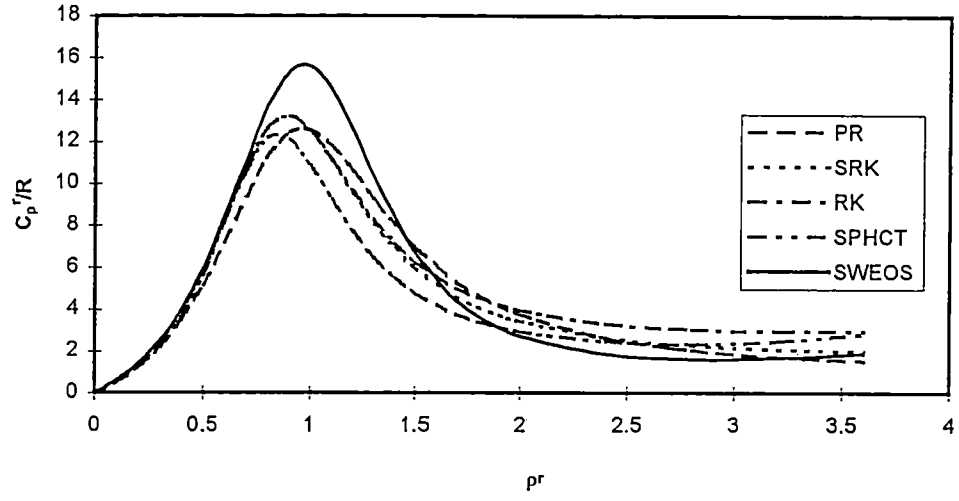

Figure 3.4 C_p^r/R **methane with model equations at** $T_r = 1.1$

All the model equations give a maximum in the isobaric heat capacity (Figure 3.4), but only the SPHCT equation is gives a minimum. Up to approximately a reduced density of 0.7 all model equations but the PR EOS gives correct values for the C_p. At near critical densities the equations underestimates the isobaric heat capacity.

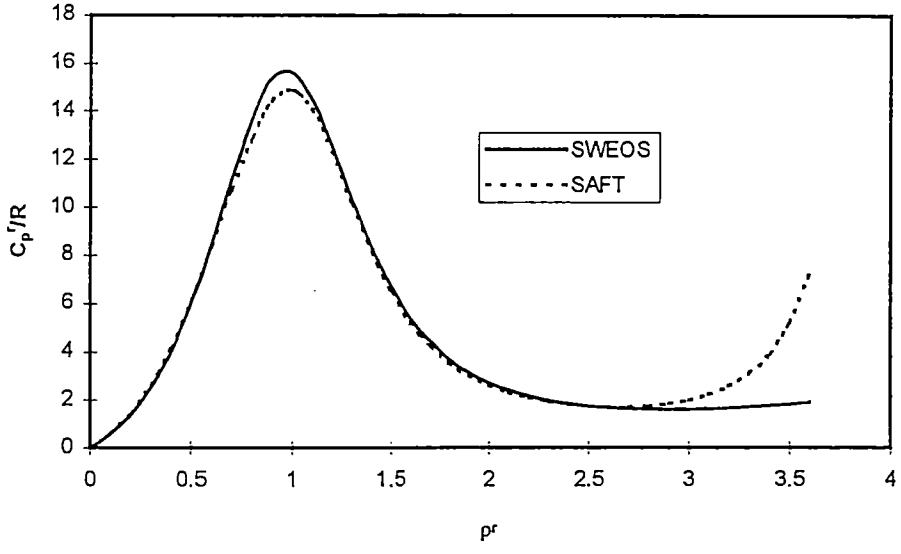

Figure 3.5 C_p^r/R **methane with the SAFT equation at** $T_r = 1.1$

As seen from Figure 3.5 the SAFT equation gives an excellent representation of the isobaric heat capacity. Its overestimation of the isobaric heat capacity at high densities is probably due to the divergence of the CS repulsion term.

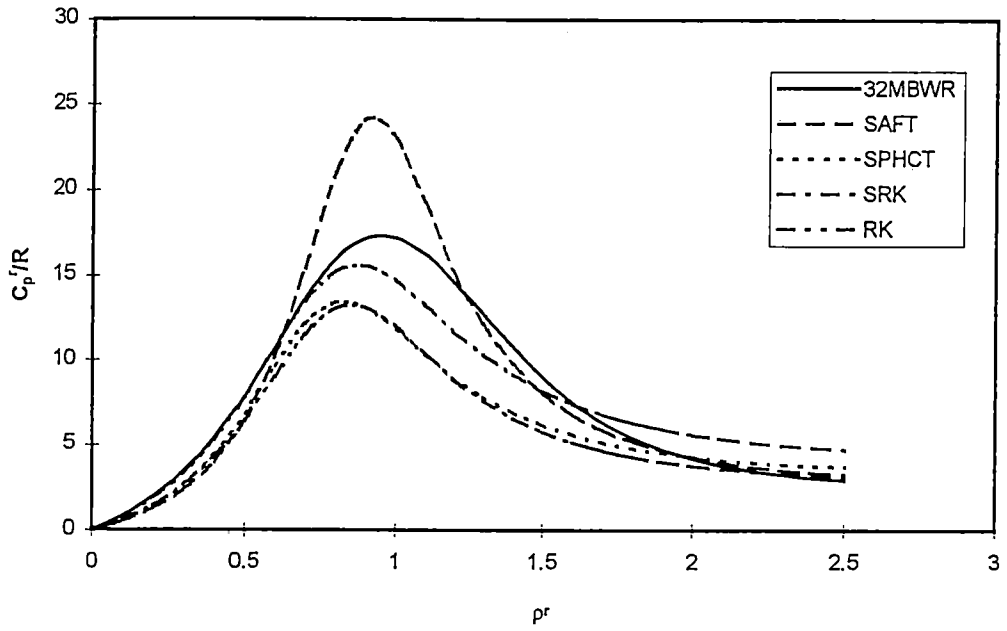

Figure 3.6 C_p^r/R n-butane with model equations

For n-butane Figure 3.6 shows that the SAFT equation is not able to give results with the same quality as it did for methane. The other equations are not very accurate since only the SRK equation is correct up to a reduced density of 0.7.

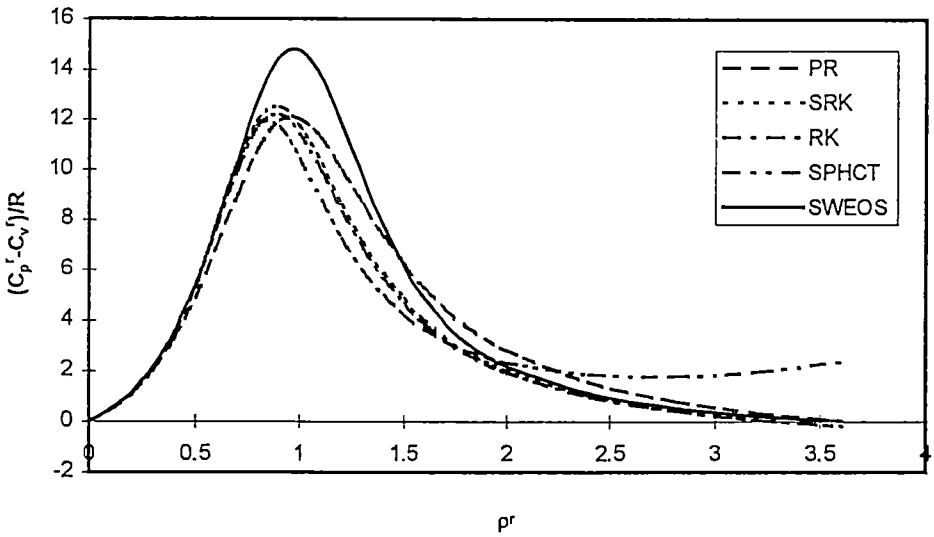

Figure 3.7 $(C_p^r-C_v^r)/R$ methane with model equations at $T_r = 1.1$

In Figure 3.7 the contribution of the isochoric heat capacity is subtracted from the isobaric heat capacity to show equation of state contributions to any deviations. This is done in order to identify the origin of the deviations in the isobaric heat capacity. Because of the relative low value of the isochoric heat capacity the deviations are in the same order as those seen for the isobaric heat capacity.

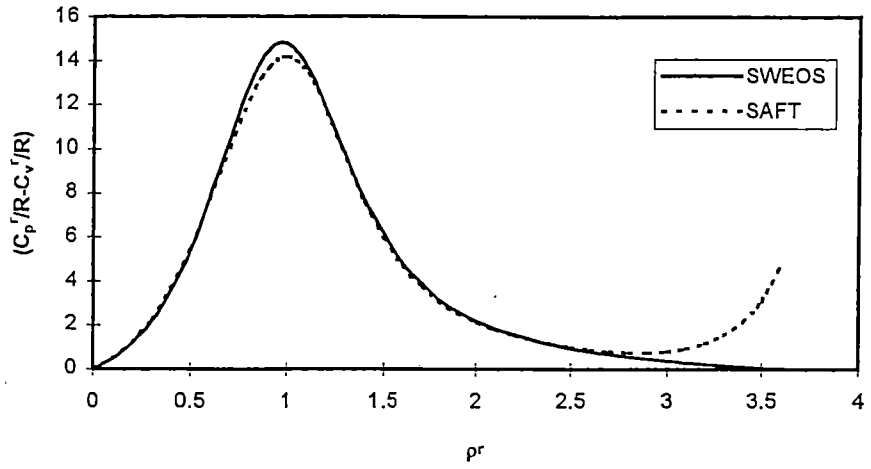

Figure 3.8 $(C_p^r-C_v^r)/R$ methane with the SAFT equation at $T_r = 1.1$

In Figure 3.8 the difference in the residual heat capacities for methane with the SAFT equation is analyzed. As before the SAFT equation gives good results.

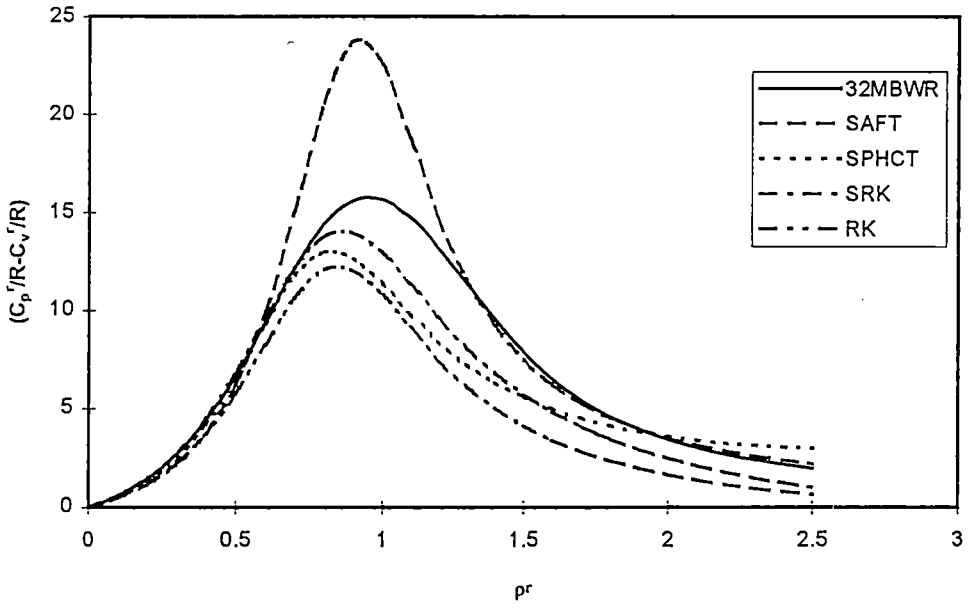

Figure 3.9 $(C_p^r/R-C_v^r/R)$ n-butane with model equations

In Figure 3.9 the difference in the residual heat capacity for n - butane is plotted. Figure 3.9 suggest that the most important deviation in the isobaric heat capacity stems from the contribution of the equation of state term heat capacity.

3.3.3. The reduced bulk modulus

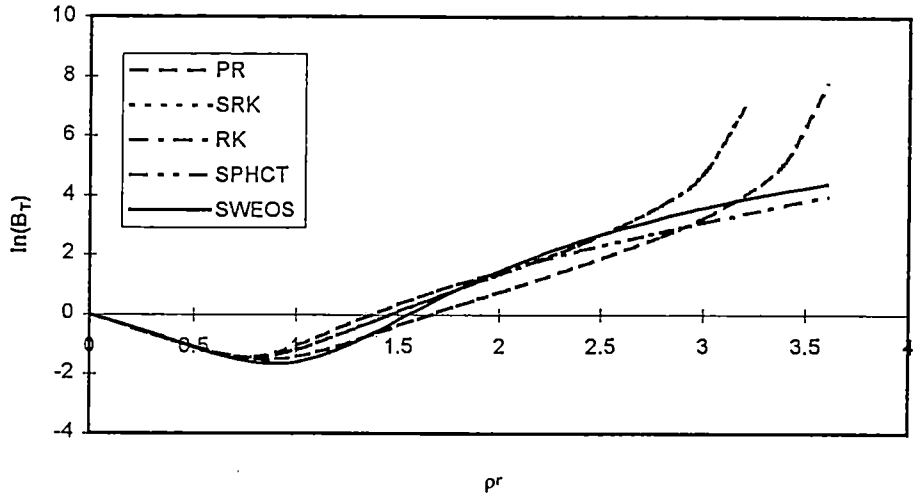

Figure 3.10 Reduced bulk modulus of methane with model equations at $T_r = 1.1$

In Figure 3.10 the reduced bulk modulus for the model equations are plotted. At low densities all the model equations gives reasonable results. All the cubic equations diverge at high densities. This is a result of the singularity in the van der Waals repulsion term. The model equations give a minimum in the reduced bulk modulus at a too low reduced density. The failure of the model equations to give correct critical densities probably contributes to this effect. The PR equation is closest to giving a good prediction of the minimum.

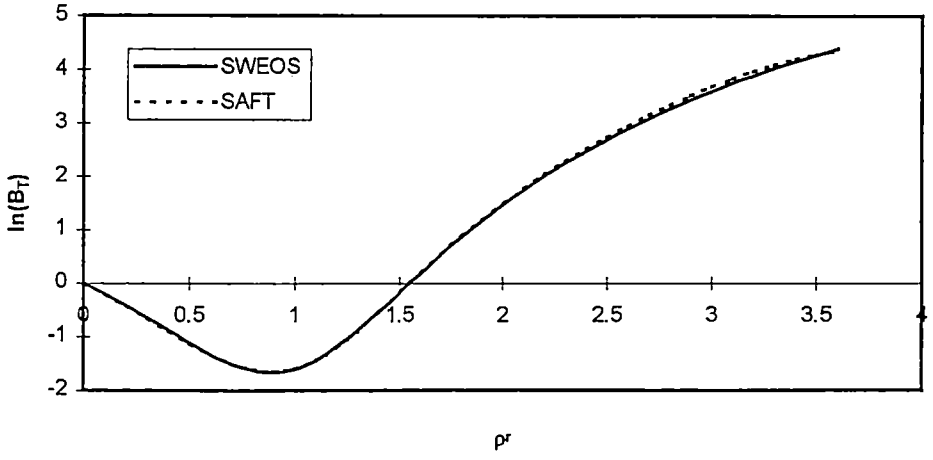

Figure 3.11 Reduced bulk modulus of methane with the SAFT equation at $T_r = 1.1$

In Figure 3.11 the reduced bulk modulus for methane with the SAFT equation is plotted. As expected from earlier discussion, the results from the SAFT equation are excellent.

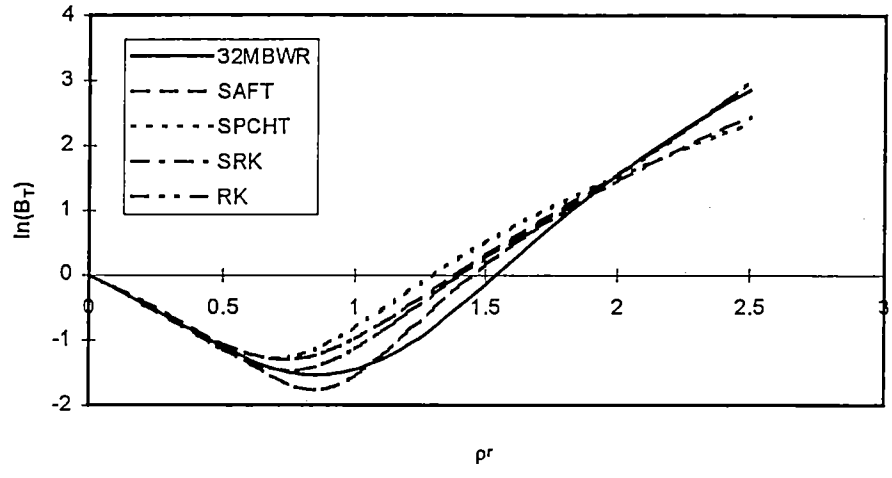

Figure 3.12 The reduced bulk modulus n-butane at $T_r = 1.1$

For n-butane all the model equations also give reasonable results at low densities (Figure 3.12). The SAFT equation is gives a minimum closest to the real density, but its value is too low. Considering that this is a logarithmic plot the deviation is expected to result in a overestimation of the C_p.

3.3.4. The Joule - Thomson coefficient

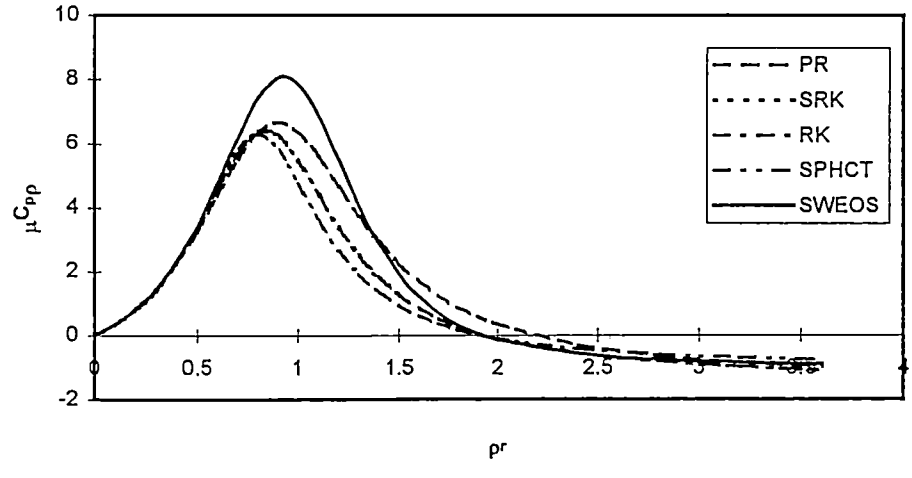

Figure 3.13 The Joule – Tomson coefficient methane with model equations at $T_r = 1.1$

All but the PR EOS give qualitatively good estimates ofr the Joule - Thomson coefficient (Figure 3.13). It is interesting to see that only the PR EOS fails to give a good estimation of the Joule - Thomson inversion point.

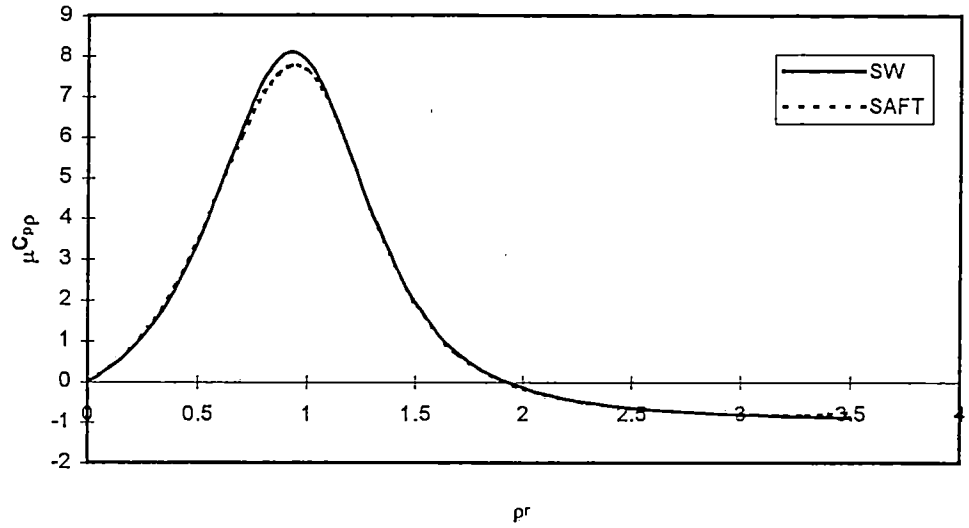

Figure 3.14 The Joule - Thomson coefficient methane with the SAFT equation at Tr = 1.1

As for the other derived properties, the SAFT equation is gives excellent predictions of the Joule - Thomson coefficient for methane (Figure 3.14).

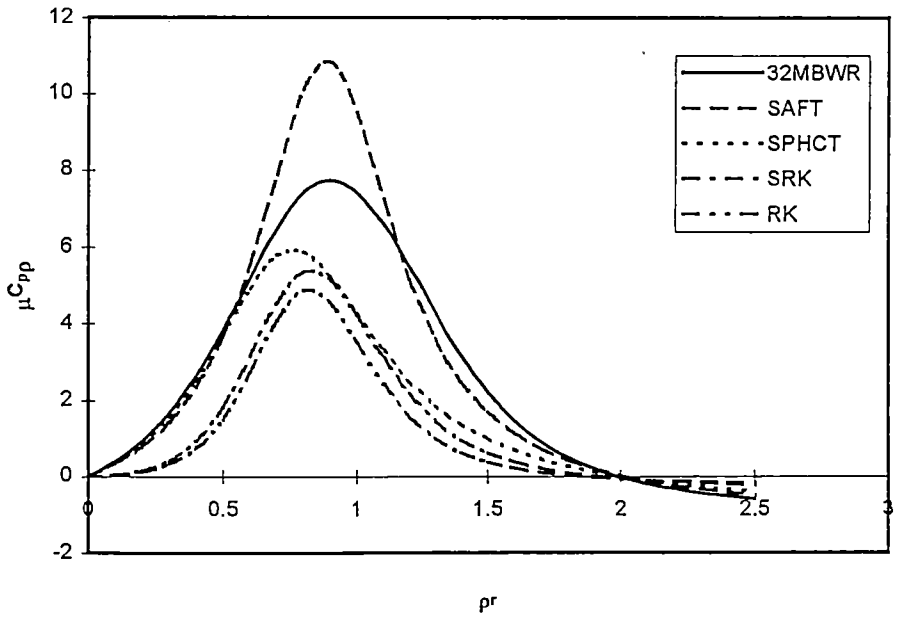

Figure 3.15 Joule - Thomson coefficient for n-butane with model equations at Tr = 1.1

Unlike the rest of the derived properties where all models gave good approximations at low densities, for the Joule Thomson coefficient for n-butane the cubic equations are not accurate at low density. (Figure 3.15) Further, the SAFT and SPHCT equations miss the maximum.

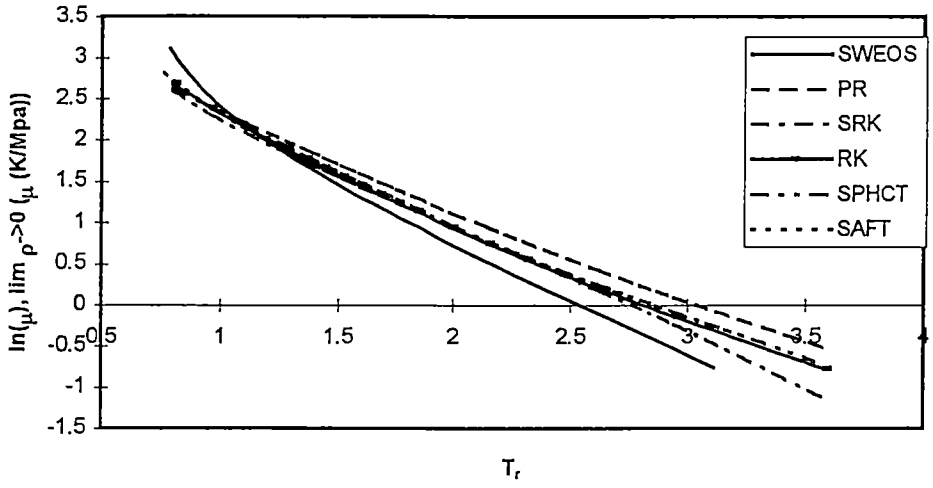

Figure 3.16 Joule - Thomson coefficient methane with model equations at zero density

In Figure 3.16 the Joule – Thomson coefficient at zero density for methane for some model equations of state is plotted. The value of the Joule - Thomson coefficient at zero density is only a function of the temperature dependencies of the linear density term of an equation of state. For methane the SAFT equation gives very good values for most derived properties, but its initial Joule - Thomson coefficient overestimate the values at high reduced temperatures. The same goes for all the other models. This indicates that the temperature dependencies of all the equations is wrong. The real behavior of this quantity, as given by the SWEOS, is interesting. At temperatures above the critical the curve is approximates a straight line. At temperatures below the critical there is a curvature.

3.3.5. Contributions to the isochoric heat capacity from the SAFT EOS

The SAFT equation is the only equation that can be analyzed for different contributions to the isochoric heat capacity. When deriving the isochoric heat capacity from all the other model equation the only term left is the contribution from the attraction term. However, because of the temperature dependence of the volume parameter in the SAFT equation, all of the terms in the equation give contributions to the isochoric heat capacity.

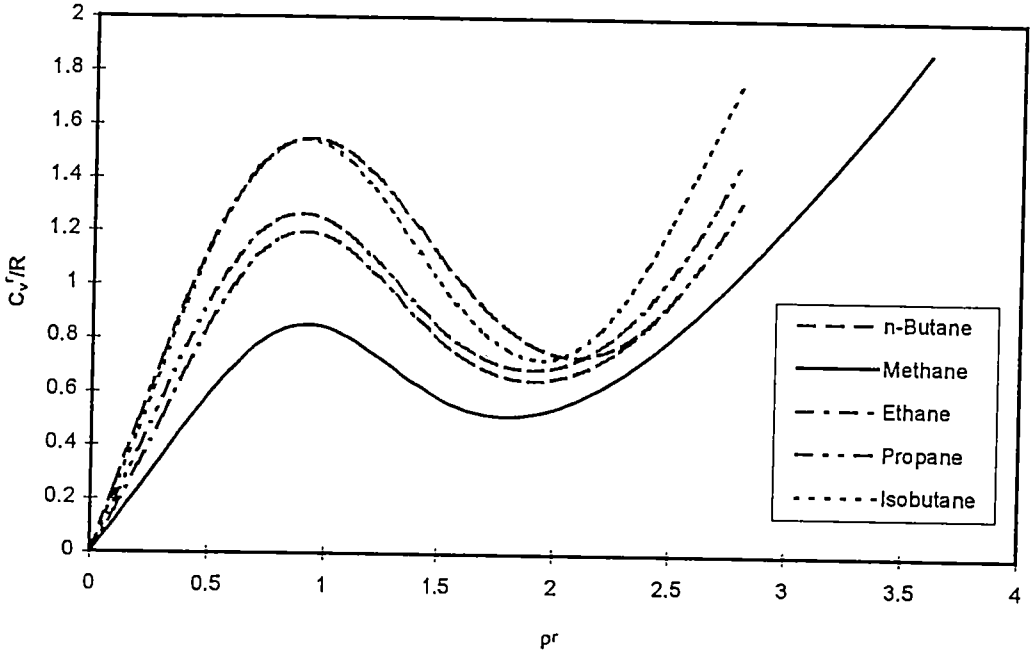

Figure 3.17 Residual isochoric heat capacities for alkanes at $T_r = 1.1$

In Figure 3.17 the residual isochoric heat capacity for the lower alkanes are plotted. This is done in order to get an idea of the trends as the chain length increases. In general, the isochoric heat capacity increases with increasing chain length. This is logical because the number of degrees of freedom increases with chain length. With higher degrees of freedom a molecule is able to absorb more heat. Note that at low densities the isochoric heat capacity can be approximated by a straight line.

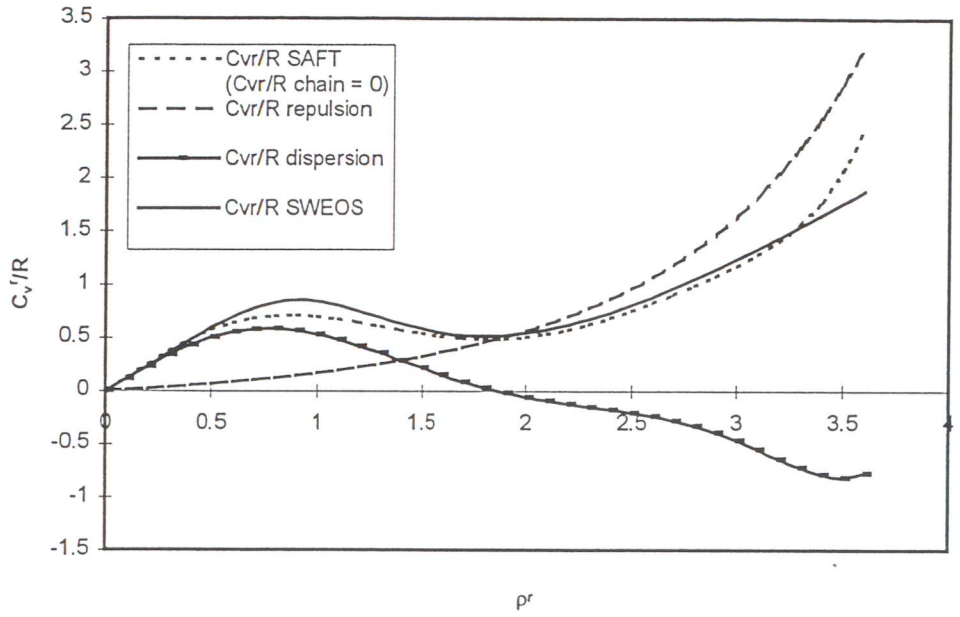

Figure 3.18 Individual contributions to the residual isochoric heat capacity from the SAFT EOS for methane at $T_r = 1.1$

In Figure 3.18 the different contributions to the isochoric heat capacity from the SAFT EOS for methane are plotted. In the case of methane there is no chain term. The maximum in the isochoric heat capacity is a result of the dispersion term. The initial slope of the heat capacity is primary dictated by the dispersion term while the minimum is where repulsion begins to dominate.

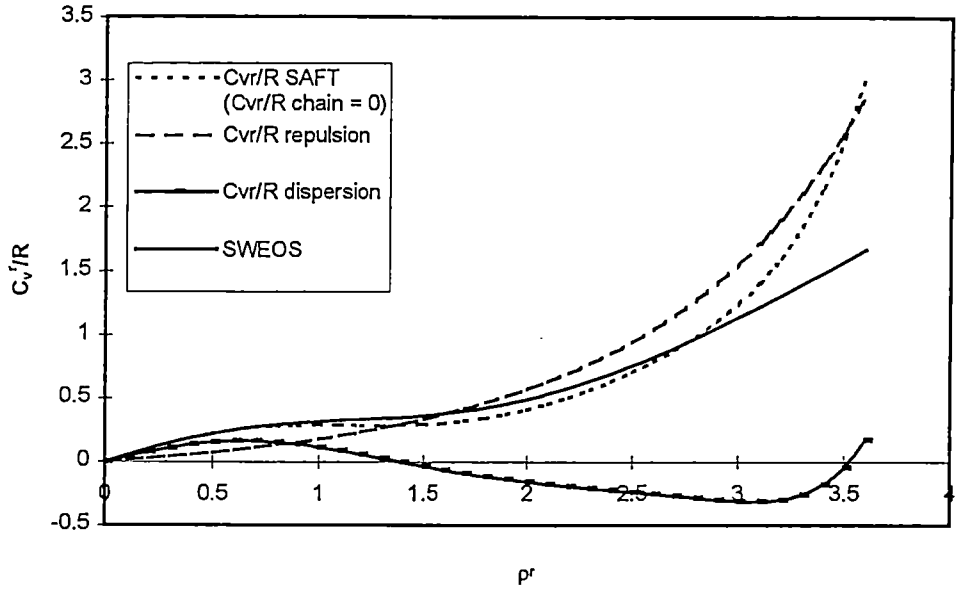

Figure 3.19 Individual contributions to the residual isochoric heat capacity from the SAFT EOS for methane at $T_r = 1.5$

In Figure 3.19 the same quantities as in Figure 3.18 are plotted, but at a higher reduced temperature. There is no maximum in the curve. At this high temperature the SAFT equation gives excellent predictions of the isochoric heat capacity for methane except at the highest densities.

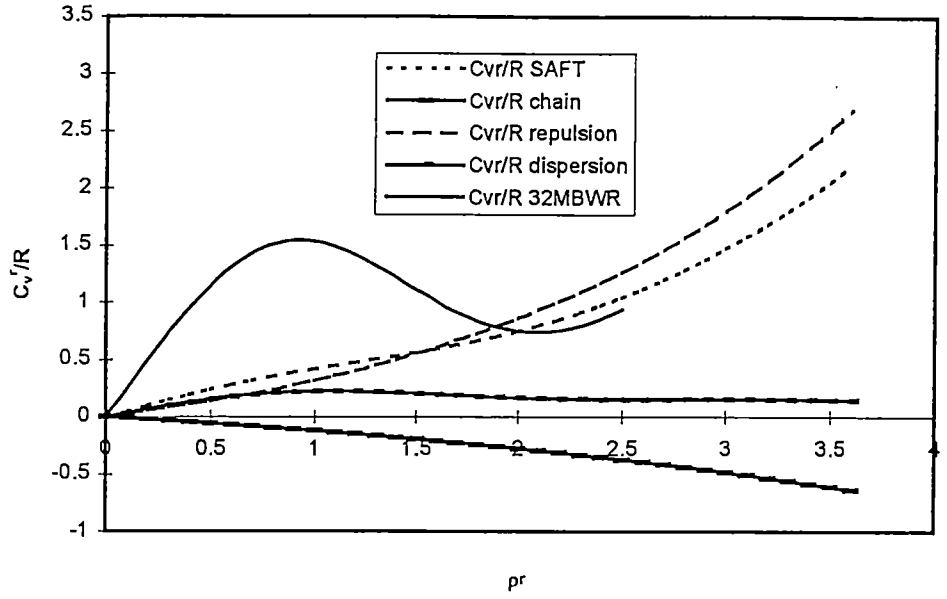

Figure 3.20 Individual contributions to the residual isochoric heat capacity with the SAFT EOS for n-butane at $T_r = 1.1$

In Figure 3.20 the individual contributions to the isochoric heat capacity for n-butane is plotted. The chain term is negative over the whole density range. The isochoric heat capacity increases with chainlength (Figure 3.17). Based on that knowledge the chainterm should be positive. However, the failure could also be a result of a wrongly behaving dispersion term. The maximum caused by the dispersion term in the case of methane is absent. In the case of methane the dispersion term has negative values at high densities. This is not the case for n-butane. If the corresponding states principle had been used there would have been a maximum in the dispersion term. The reducing parameters in the SAFT dispersion term are :

u/k : reducing temperature
$1/mv^0$: reducing density

If the corresponding states principle is valid the fraction of the critical temperature to the reducing temperature for both fluid would be approximately the same. The same would be valid for the densities. Those fractions are at this temperature :

Methane : $T_c/(u/k) = 0.96$ $\rho_c * mv^0 = 0.21$
n-Butane : $T_c/(u/k) = 2.13$ $\rho_c * mv^0 = 0.17$

The reason there is no maximum in the isochoric heat capacity for methane is that the reducing parameter for the temperature is far from its corresponding states value. The reducing parameters for the density are closer to obeying the corresponding states principle.

3.3.6. Contributions to the reduced bulk modulus from the SAFT EOS

Just as the case is with the isochoric heat capacity the reduced bulk modulus can be analyzed with regard to the contributions from the different terms in the equation of state. In the case of no associating molecules the reduced bulk modulus from the SAFT equation can be written as :

$$B_T - 1 = \left(Z + \rho \left(\frac{dZ}{d\rho} \right)_T \right)^{hs} + \left(Z + \rho \left(\frac{dZ}{d\rho} \right)_T \right)^{disp} + \left(Z + \rho \left(\frac{dZ}{d\rho} \right)_T \right)^{chain} \qquad (3.6)$$

In this paragraph the different contributions to the variable (B_T-1) and their sum are evaluated. The symbol SAFT, SWEOS, and 32MBWR denotes the variable (B_T-1) from the respective equations of state. The factors HS, DISP, and CHAIN denote the individual contributions to the reduced bulk modulus from the SAFT equation.

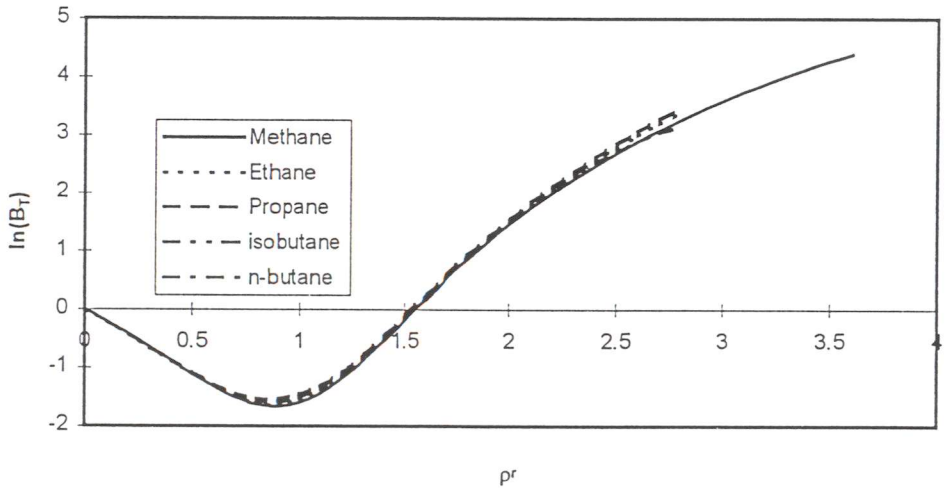

Figure 3.21 Reduced bulk modulus for the alkenes at T_r = 1.1

In Figure 3.21 the reduced bulk modulus for the lower alkanes are plotted as a function of reduced density. The variations with molecular structure are small.

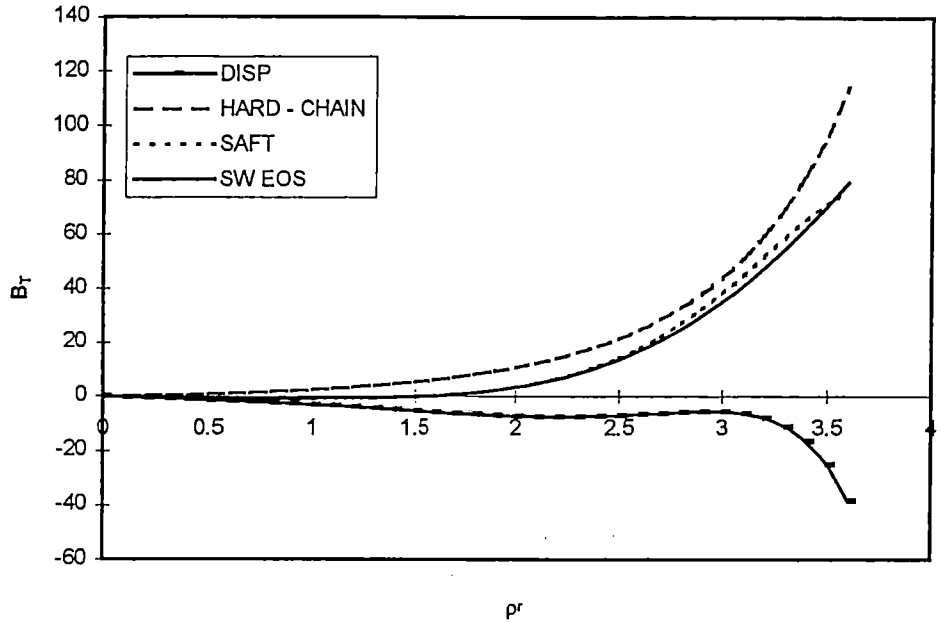

Figure 3.22 Individual contributions to the reduced bulk modulus from the SAFT EOS with methane at $T_r = 1.1$

In Figure 3.22 the contributions of the reduced bulk modulus from the individual terms in the SAFT EOS are plotted as function of reduced density for methane at a reduced temperature of 1.1. The chain term in the SAFT EOS is zero. As mentioned earlier the prediction from the SAFT EOS is good. There seem to be small deviations at high densities, though this occurs because of competing divergences.

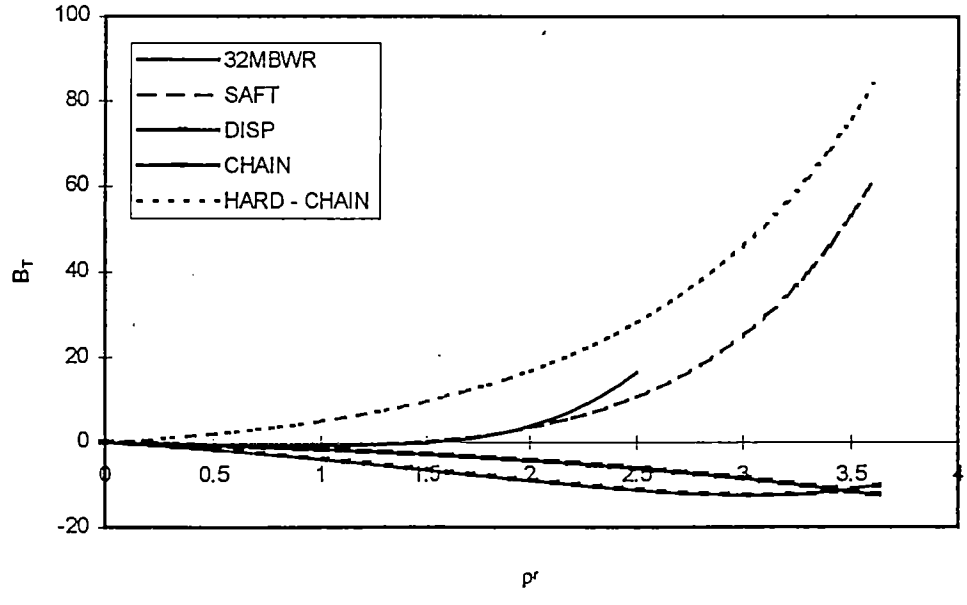

Figure 3.23 Individual contributions to the reduced bulk modulus from the SAFT EOS for n-butane at $T_r = 1.1$

In Figure 3.23 the contributions to the bulk modulus for n-butane are plotted as a function of reduced density at a reduced temperature of 1.1. The contribution from the chain term is negative. At reduced densities higher than 2 the reduced bulk modulus is underestimated.

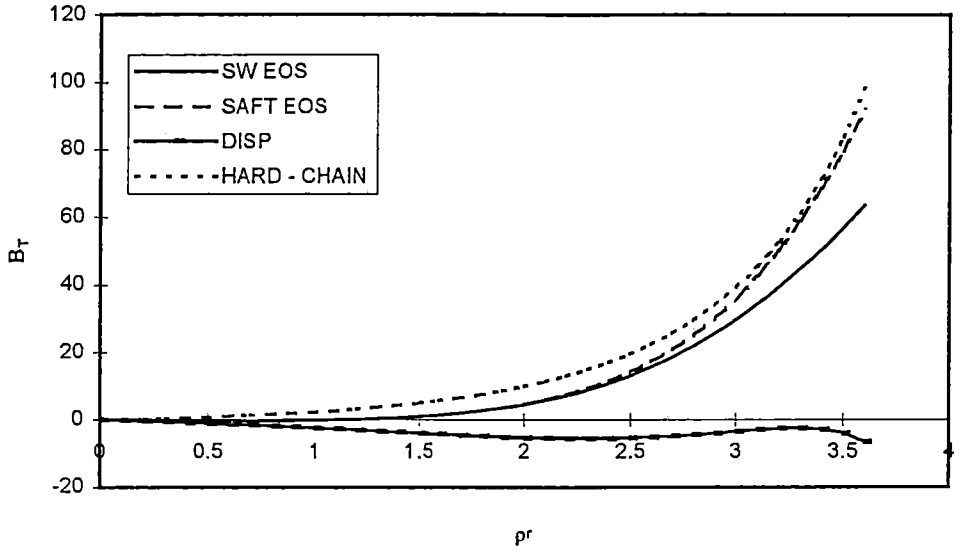

Figure 3.24 Individual contribution to the reduced bulk modulus from the SAFT EOS for methane at $T_r = 1.5$

In Figure 3.24 the different contributions to the reduced bulk modulus for methane are plotted as function of reduced density at a reduced temperature of 1.5. At reduced densities higher than 2.5 the SAFT equation overestimates the reduced bulk modulus. Thus as temperature increases the SAFT equation shows too strong a variation at fixed high densities.

3.3.7. The initial slope of the isochoric heat capacity from cubic equations

For cubic equations of state the initial slope of the isochoric heat is a function of acentric factor. In this case the relationship for the initial slope is :

$$\frac{P_c}{RT_c}\frac{dC_v^r / R}{d\rho} = \frac{T_r P_c}{R^2}\frac{d^2 a}{dT^2} \qquad (3.7)$$

For the PR and the SRK equations this quantity is a function of the acentric factor. For the RK equation this quantity is a constant. By studying the initial slopes from the multi parameter equations of state the effectiveness of the acentric factor in the supercritical region can be studied.

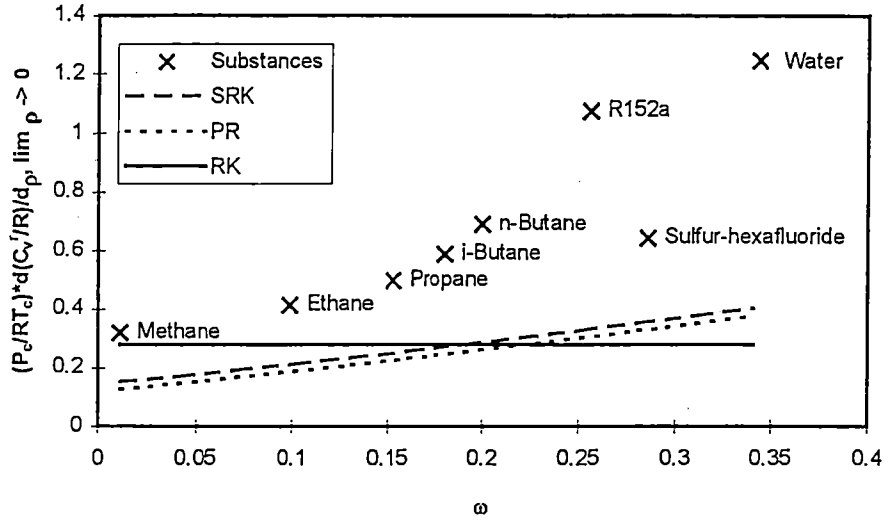

Figure 3.25 Initial slope of (C_v^r/R) as a function of acentric factor at $T_r = 1.1$

In Figure 3.25 the dimensionless initial slopes of the isochoric heat capacities resulting from the cubic equations of state are plotted against acentric factor. The PR and the SRK equations give approximately the right slope, but the wrong intercept. The RK equation give a better intercept, but is fixed with chain length.

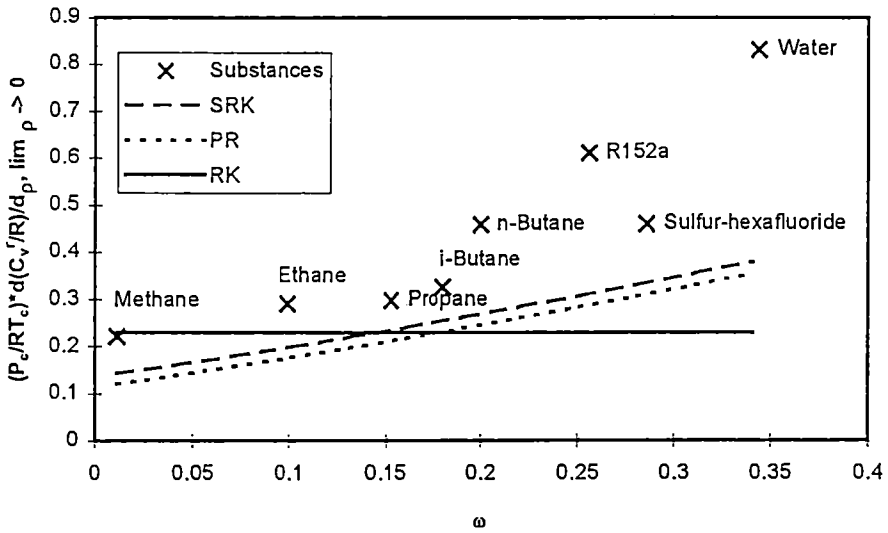

Figure 3.26 Initial slope of (C_v^r/R) as a function of acentric factor at $T_r = 1.25$

Figure 3.26 shows that this behavior is less obvious at $T_r = 1.25$ but still present.

3.4 Graphical evaluation of the equations of state for mixtures

The methane/ethane mixture is used as a reference to describe mixture behavior. The range of the 32MBWR surfaces covering ethane and methane makes evaluation possible for all mole fractions over many state points. The Peng - Robinson equations is used to calculate the derived properties from a model equation. All properties are calculated at a temperature of 330 K. All properties are dependent on the reduced mixture density. The mixture critical density is calculated with the following relationship :

$$\rho_{c,mix} = \frac{1}{\sum_i x_i / \rho_{c,i}} \qquad (3.8)$$

All binary interaction parameters both for the PR EOS and for the ECS calculations are set equal to unity. Since the focus of this study primarily has been on pure substances this paragraph will serve as a reference for future work.

3.4.1. The behavior of the isochoric heat capacity

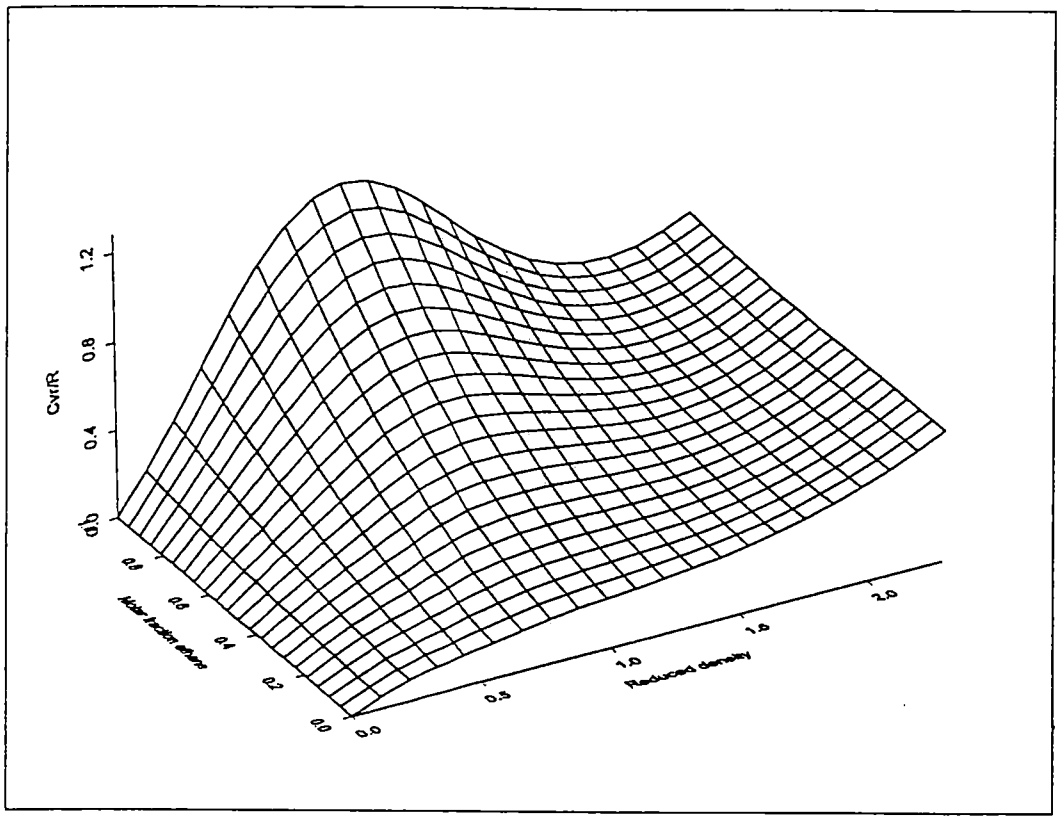

Figure 3.1 **Isochoric heat capacity with the ECS principle for methane/ethane mixtures at T = 330 K**

In the limit of pure methane non - physical behavior is calculated at low densities. This is believed to be a result of convergence problems of the theory. In Figure 3.2 this region has been plotted to give a closer look at the non - physical behavior. The value should go smoothly and uniformly to zero at zero density.

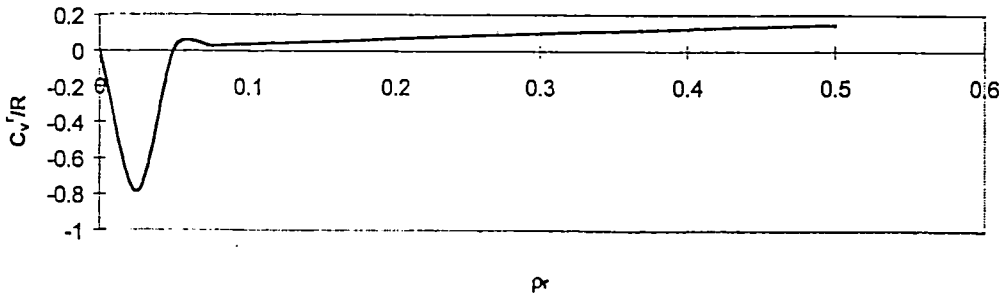

Figure 3.2 **C_v^r/R methane with the ECS principle at T = 330 K**

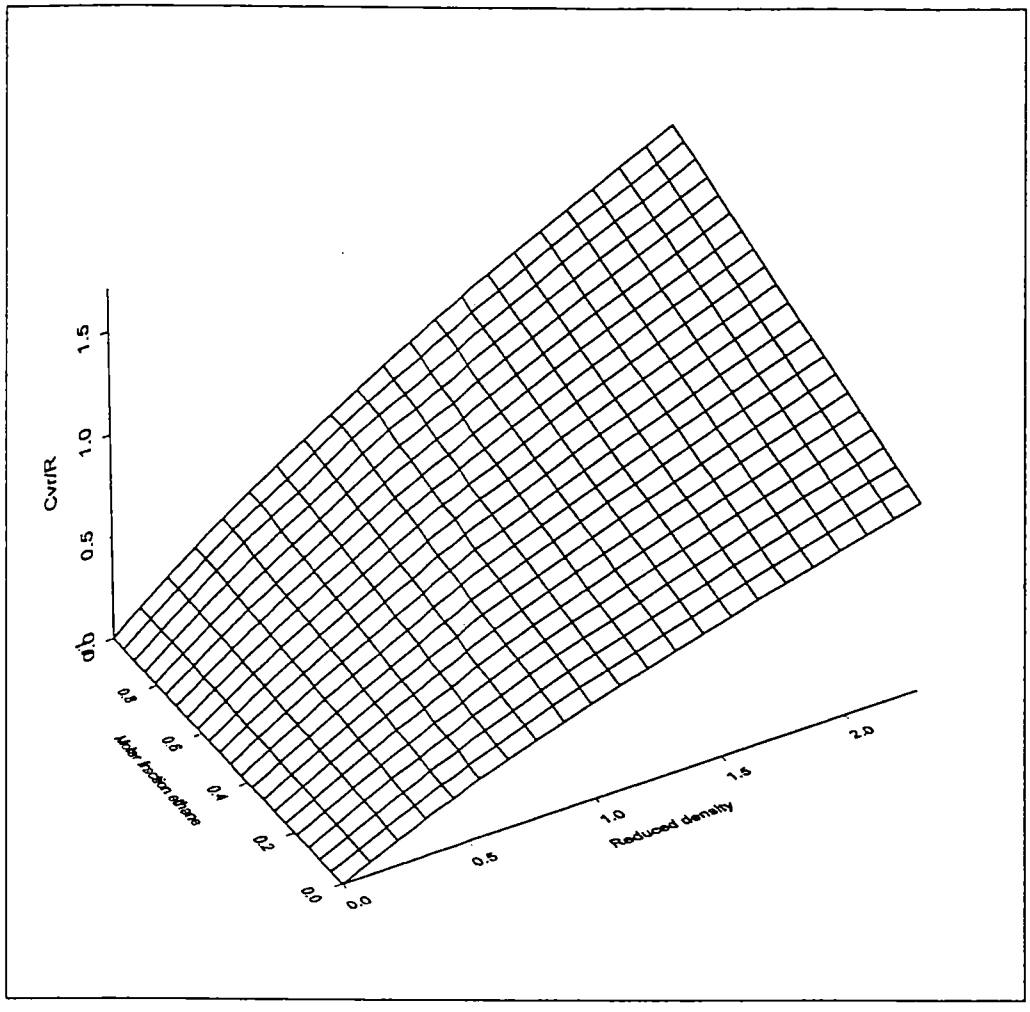

Figure 3.3 **Isochoric heat capacity for methane/ethane mixtures with PR – EOS** at T = 330 K

Because of its failure to give correct values for the isochoric heat capacities for pure substances (Figure 3.1) the Peng Robinson equation also gives wrong values in the case of mixtures. Judging from the results of the pure component, analysis all the model equations will fail to give good results for mixtures as well.

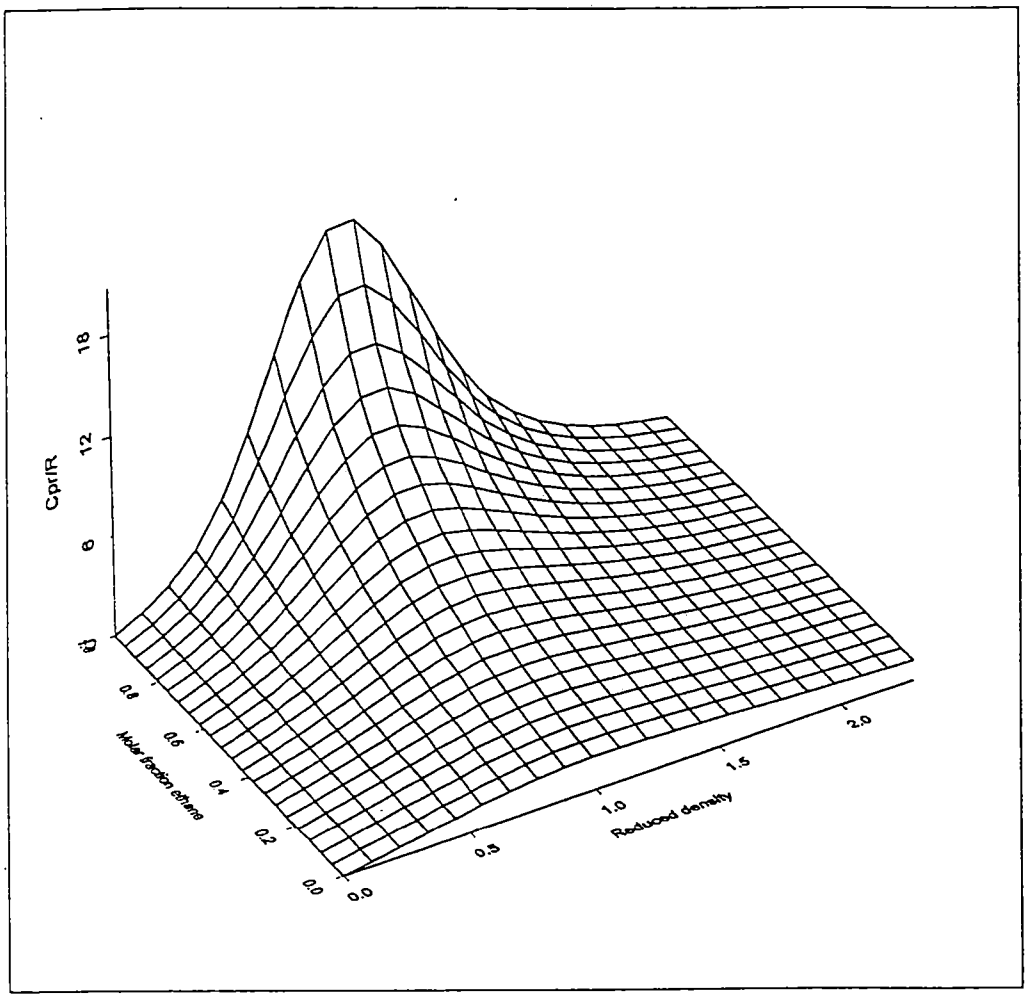

Figure 3.4 Isobaric heat capacity calculated with the ECS principle for methane/ethane mixtures at T = 330 K

In Figure 3.4 the isobaric heat capacity calculated with the ECS principle is plotted as a function of reduced density and mole fraction methane. The ECS principle predicts a smooth behavior in all directions of the surface.

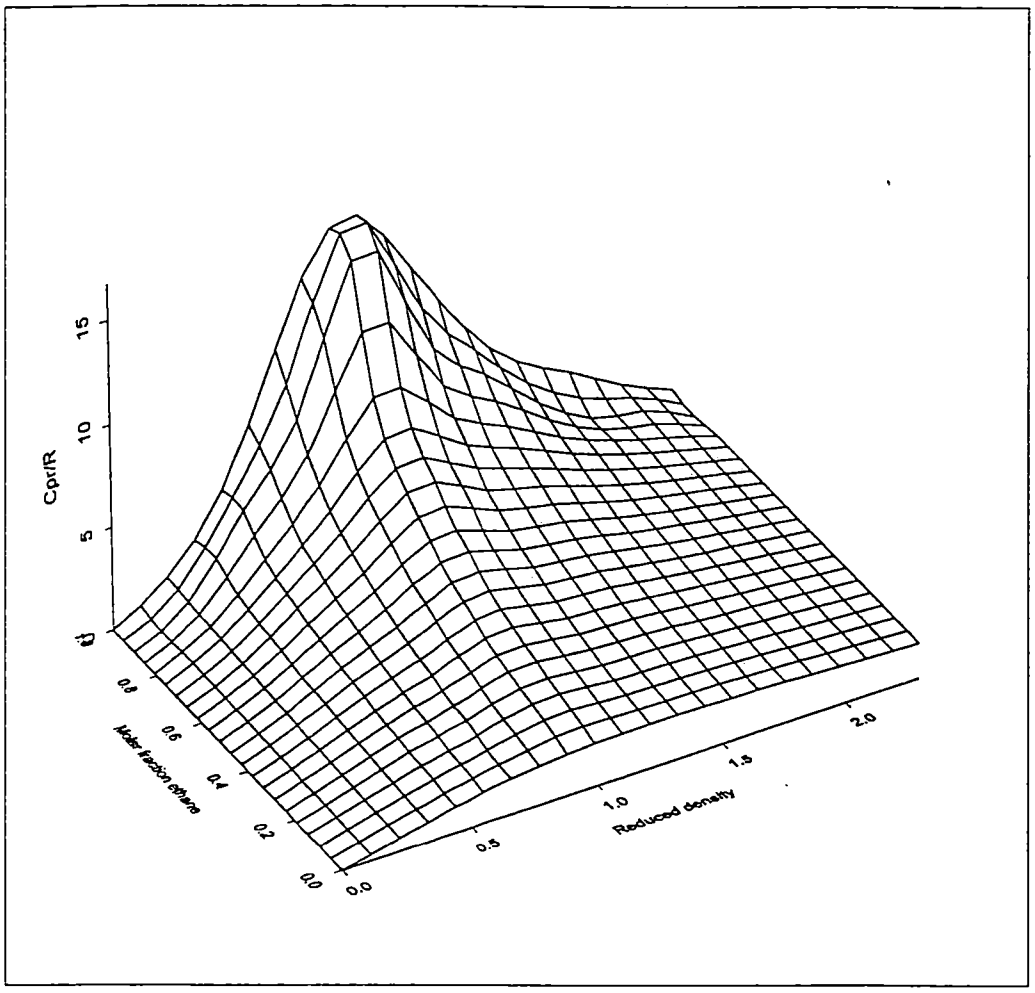

Figure 3.5 Isobaric heat capacity calculated with the PR - EOS methane/ethane mixtures at T = 300 K

The PR equation gives quantitatively correct dependencies for the isobaric heat capacity. The ECS calculation (Figure 3.4) is predicting a smooth curves all over the surface. However, it has irregular curves in the limit of pure ethane. This could also be a result of the mixing rule used for the critical density.

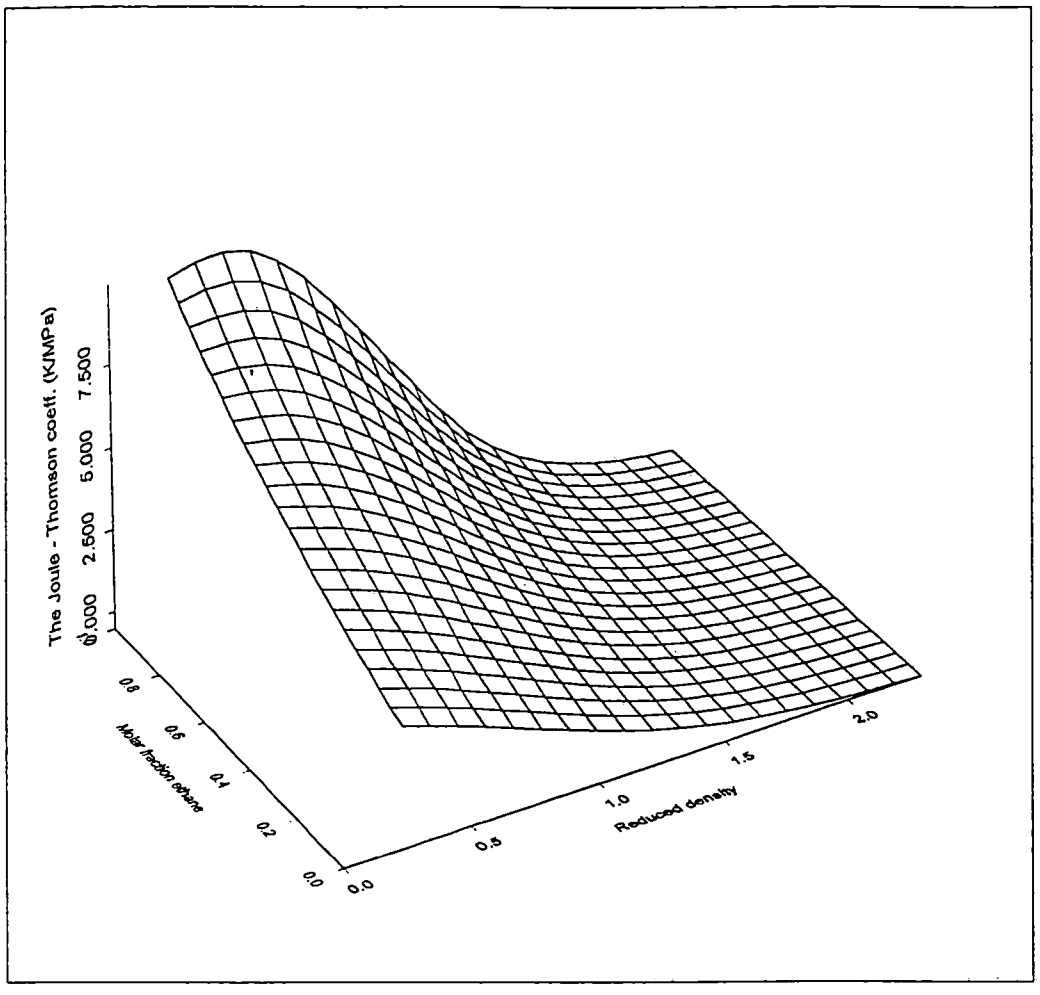

Figure 3.6 Joule - Thomson coefficient with the ECS principle for methane/ethane mixtures at T = 300 K

Figure 3.6 shows the Joule - Thomson coefficient in the reduced density range 0.23 - 2.3 from the ECS principle.

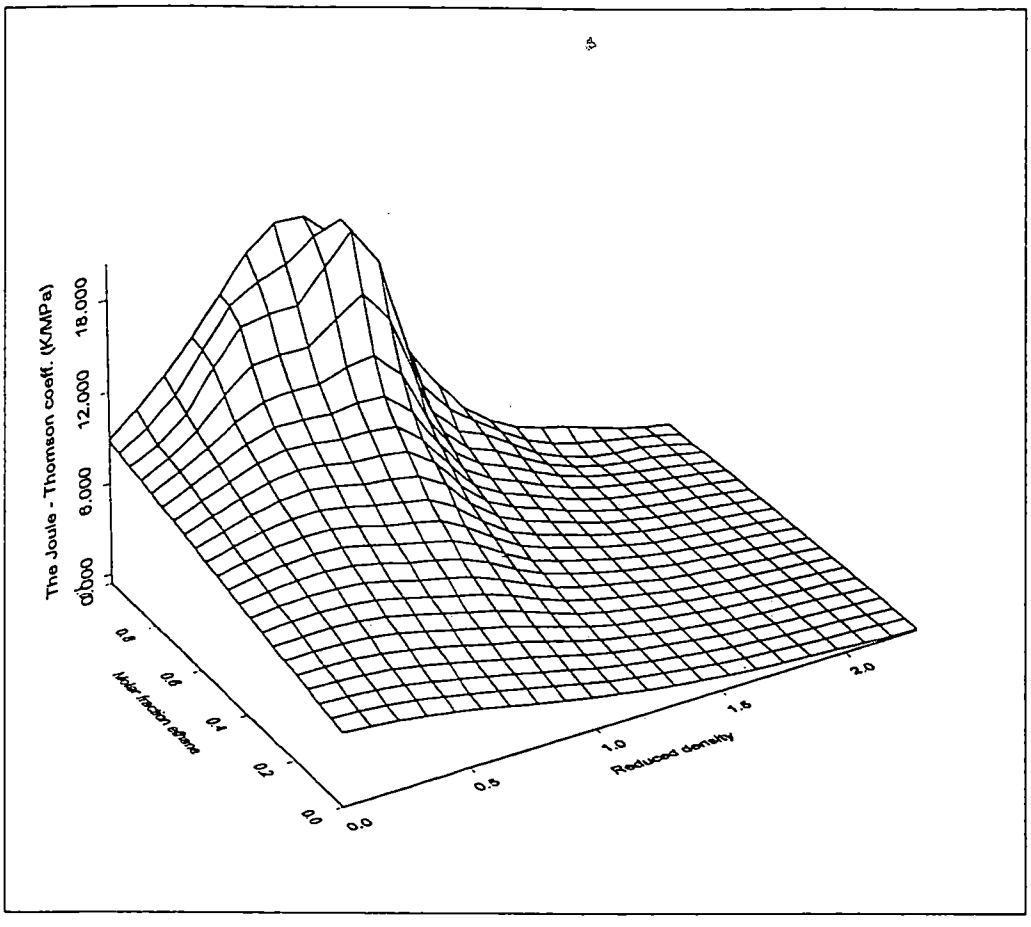

Figure 3.7 Joule - Thomson coefficient with the PR - EOS for methane/ethane mixtures at T = 300 K

Figure 3.7 shows the Joule - Thomson coefficient calculated with the PR EOS. It has irregular and non - physical behavior in almost in the entire plotted range below high mole fractions of methane.

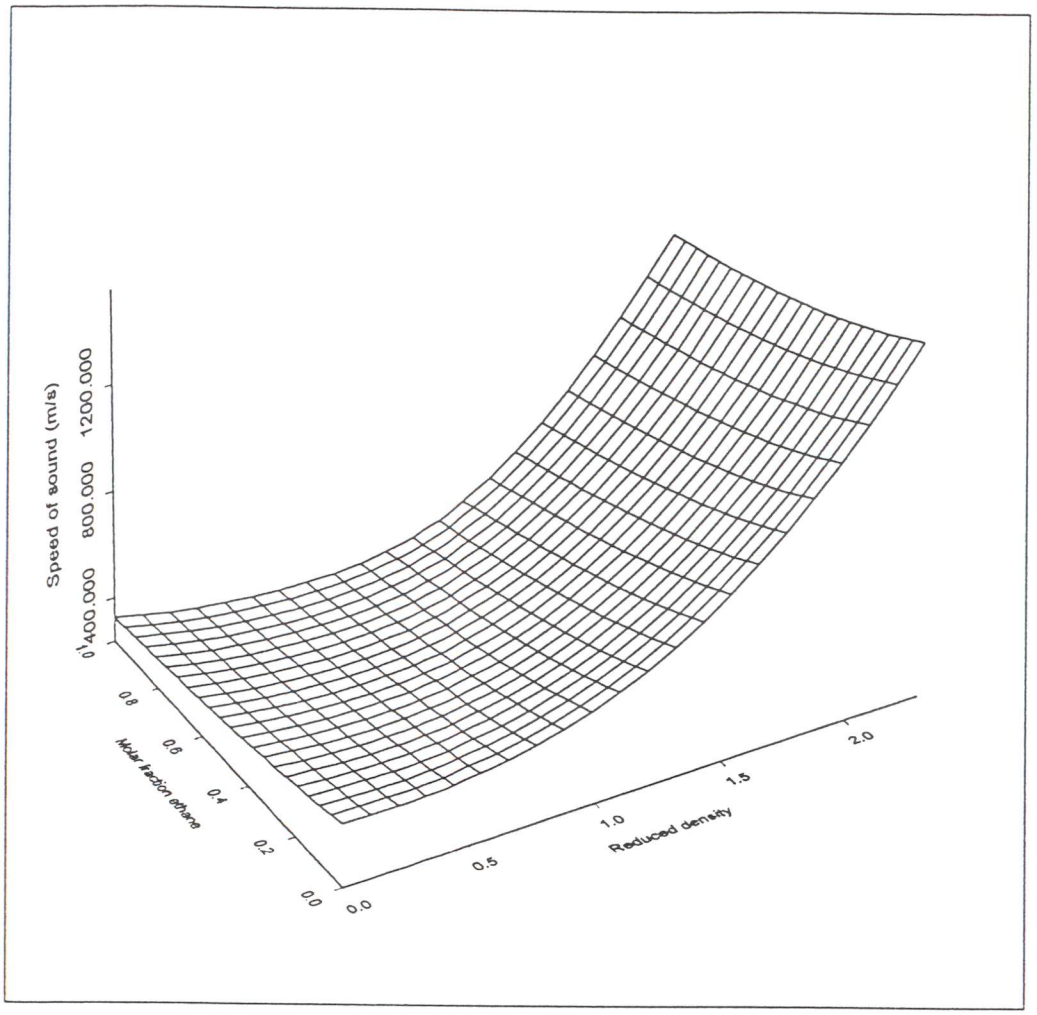

Figure 3.8 **Speed of sound from the ECS principle for methane/ethane mixtures at T = 300 K**

In Figure 3.35 the speed of sound for mixtures of methane and ethane is plotted. The speed of sound is not very dependent on mixture.

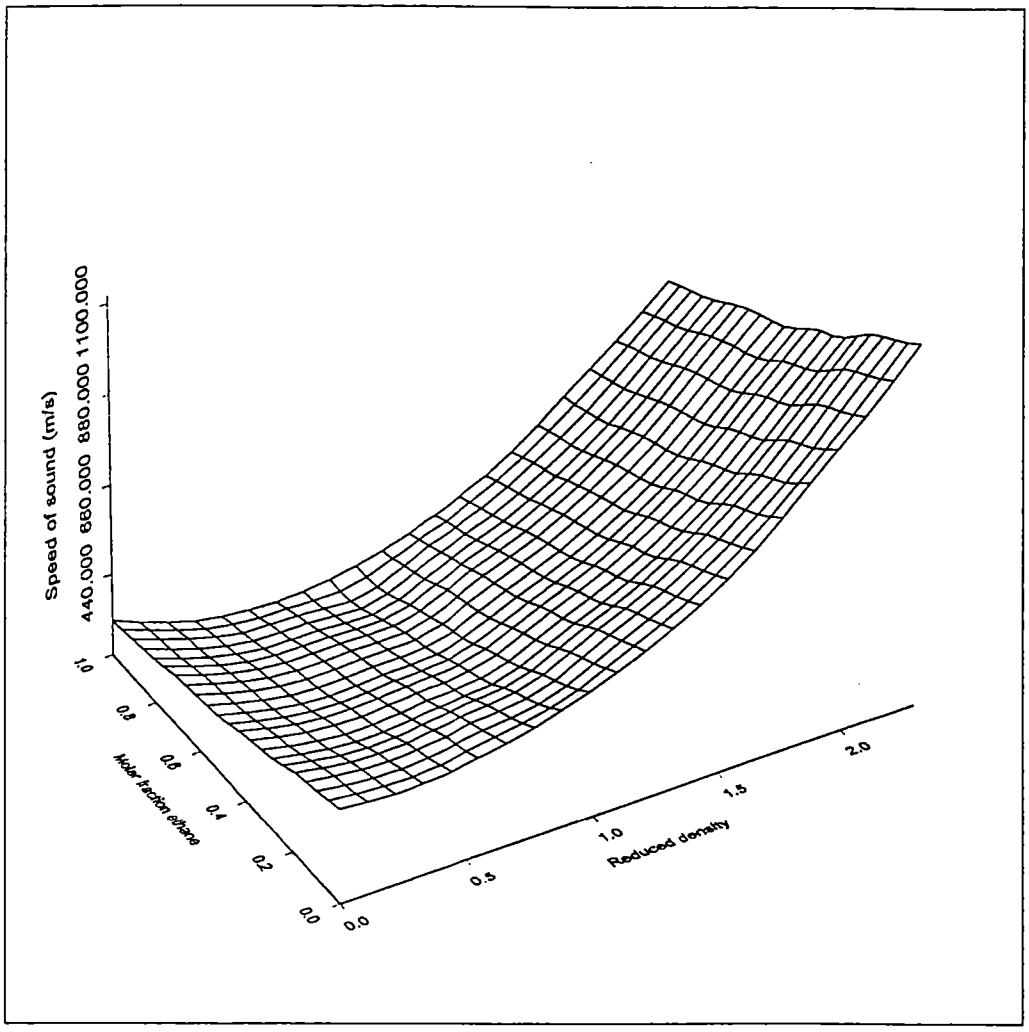

Figure 3.9 Speed of sound with the PR - EOS for methane /ethane mixtures at T = 300 K

The speed of sound for methane/ethane mixtures calculated with the PR EOS seems to give good qualitative results as shown by comparing Figures 3.35 and 3.36.

3.5. Discussion of results

The analysis of the model equations has revealed some weaknesses in their ability to describe the derivative properties for pure components. In this evaluation the substances methane and n-butane have been chosen for evaluation in order to study the ability of the equations to describe both spherical and chain - like molecules.

The residual isochoric heat capacity is poorly predicted by all the model equations, except for the SAFT equation with methane. The equations fail to give both a maximum and a minimum. The SPHCT equation gives a maximum for methane, but at too high densities. In the case of the cubic equations and the SPHCT equation the failure is partly a result of having no temperature dependence in the repulsion terms. Without any temperature dependence, the whole term disappears in the isochoric heat capacity. In the case of the SAFT equation the repulsion term is a function of temperature, so intermolecular repulsion gives a contribution to the isochoric heat capacity. By studying the SAFT equation we see that the maximum in the isochoric heat capacity for methane stems from a maximum in the attraction term. This leads us to believe that the attraction contribution in the cubic equations and the SPHCT equation must be modified to give a maximum in order to improve the estimations of the isochoric heat capacity. Another interesting result of the analysis is the failure of the SAFT equation to give a correct isochoric heat capacity for n-butane. The attraction term behaves different from methane. According to the principle of the corresponding states the attraction term should have approximately the same behavior, but the characteristic temperature for the SAFT model does not vary with molecular size.

The isobaric heat capacity is qualitatively correct from all equations and substances, though the cubic equations do not give minima in the isobaric heat capacity. Again the prediction from the SAFT equation for methane is excellent, but its prediction for n-butane is too high at densities close to the critical. All other equations are underestimate the isobaric heat capacity at the critical density.

The reduced bulk modulus is predicted qualitatively correct for both methane and n-butane with all the equations. The SAFT equation gives the best predictions, especially for methane.

The Joule - Thomson coefficient is well predicted from all the equations for methane, though the PR equation fails to give the correct inversion point. The cubic equations do not yield good predictions for n-butane. In all cases the initial slope of the curve is far to low.

For the cubic equations the initial slope of the residual isochoric heat capacity was studied as a function of acentric factor. It is expected to be roughly a linear function of acentric factor for the lower alkanes The SRK and the PR equation, do yield appropriate slopes but the intercepts are too low. The RK equation has a better intercept, but its initial slope is not a function of acentric factor.

4. General behavior

4.1. Introduction

In order to reduce the number of unknown parameters in a equation of state, it is useful to make use of behavior that are common to classes of substances. An example of this is using mathematical constraints valid at the critical point in order to connect the parameters of the cubic equations to critical temperature and pressure. Here we use variables of temperature and density reduced by their critical values to explore similarities and differences among substances and states.

4.2. Comparisons of extreme points

In this paragraph the extreme points of the different derivative properties and the Joule - Thomson inversion curve for water and ethane are compared to the same quantities for methane. This is similar to the work of Grogorowicz et al.[26]

4.2.1. Extrema water and methane

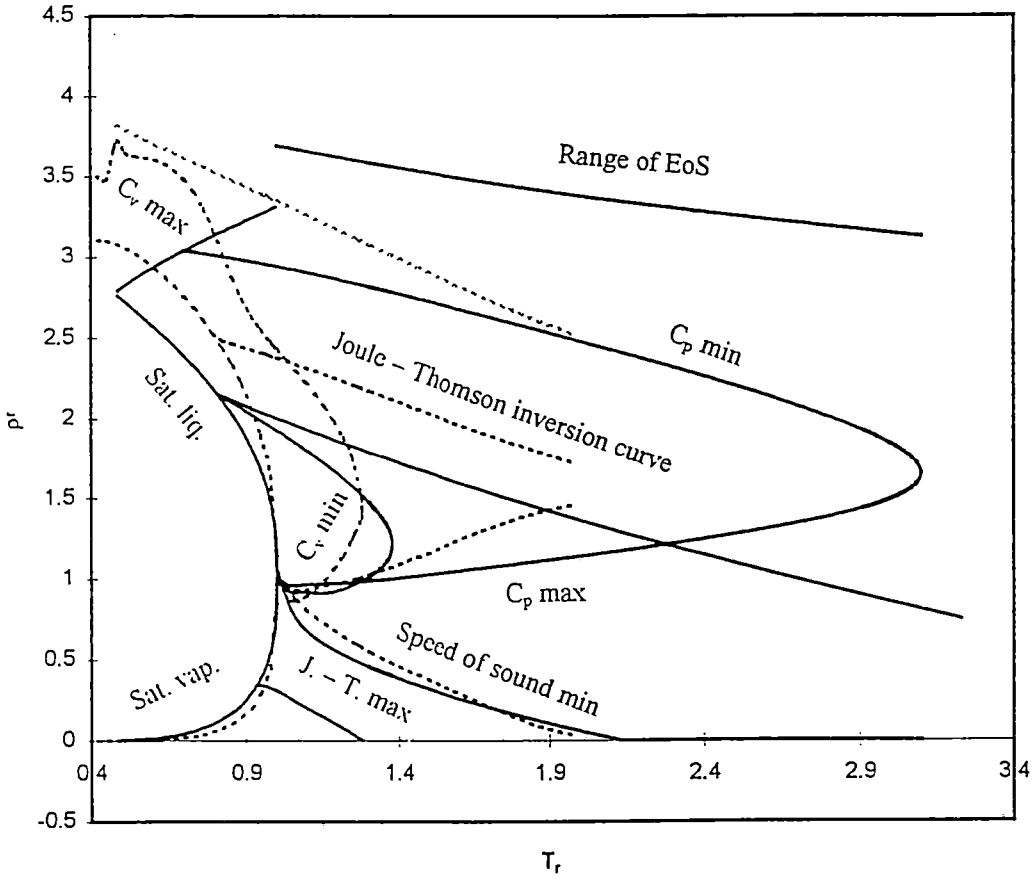

Extrema methane, -- Extrema water

Figure 4.1 Extrema water and methane

In Figure 4.1 we see that the behavior of water is differs from the behavior of methane, especially in the liquid region. This is expected because water is a self associating compound and methane is not. Major differences are associated with the C_v and C_p extrema. Water does not have a minimum in the C_p. The C_v is not entering the saturated liquid curve.

4.2.2. Extrema ethane and methane

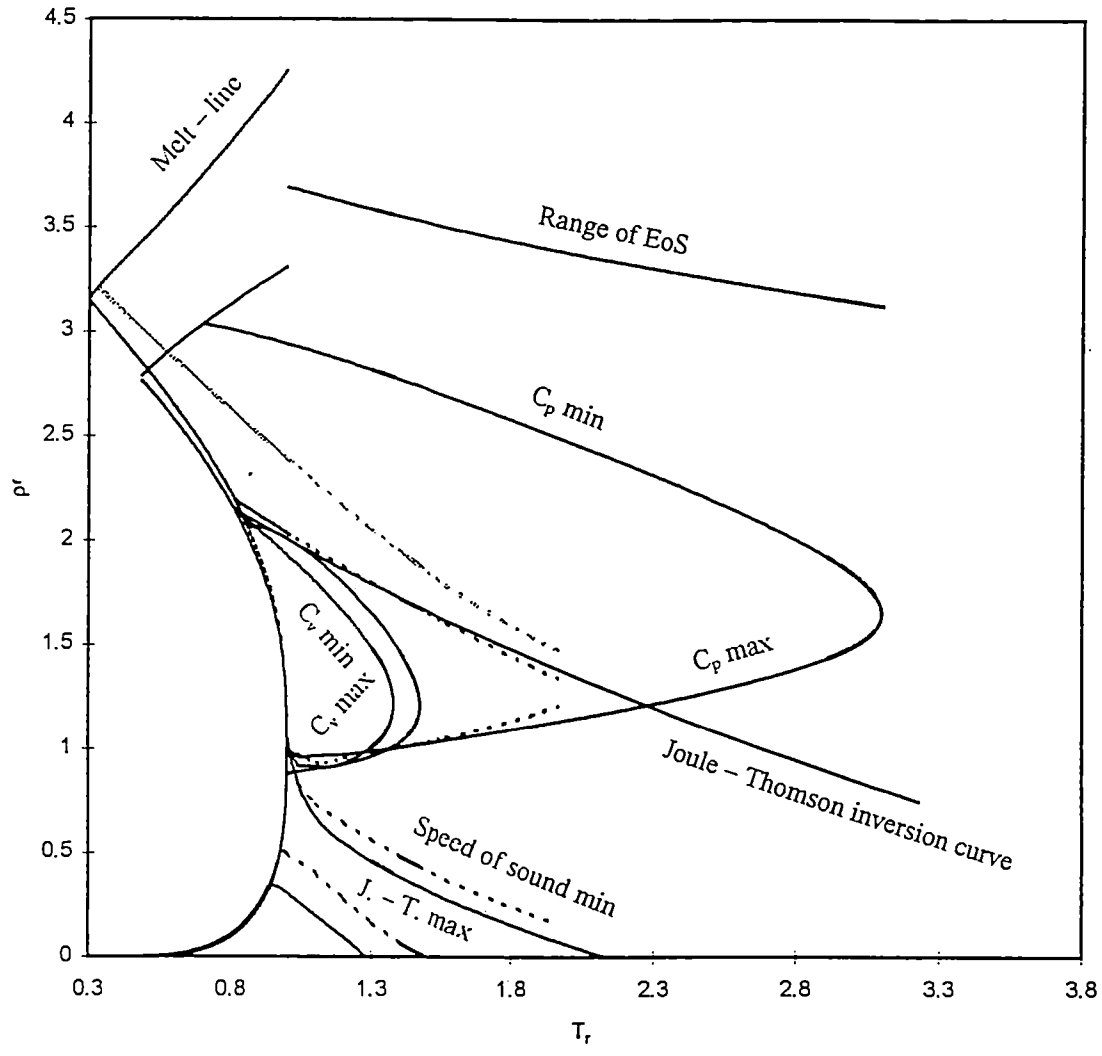

— Extrema methane, -- Extrema ethane

Figure 4.2 Extreme points ethane and methane

In Figure 4.2 the extreme points and the Joule - Thomson inversion curve for ethane are compared to the same properties for methane. Both components are approximately spherical and should have a similar behavior when the properties are plotted in reduced coordinates. However there are differences, mainly because the triple point of ethane is at a lower temperature than methane.

4.3. The Joule - Thomson curve

The Joule - Thomson inversion curve seems to have a simple form for all substances studied.

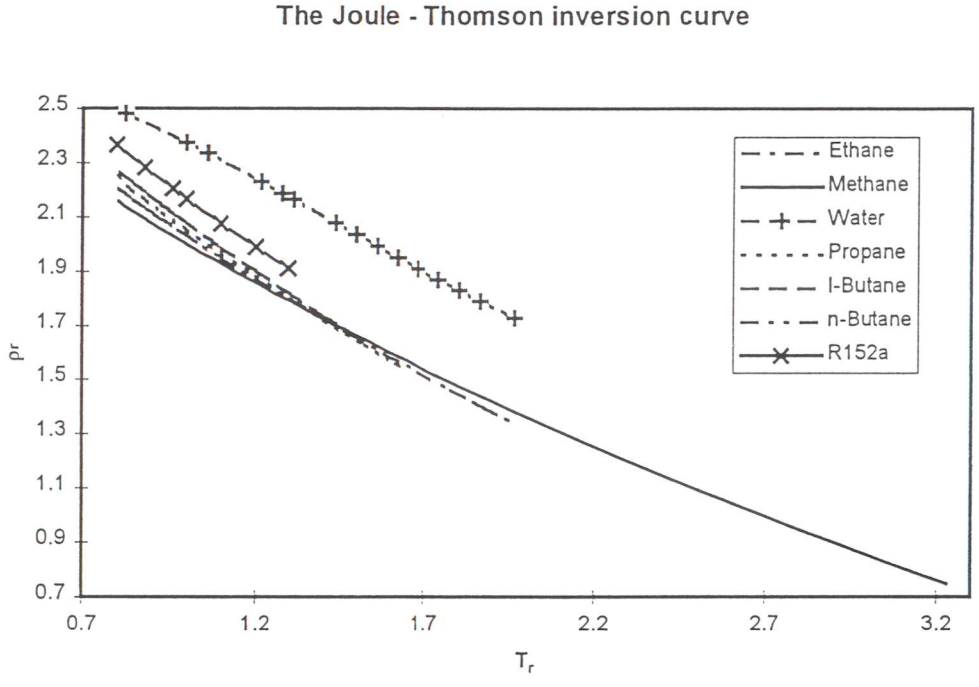

Figure 4.3 The Joule – Thomson inversion curve

Within the normal alkanes there is a regular behavior. The curves should be relatively easy to model as a function of the acentric factor.

Table 4.1 Intercept of the Joule Thomson inversion curve with the saturated liquid line

Substance	ρ_r	T_r
Methane	2.207	0.805
Ethane	2.157	0.806
Propane	2.260	0.801
I-Butane	2.266	0.798
n-Butane	2.366	0.807
R152a	2.482	0.800
Water	2.246	0.824

Another intriguing fact is that the inversion curves are touching the saturated liquid curve at approximately the same reduced temperature. (Table 4.1) The value of this information is limited in light of the good representations of the inversion points given by all model equations accept the PR - EOS. (Chapter 3.)

4.4. The minimum in the speed of sound

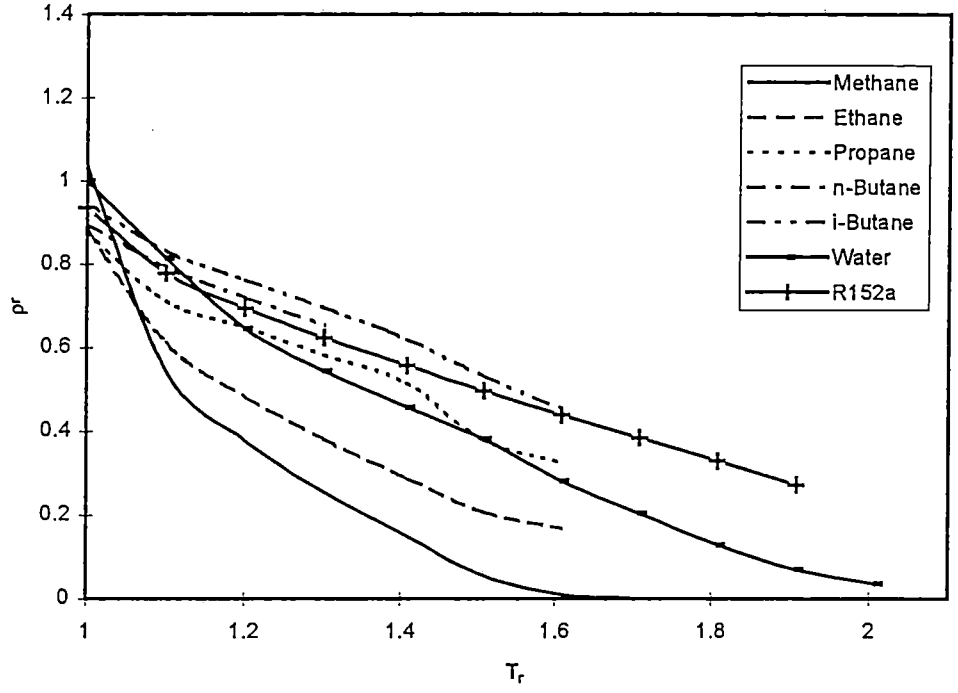

Figure 4.4 Minimum of speed of sound

In Figure 4.4 the minima of the speed of sound are plotted in reduced density and temperature coordinates. Again there is a regular behavior within the normal akenes. The accuracy of the surfaces used may be uncertain as shown by the non - smooth behavior of the curves.

4.5. The maximum in the Joule - Thomson curve

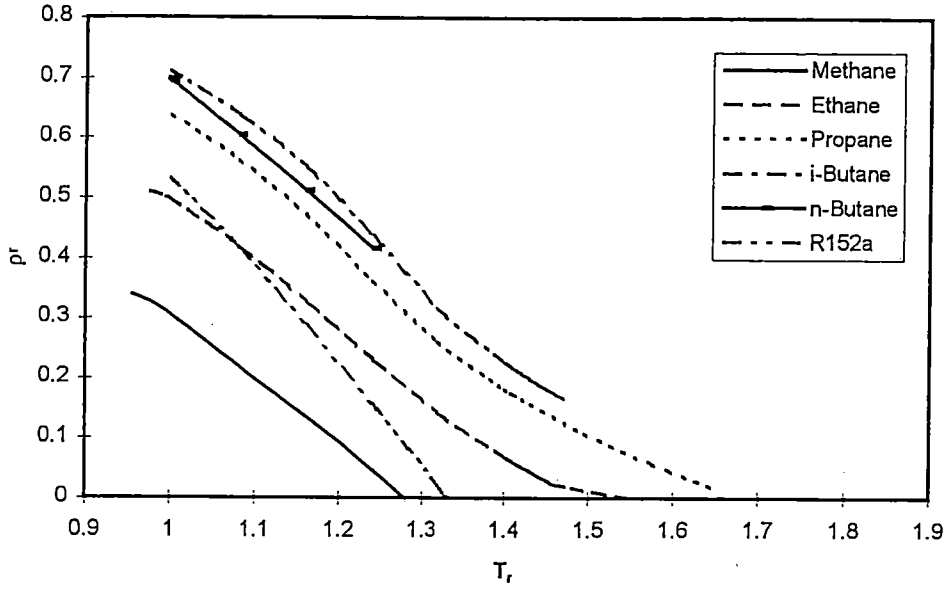

Figure 4.5 Maximum in the Joule - Thomson coefficient

In Figure 4.5 the maximums in the Joule - Thomson coefficient are plotted in the reduced temperature and reduced density plane. Only the the lower alkanes (C_1-C_3) shows some regularity in their behavior. Again the accuracy of the pure component surfaces has to be questioned.

Table 4.2 Points of intercept of the maximum in the Joule – Thomson inversion curve with the saturated vapor line

Substances	T_r	p_r
Methane	0.956	0.340
Ethane	0.976	0.510
Propane	1.000	0.637
I-Butane	0.998	0.711
n-Butane	0.997	0.698
R152a	1.000	0.531

Among the three first alkanes (C_1 - C_3) there seems to be a approximately lineair relationship between in the reduced temperatures at saturated vapor line. The bigger molecules have a starting point close to the critical point. Water is the only compound studied with no maximum in the Joule - Thomson coefficient.

4.5. Extreme points isochoric heat capacity

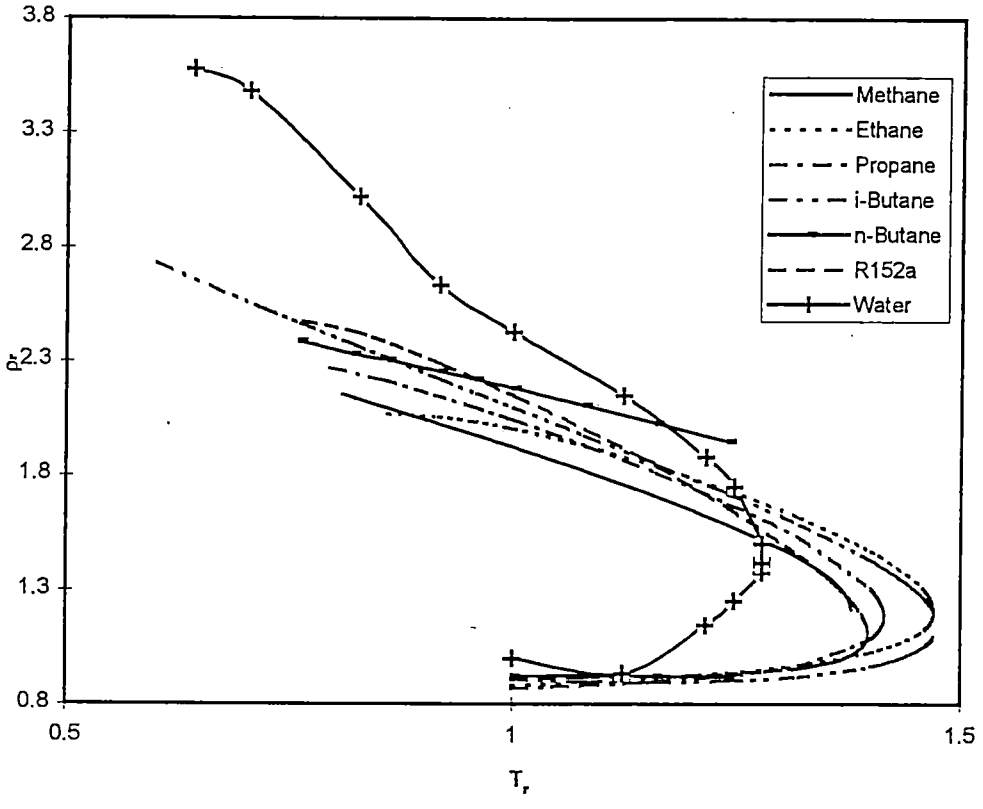

Figure 4.6 Extreme points C_v

In Figure 4.6 the extreme points of the C_v are plotted in the reduced temperature and reduced density plane. Water shows a different behavior from the rest of the compounds. The minimum is at higher densities and the transition to a maximum at lower temperatures than the others.

Table 4.3 Intercept of the C_v with the saturated liquid line

Substances	T_r	ρ_r
Methane	0.806	2.155
Ethane	0.856	2.069
Propane	0.791	2.271
I-Butane	0.598	2.730
n-Butane	0.757	2.386
R152a	0.760	2.475

Table 4.4 Points where : $(d^2C_v/d\rho^2)_T = 0$

Substance	T_r	ρ_r
Methane	1.378	1.217
Ethane	1.471	1.209
Propane	1.415	1.188
R152a	1.397	1.113
Water	1.278	1.419

4.6. The phase - envelope

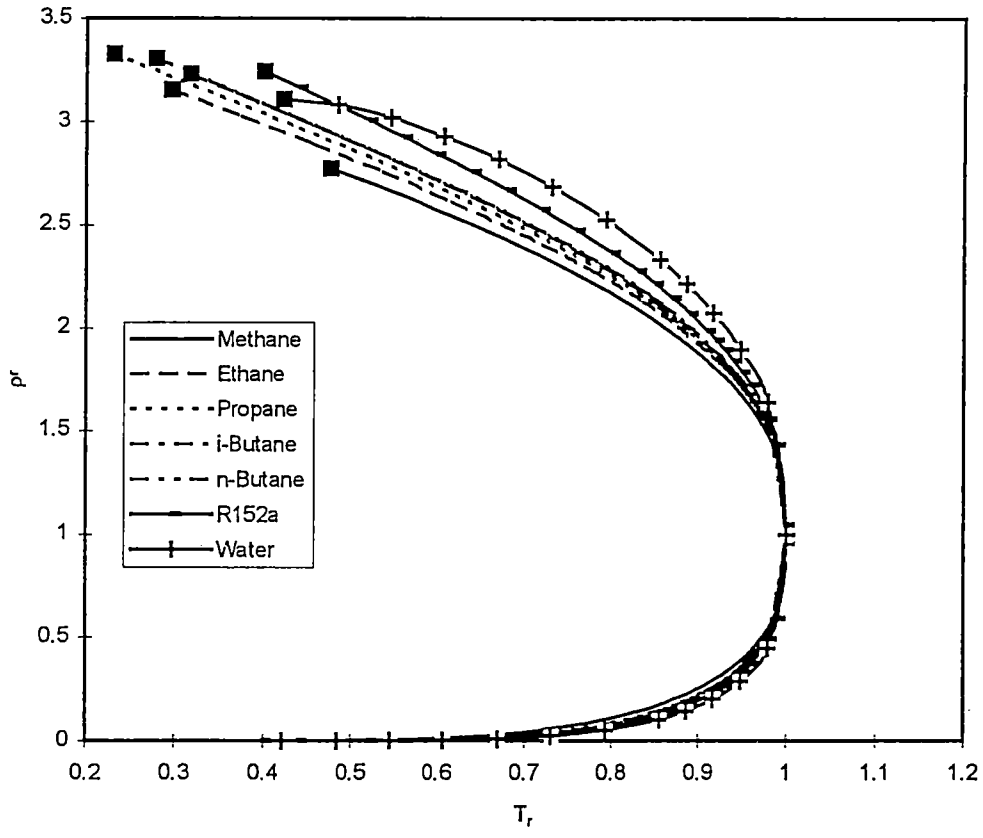

■ = triple point

Figure 4.7 The phase envelope

In Figure 4.7 the phase envelopes the pure components are plotted in the reduced temperature and the reduced density plane. The liquid densities are larger for larger molecules. This may be a regular variation with acentric factor.

4.7. Discussion of results

It is evident that the behavior of water is different from the behavior of the alkanes. This is probably a result of the association of the water molecules.

The Joule - Thomson inversion curve is the property that behaves in the most regular fashion. The value of this knowledge is lowered by the fact that most of the model equations studied here are able to predict the Joule - Thomson inversion curve.

The extrema of the isochoric heat capacity behave in a regular fashion. The behavior of the curves is sensitive to the accuracy of the equations used. As earlier pointed out most of the model equations studied are not able to give a qualitatively correct behavior of the isochoric heat capacity. Using the information gained from the plot of the extrema for the different pure components would probably allow us to improve the predictions of the isochoric heat capacities given by the model equations.

Conclusions

The object of this thesis was to study the real behavior of derivative propertries for pure substances and mixtures and to compare this behavior to the predictions obtained from model equations of state. The primary focus has been on pure components. In order to be able to avaluate the behavior of mixtures the extended corresponding states principle (ECS) has been studied on its ability to produce reference data. Analytical relationships were derived for isochoric heat capacity, isobaric heat capacity, the Joule - Thomson coefficient, and the speed of sound.. The ECS calculations were compared to experimental isobaric heat capaciy data for the methane/propane mixture. All derived properties were evaluated against a pure component surface for the methane/ethane mixturte and the principle of congruence for the same mixture. The ECS principle was found to generate data of a high quality. Deviations were found in the vicinity of the pseudo critical point for the mixture. Also the sensitivity of the derived priperties to binary interaction parameters in the mixingrule was studied. The sensitivity was found to be small.

The study of the behavior of pure components showed two types of behavior. The properties of pure components were evaluated as a function of density at a reduced temperature of 1.1. At this temperature the non - associating components were showing some common behavior :

- The isochoric heat capacity has both a minimum and a maximum.
- The isobaric heat capacity has both a maximum and a weak minimum.
- The Joule - Thomson coefficient has a maximum and a weak minimum.
- The speed of sound has a minimum.

The associating substances lacked the maximum in the Joule - Thomson coefficient. The isochoric heat capacity had a highly irregular behavior. A minimum in the isobaric heat capacity was at a high density, or absent depending on the range of the equations used.

Expressions for the derived properties from five model equations were derived :

- The RK - EoS
- The SRK - EoS
- The PR - EoS
- The SPHCT - EoS
- The SAFT - EoS

All the equations are in the simplest form dependent on three parameters; a parameter describing the volume of molecules, a parameter describing the interaction energy between molecules, and a parameter describing the chain length of molecules.

The model equations mentioned above were studied on their ability to predict derivative properties. Methane and n-butane were used as a reference in order to explore the ability to describe effects stemming from the chainlength of molecules. In all cases but methane with the SAFT equation the isochoric heat capacity was not well predicted. All equations were able to give a maximum in the isobaric heat capacity. All

equations were able to give a maximum in the Joule - Thomson coefficient as well as a minimum in the speed of sound. The SAFT equation was found to give excellent predictions for methane, but was not able to predict properties for n-butane with the same accuracy.

The extreme points of pure components were compared in the reduced density - temperature plane. This was done in order to explore regular behavior as a function of molecular structure. This behavior can be used to improve the model equations available. The extrema in the isochoric heat capacity were found to serve as a good tool for improvement of model equations. This conclusion is drawn from the fact that most equations of state have trouble in predicting them, and that there is a certain regularity in the behavior among different substances.

Recommendations

In this study the ECS principle has only been tested on mixtures of lower alkanes. This class of molecules can generally be described well with the van der Waals mixing rules. In order to use the ECS principle on more complex mixtures, other mixing rules should be tested. Hopefully, the ECS principle can produce good results for more complex mixtures as well. If so, this will allow us to calculate reference data for complex mixtures and test equations of state for mixtures.

The equations tested in this study should also be tested on their ability to produce accurate derivative properties for mixtures. Even now testing is possible for the lower alkanes based on reference data produced from the ECS calculations.

The full PHCT equation should be tested and compared to the results obtained with the SAFT equation since both equations have a similar theoretical basis. The difference is that there are extra temperature dependencies in the SAFT equations, and the treatment of chain - like molecules is different; the effect of this is not known.

In future work, models for pure components could be designed using the behavior of the multiparameter equations as a reference. Based on experience so far, a strategy of design can be suggested. In order to capture the temperature dependence of the equation of state the isochoric heat capacity should be modeled first. The residual isochoric heat capacity has some advantages over the other properties :

- The property links the microscopic structure of the molecules with the macroscopic behavior. The isochoric heat capacity is proportional to the degrees of freedom of the molecules. If the influence of density on the internal degree of freedom of the molecules can be understood, it should be possible to link the structure of the molecules to the macroscopic behavior of a fluid.
- In terms of different contributions the property seems to be additive. This means that the property is the sum of contributions from different effects on the thermodynamic surface.
- The property is very sensitive to the temperature dependence of the thermodynamic surface.

In order to give the equation the right volumetric behavior one other property should be used in the development of the equation. The reduced bulk modulus is not very temperature dependent, but has a strong density dependence which provides complementary information to the heat capacity. The different contributions to this property are also additive.
If the residual isochoric heat capacity is modeled, it can be transformed into the residual Helmholtz energy according to :

$$A^r = K(\rho,T) + TL(\rho) + M(\rho) \qquad (5.1)$$

with :

$$K(\rho,T) = -\int\int \frac{C_v^r(\rho,T)}{T} dTdT \qquad (5.2)$$

The next step would be to derive the reduced bulk modulus from residual Helmholtz energy :

$$B_T = 1 + 2\rho\left(\frac{dA^r / RT}{d\rho}\right)_T + \rho^2\left(\frac{d^2A^r / RT}{d\rho^2}\right)_T \qquad (5.3)$$

We see that from transforming the residual isochoric heat capacity into the residual Helmholtz energy two functions of density (L,M in equation (5.2)) appear that give us an extra degree of freedom in modeling the reduced bulk modulus. This scheme can also be used the other way around. Starting with a model of the reduced bulk modulus, this model can be transformed into the residual Helmholtz energy according to :

$$\frac{A^r}{RT} = K(T) + \frac{L(T)}{\rho} - \ln(\rho) + \int \frac{1}{\rho^2}\left(\int B_T d\rho\right)d\rho \qquad (5.4)$$

If this relationship is transformed into the isochoric heat capacity according to

$$\frac{C_v^r}{R} = -\frac{T}{R}\left(\frac{d^2A^r}{dT^2}\right)_\rho \qquad (5.5)$$

we have two temperature functions (K and L in equation (5.4)) that can be modeled to give the right behavior of the isochoric heat capacity. These steps should be undertaken in addition to the modeling of saturation properties.

The dispersion term in the SAFT equation does not show the same qualitative behavior for methane and n-butane. Probably should this term be critically reviewed and remodeled in order to improve the ability of the SAFT equation to estimate correct values for the isochoric heat capacity.

List of symbols

A	Helmholtz energy	(J/mol)
$a = [A-A^{id}]/RT$	Dimensionless residual Helmholtz energy	(-)
b	Co – volume in cubic equations of state	(L/mol)
B_T	Reduced bulk modulus	(-)
c	Number of segments (SPHCT EOS)	(-)
C_p	Isobaric heat capacity	(J/K.mol)
$c_p^r = [C_p-C_p^{id}]/R$	Dimensionless residual isobaric heat capacity	(-)
C_v	Isochoric heat capacity	(J/K.mol)
$c_v^r = [C_v-C_v^{id}]/R$	Dimensionless residual isochoric heat capacity	(-)
d	Diameter of segment (SAFT EOS)	(dm)
D_{ij}	Constants in dispersion term (SAFT EOS)	(-)
G	Gibbs energy	(J/mol)
$g = [G-G^{id}]/RT$	Dimensionless residual Gibbs energy	(-)
H	Enthalpy	(J/mol)
$h = [H-H^{id}]/RT$	Dimensionless reduced enthalpy	(-)
h	Transformation parameter (ECS)	(-)
f	Transformation parameter (ECS)	(-)
k	Bolzman's constant	(J/K)
M_r	Molar mass	(g/mol)
m	Chain length of molecules	(-)
N^t	Total number of moles	(-)
N_{AV}	Avogadro's number	(1/mol)
n_i	Number of moles of component I	(-)
P	Pressure	(MPa)
R	Gas constant	(J/K.mol)
S	Entropy	(J/K.mol)
$s = [S-S^{id}]/R$	Reduced residual entropy	(-)
T	Absolute temperature	(K)
x_i	Mole fraction of component i	(-)
Z	Compressibility factor	(-)
Z_M	Coordination number (SPHCT EOS)	(-)
$z = Z-1$	Residual compressibility factor	(-)
U	Energy	(J/mol)
$u = [U-U^{id}]/RT$	Dimensionless energy	(-)
u/k	Segment – segment interaction energy	(K)
u^0/k	Segment – segment interaction energy at $T \rightarrow \infty$	(K)
v^0	Segment volume	(L/mol)
v^{00}	Segment volume at zero temperature	(L/mol)
w	Speed of sound	(m/s)
$1-C_{ij}$	The direct correlation function	(-)

Greek :

δ	Dimensionless density (ρ/ρ_c)	(-)
ω	Pitzers acentric factor	(-)
ρ_r	Reduced density	(-)
ρ	Density	(mol/L)
τ	Dimensionless temperature (T_c/T)	(-)
τ	Geometrical constant (= 0.74048)	(-)
Φ^0	Dimensionless ideal gas Helmholtz energy (A^{id}/RT)	(-)
Φ^r	Dimensionless residual Helmholtz energy ($A-A^{id}$)/RT	(-)
μ	The Joule – Thomson coefficient	(K/Pa)
θ	Shapefactor (ECS)	(-)
ϕ	Shapefactor (ECS)	(-)
εq	Segment energy (SPHCT EOS)	(J)
ε_{ij}	Binary interaction parameter (ECS)	(-)
η_{ij}	Binary interaction parameter (ECS)	(-)
ϕ_i	Fugacity	(-)

Indices :

r	Reduces properties
c	Critical properties
id	Ideal gas state
x	Mixture property
i	Target fluid
0	Reference fluid
hs	Carnahan – Starling contribution SAFT EOS
seg	Segment contribution SAFT EOS
chain	Chain contribution SAFT EOS
assoc	Association contribution SAFT EOS

References

1. J. F. Ely, "A Predictive, Exact Shape Factor Extended Corresponding States Model for Mixtures", *Advances in Cryogenic Engineering*, **35**, 1511 (1990)
2. C. H. Kim,P. Vimalchand, M. D. Donohue, and S. I. Sandler, "Local Composition Model for Chainlike Molecules : A New Simplified Version of the Perturbed Hard Chain Theory", *AIChE J.*, **32**, p1726-1734
3. S. H. Huang and M. Radosz, "Equation of State for Small, Large, Polydisperse, and Associating Molecules", *Ind. Eng. Chem. Res.*, **29**, No. 11, 2284 (1990)
4. B. A. Younglove and J. F. Ely, "Thermophysical Properties of Fluids. II. Methane, Ethane, Propane, Isobutane and Normal Butane", *J. Phys. Chem. Ref. Data*, **16**, No. 4, 577 (1987)
5. S. L. Outcalt and M. O. Mc Linden, "A Modified Benedict-Webb-Rubin Equation of State for the Thermodynamic Properties of R152a (1,1-difluoroethane)", *J. Phys. Chem. Ref. Data*, **25**, 605 (1996)
6. R. D. McCarty, "Extended Corresponding States as a Tool for the Prediction of the Thermodynamic Properties of Mixtures", *Int. J. Thermophys.* **7**, 901 (1986)
7. V.F. Yesavage, "The Measurement and Prediction of the Enthalpy of Fluid Mixtures Under Pressure", Department of Chemical and Metallurgical Engineering, The University of Michigan, (1968)
8. O. Redlich and J. N. S. Kwong, "On Thermodynamics of Solutions V : An Equation of State. Fugacities of Gaseous Solutions", *Chem. Rev.*, **44**, 233-244 (1949)
9. G. Soave, "Equilibrium Constants from a Modified Redlich - Kwong Equation of State", *Chem. Eng. Sci.*, **27**, 1197-1203 (1972)
10. D. Y. Peng and D. B. Robinson, "A New Two - Constant Equation of State", *Ind. Eng. Chem. Fund.*, **15**, 59-64 (1976)
11. S. Beret and J. M. Prausnitz, "Perturbed Hard - Chain Theory : An Equation of State for Fluids Containing Small and Large Molecules", *AIChE J.*, **21**, 1123 (1975)
12. N. F. Carnahan and K. E. Starling, "Intermolecular Repulsion and the Equation of State for Fluids", *AIChE J.*, **18**, 1184 (1972)
13. B. J. Alder, D. A. Young, and M. A. Mark, "Studies in Molecular Dynamics. X. Corrections to the Augmented van der Waals Theory for the Square - Well Fluid", *J. Chem. Phys.*, **56**, 3013 (1972)
14. K. H. Lee, M. Lombardo, and S. I. Sandler, "The Generalized van der Waals Partition Function. II. Application to the Square - Well Fluid", *Fluid Phase Eq.*, **21**, 177-196 (1985)
15. C. H. Kim, P. Vimalchand, M. D. Donohue, and S. I. Sandler, "Local Composition Model for Chain - Like Molecules : A New Simplified Version of the Perturbed Hard Chain Theory", *AIChE J.*, **32**, 1726-1734 (1986)
16. C. J. Peters, J. M. H. Levelt Sengers, J. de Swaan Arons, and J. S. Gallagher, "Global Phase Behavior of Mixtures of Short and Long n-Alkanes", *AIChE J.*, **34**, 834 (1988)
17. S. S. Chen, and A. Kreglewski, "Application of the Augmented van der Waals Theory of Fluids. I. Pure Fluids", *Ber. Bunsenges, Phys. Chem.*, **81**, 1049 (1977)

18. W. G. Chapman, K. E. Gubbins, G. Jackson, and Maciej Radosz, "New Reference Equation of State for Associating Liquids", *Ind. Eng. Chem. Res.*, **29**, No. 8, 1709-1721 (1990)
19. T. M. Reed, and K. E. Gubbins, "Applied Statistical Mechanics", McGraw-Hill: New York, 1973.
20. S. G. Penoncello, R. T. Jacobsen, and A. R. H. Goodwin, "A Thermodynamic Property Formulation for Cyclohexane", *Int. J. Thermophys.*, **16**, 519 (1995)
21. U. Setzmann, and W. Wagner, "A New Equation of State and Tables of Thermodynamic Properties for Methane Covering the Range from the Melting Line to 625 K at Pressures up to 1000 MPa", *J. Phys. Chem. Ref. Data*, **20**, 1061 (1991)
22. P. G. Hill, "A Unified Equation for the Thermodynamic Properties of H_2O", *J. Phys. Chem. Ref. Data*, **19**, 1233 (1990)
23. A. Saul, and W. Wagner, "A Fundamental Equation for Water Covering the Range from the Melting Line to 1273 K at Pressures up to 25000 MPa", *J. Phys. Chem. Ref. Data*, **18**, 1537 (1989)
24. K. M. de Reuck, and R. J. B. Craven, "METHANOL - International Thermodynamic Tables of the Fluid State - 12", *Blackwell Scientific Publications*, Oxford (1993)
25. W. A. Cole, and K. M. de Reuck, "An Interim Analytic Equation of State for Sulfurhexafluoride", *Int. J. Thermophys.*, **11**, 189 (1990)
26. J. Gregorowics, J. P. O'Connell, and C. J. Peters, "Some Characteristics of Pure Fluid Properties that Challenge Equation-of-State Models", *Fluid Phase Eq.*, **116**, 94-101 (1996)
27. S. I. Sandler, "Models for Thermodynamic and Phase Equilibria Calculations", Marcel Dekker Inc., New York, 87-186 (1994)
28. C. H. Kim, P. Vimalchand, M. P. Donohue, and S. I. Sandler, "Local Composition Model for Chainlike Molecules : A New Simplified Version of the Perturbed Hard Chain Theory", AIChE J., **32**, 1726-1734 (1986)

Appendices

Appendix 1. Derivative properties methane

C_v^r/R for methane with the Wagner EOS

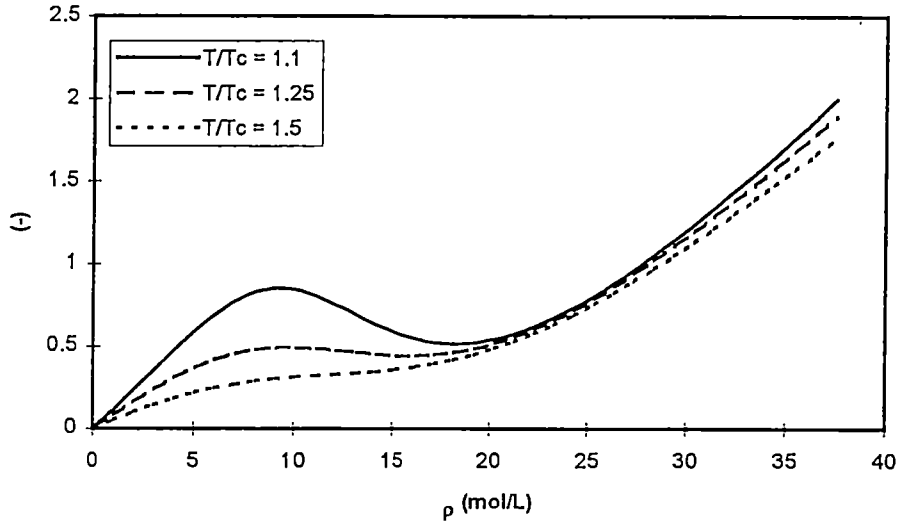

C_p methane with the wagner EOS

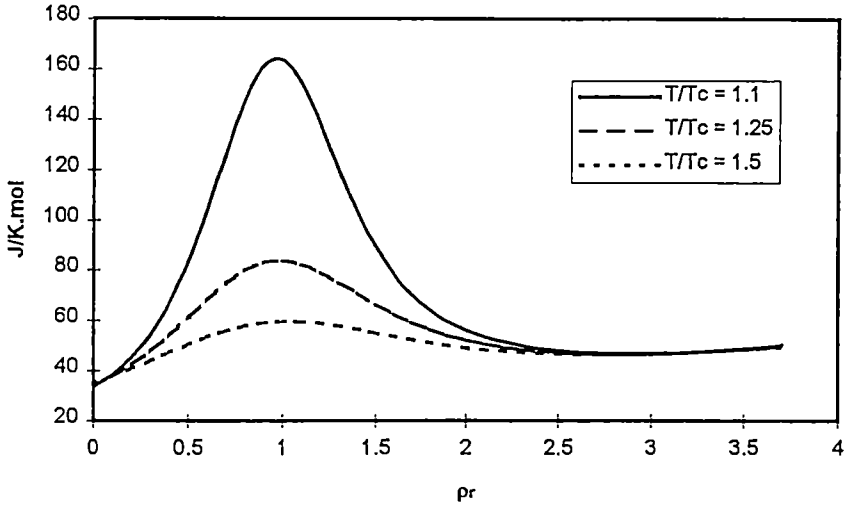

Speed of Sound methane with the wagner EOS

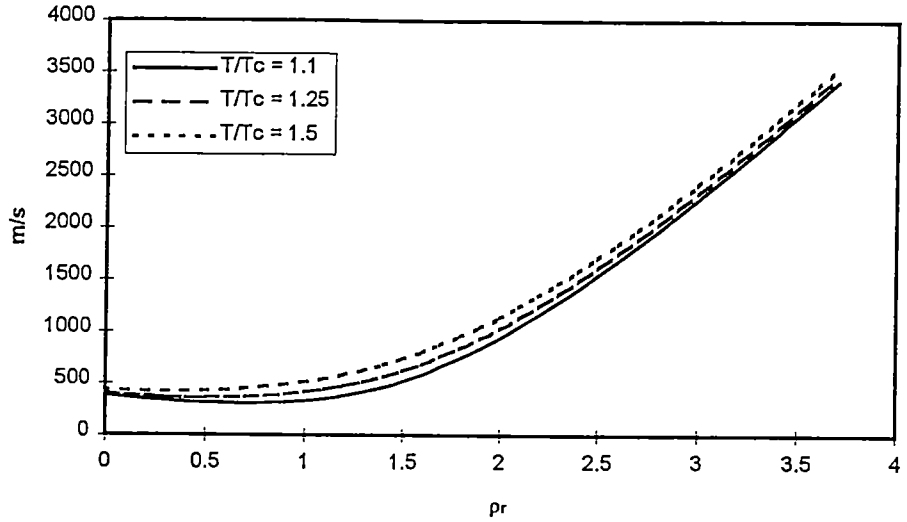

The Joule - Thomson coeff. methane with the wagner EOS

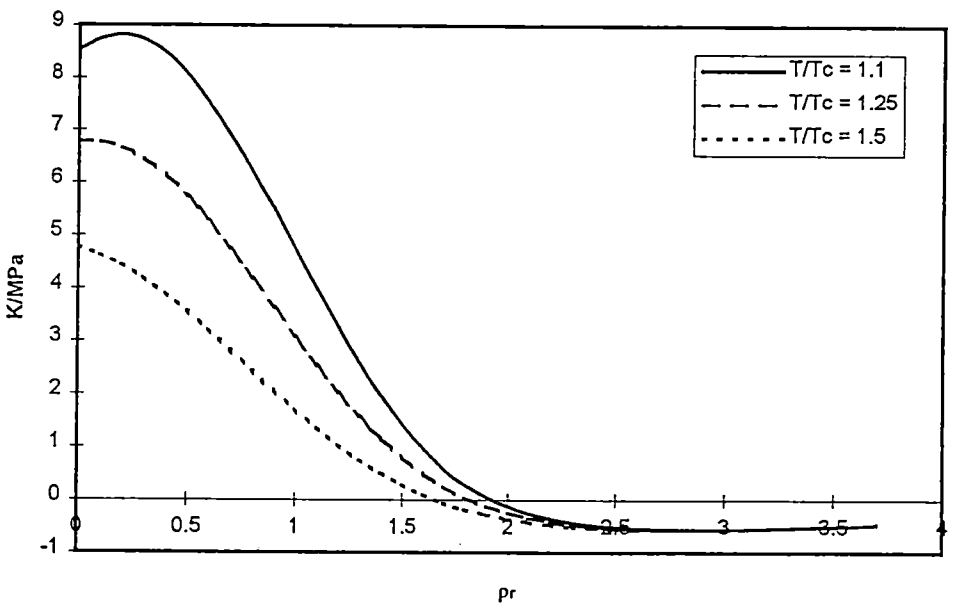

Appendix 2. Derivative properties ethane

C_v^r/R ethane with the 32-MBWR EOS

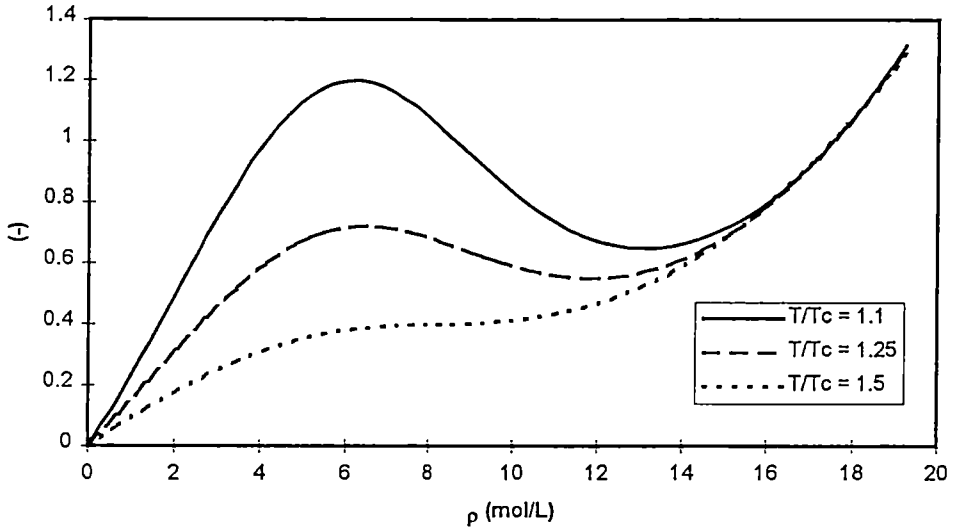

C_p ethane with the 32-MBWR EOS

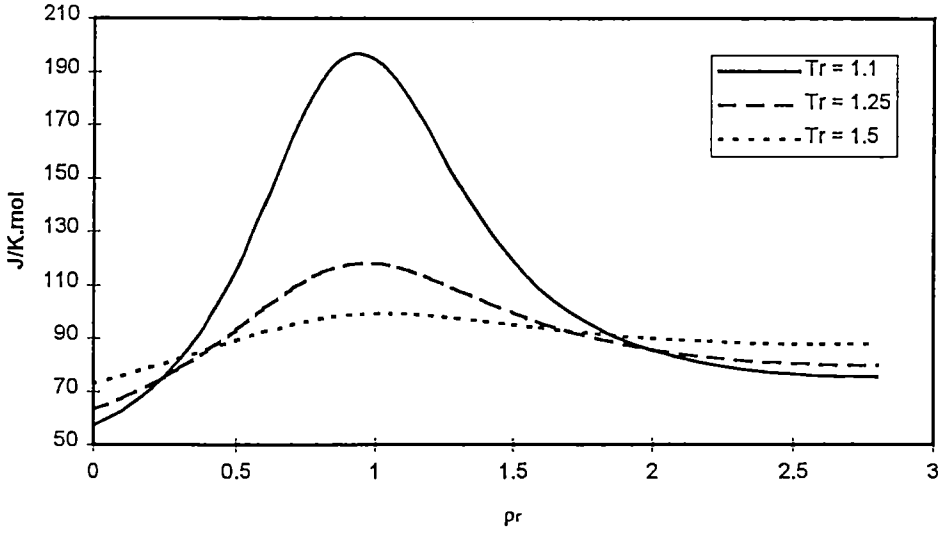

Speed of sound ethane with the 32-MBWR EOS

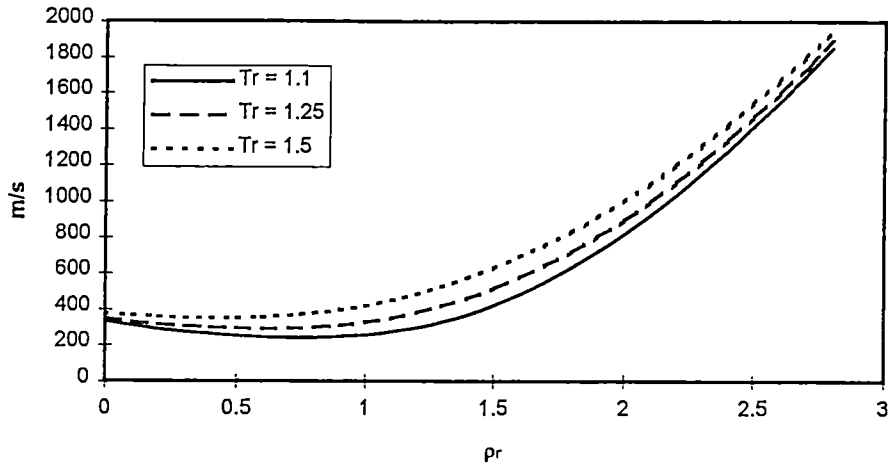

The Joule - Thomson coeff. ethane with the 32-MBWR EOS

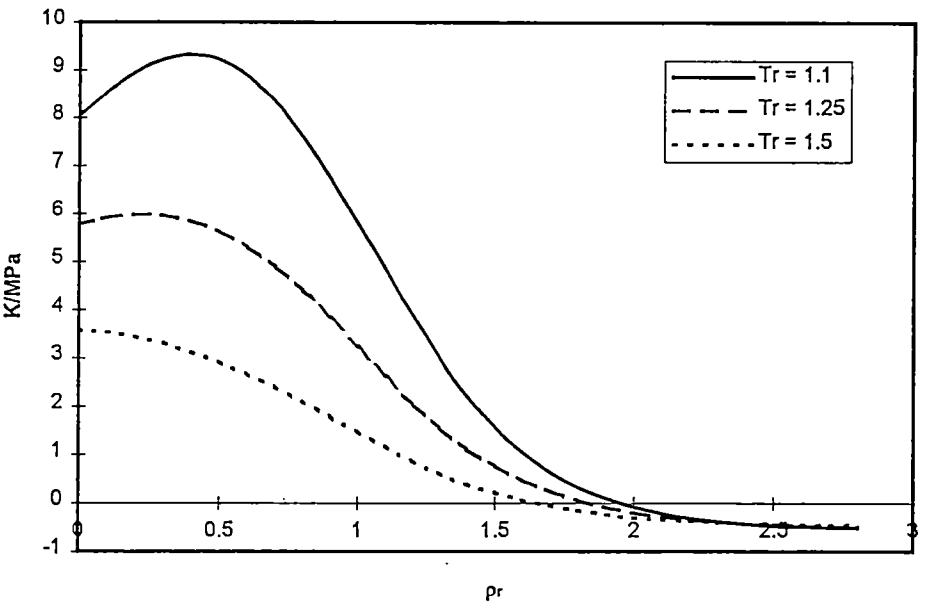

Appendix 3. Derivative properties propane

C_v^r/R propane with the 32-MBWR EOS

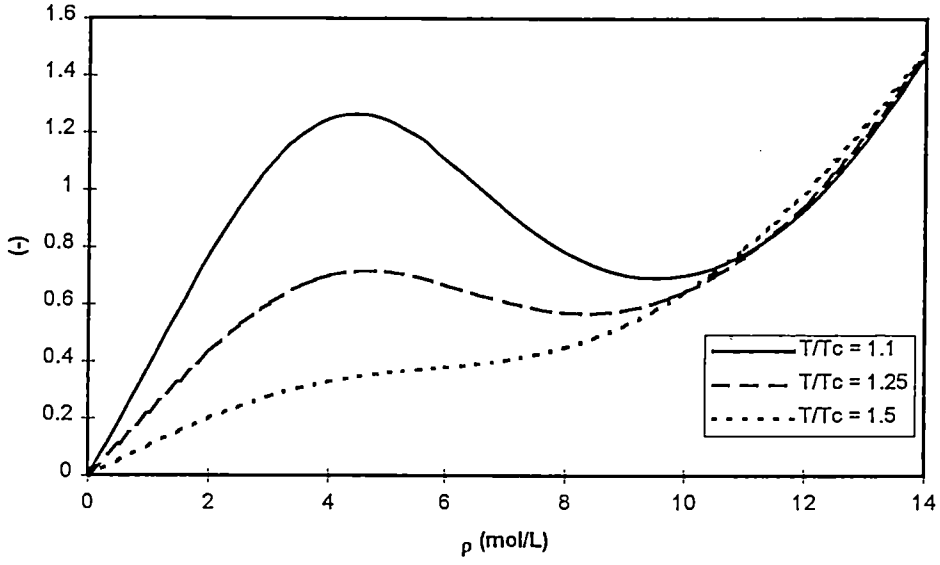

C_p propane with the 32-MBWR EOS

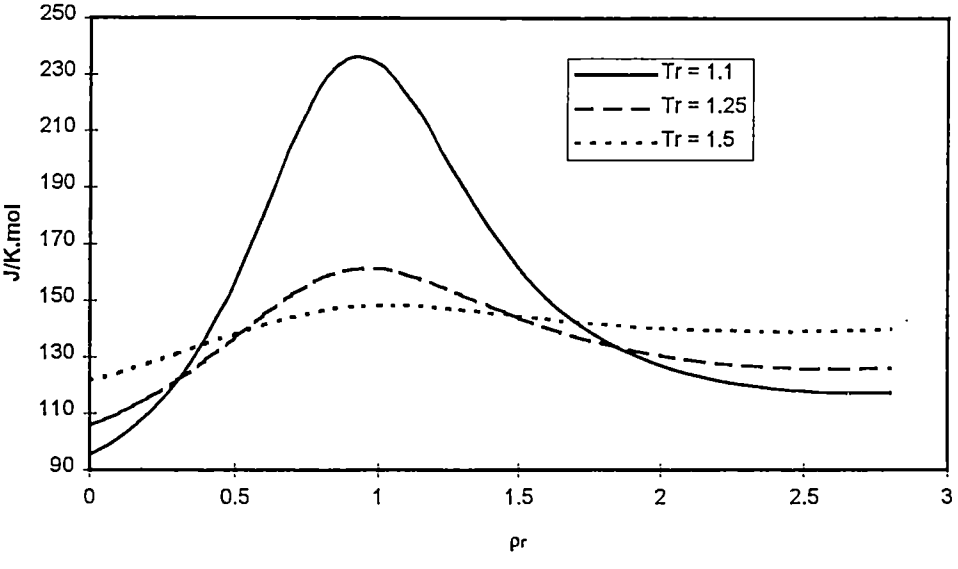

Speed of Sound propane with the 32-MBWR EOS

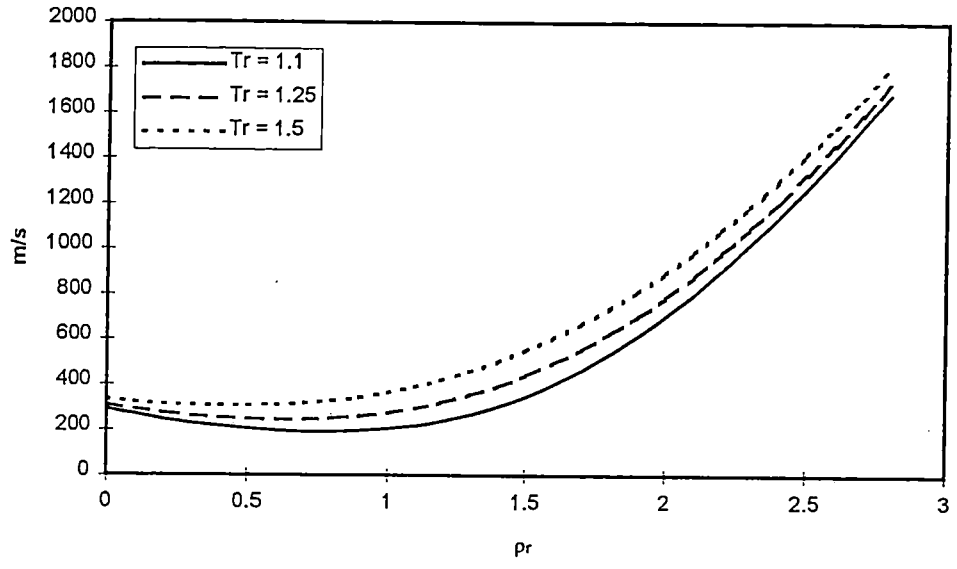

The Joule - Thomson coeff. propane with the 32-MBWR EOS

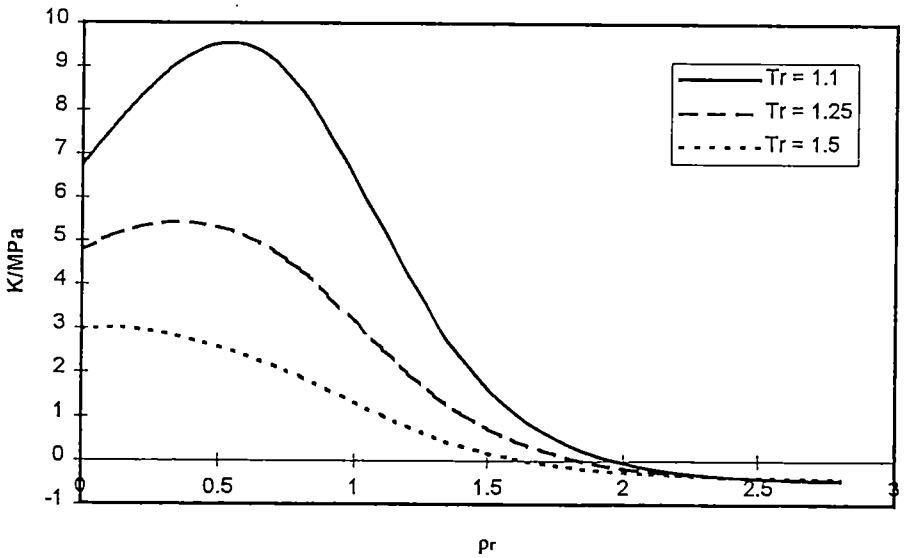

Appendix 4. Derivative properties i-butane

C_v^r/R i-butane with the 32-MBWR EOS

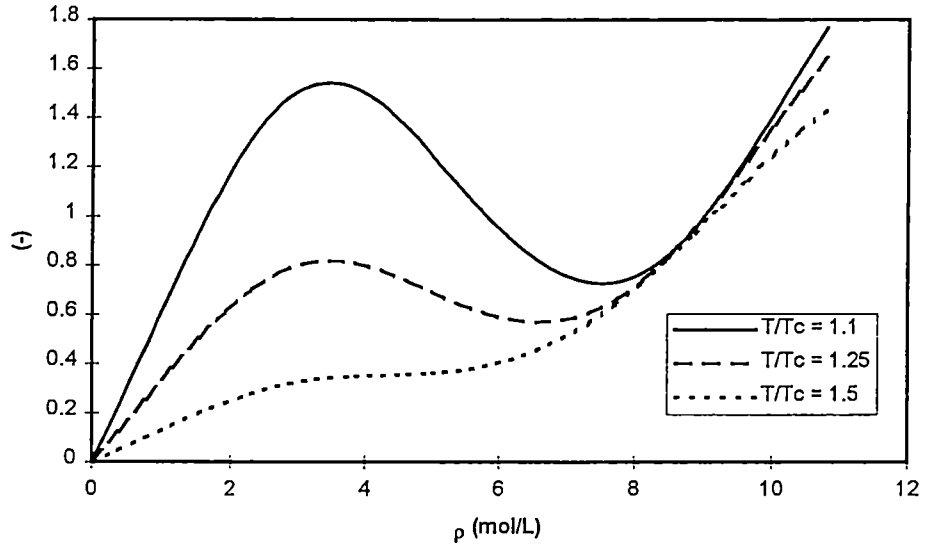

C_p i-butane with the 32-MBWR EOS

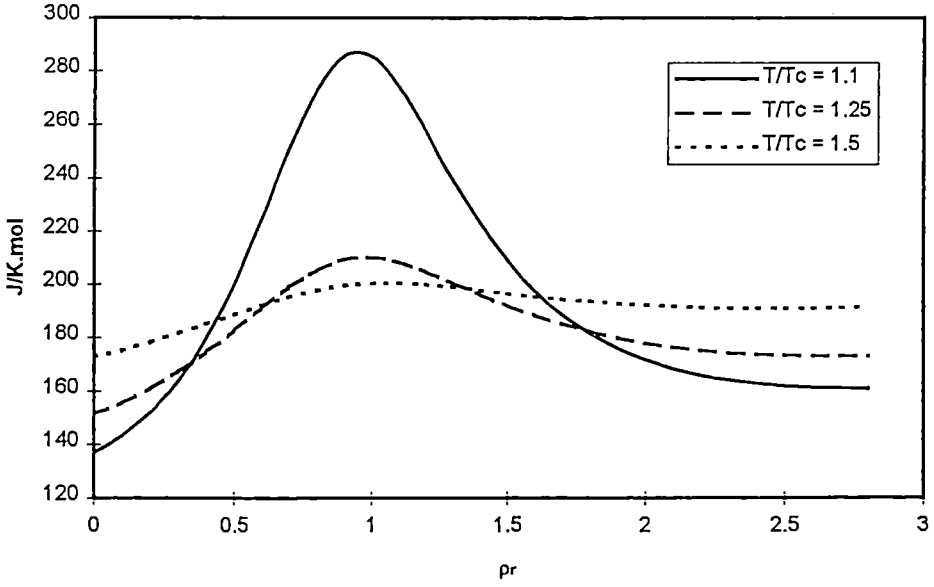

Speed of Sound i-butane with the 32-MBWR EOS

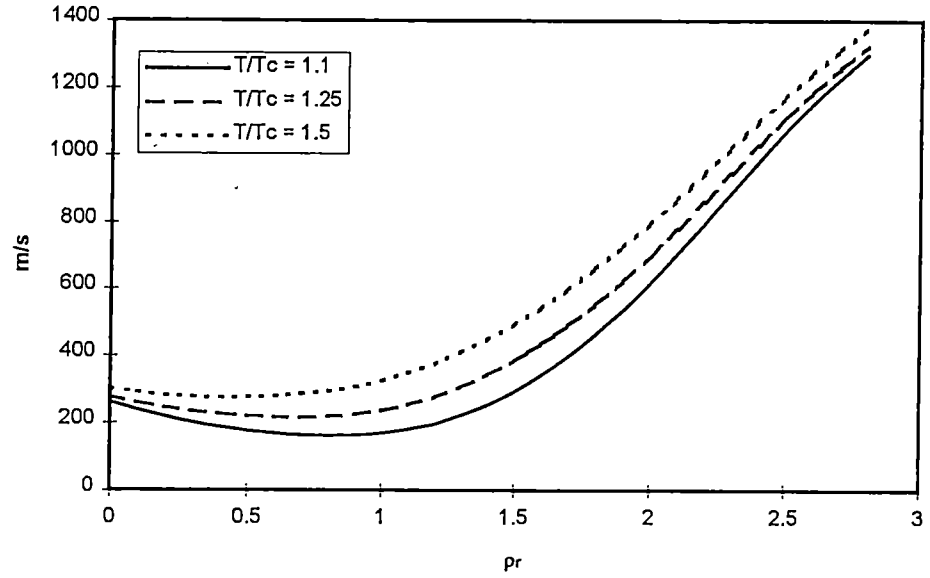

The Joule - Thomson coeff. i-butane with the 32-MBWR EOS

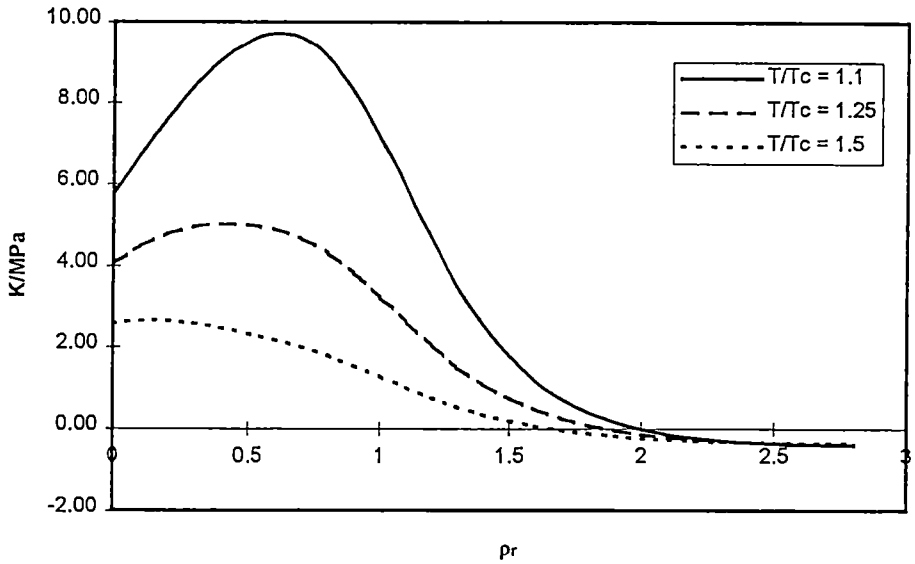

Appendix 5. Dèrivative properties n-butane

C_v^r/R n-butane with the 32-MBWR EOS

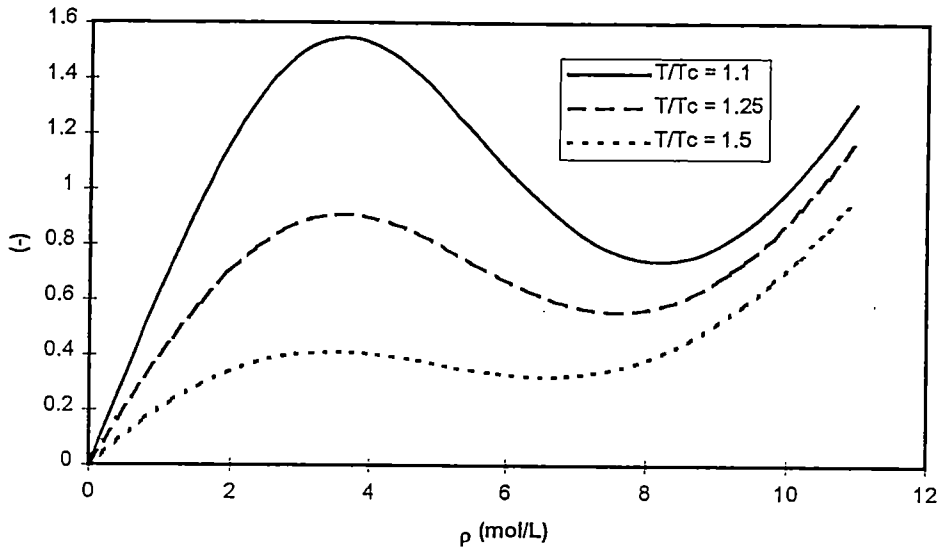

C_p n-butane with the 32-MBWR EOS

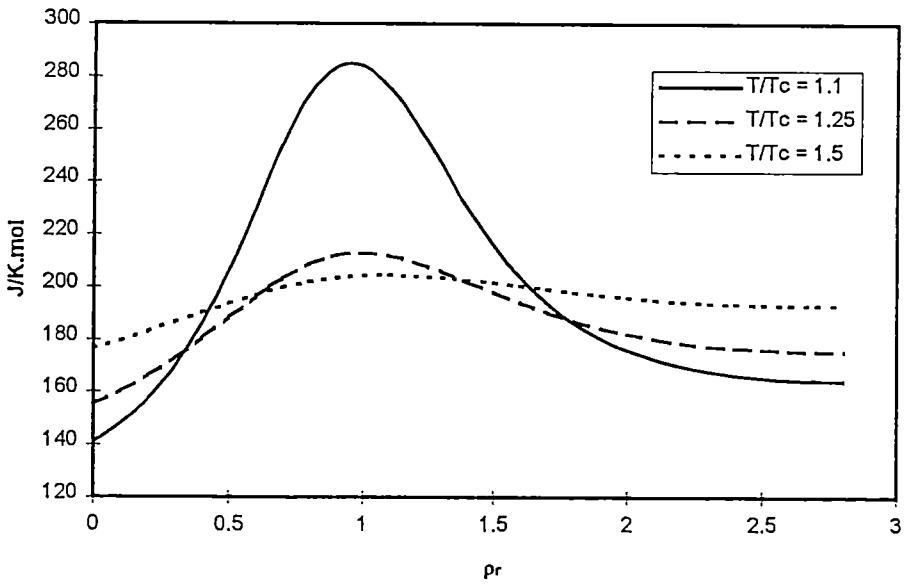

Speed of Sound n-butane with the 32-MBWR EOS

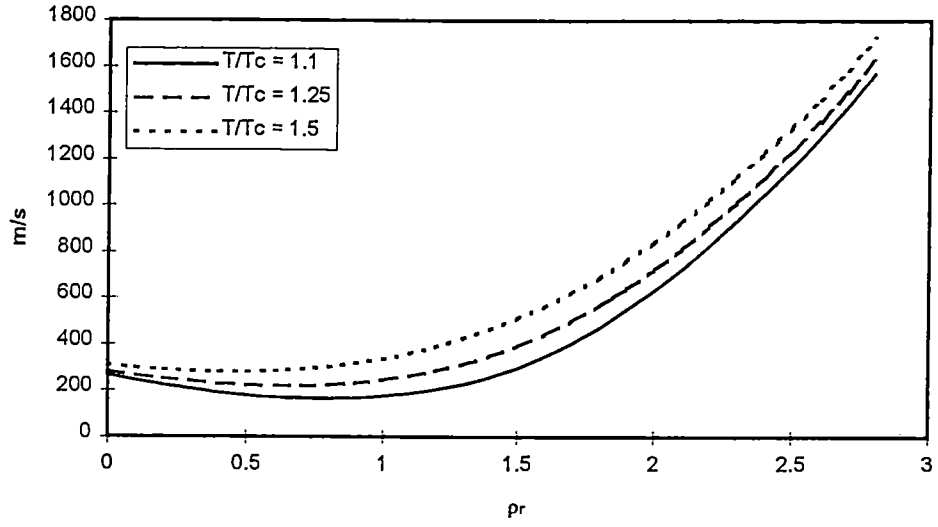

The Joule - Thomson coeff. n-butane with the 32-MBWR EOS

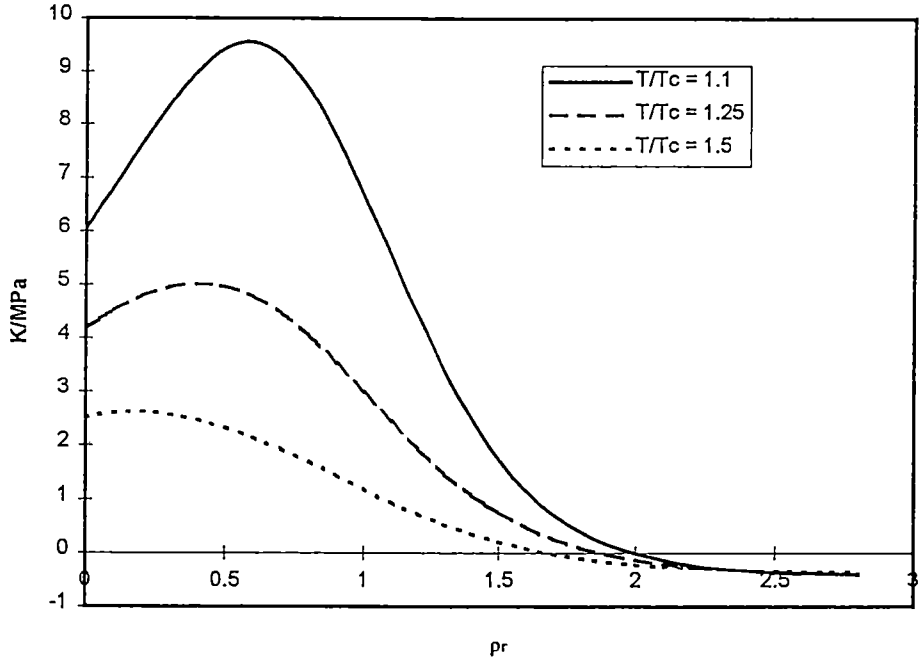

Appendix 6. Derivative properties cyclohexane

C_v^r/R cyclohexane with the Wagner EOS

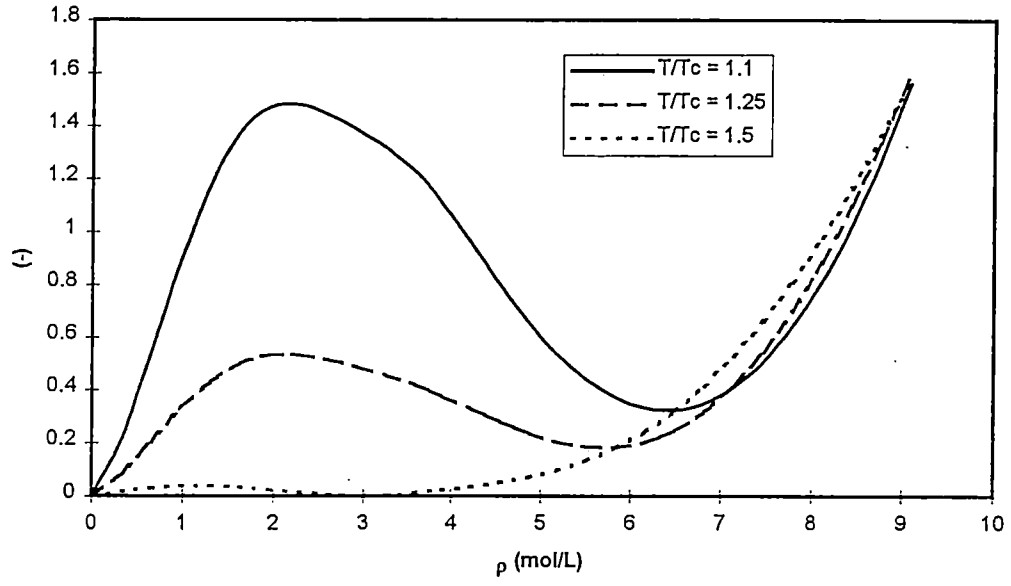

C_p cyclohexane with the wagner EOS

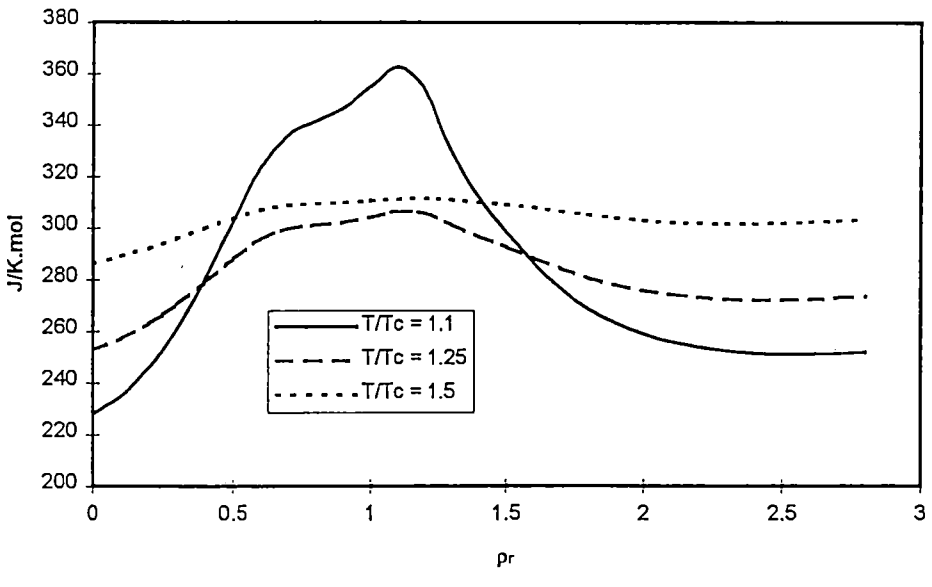

Speed of Sound cyclohexane with the wagner EOS

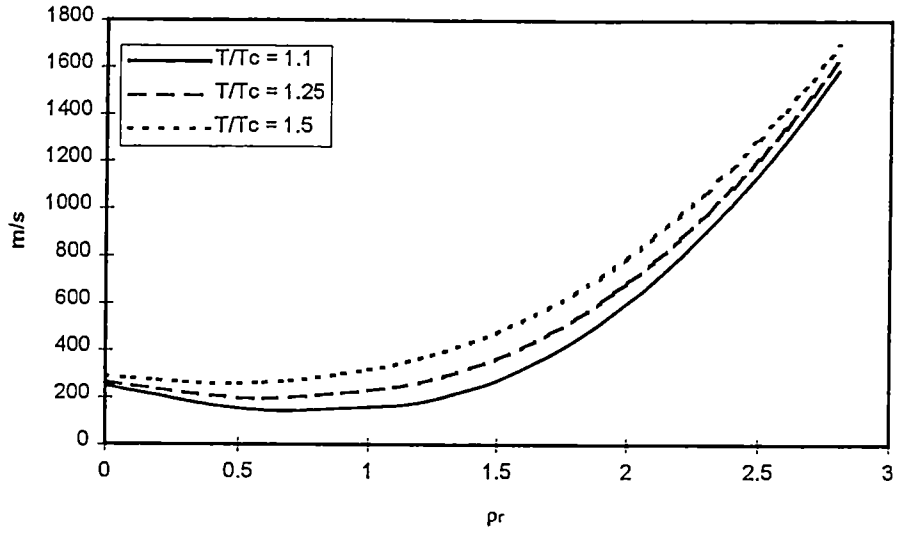

The Joule - Thomson coeff. cyclohexane with the wagner EOS

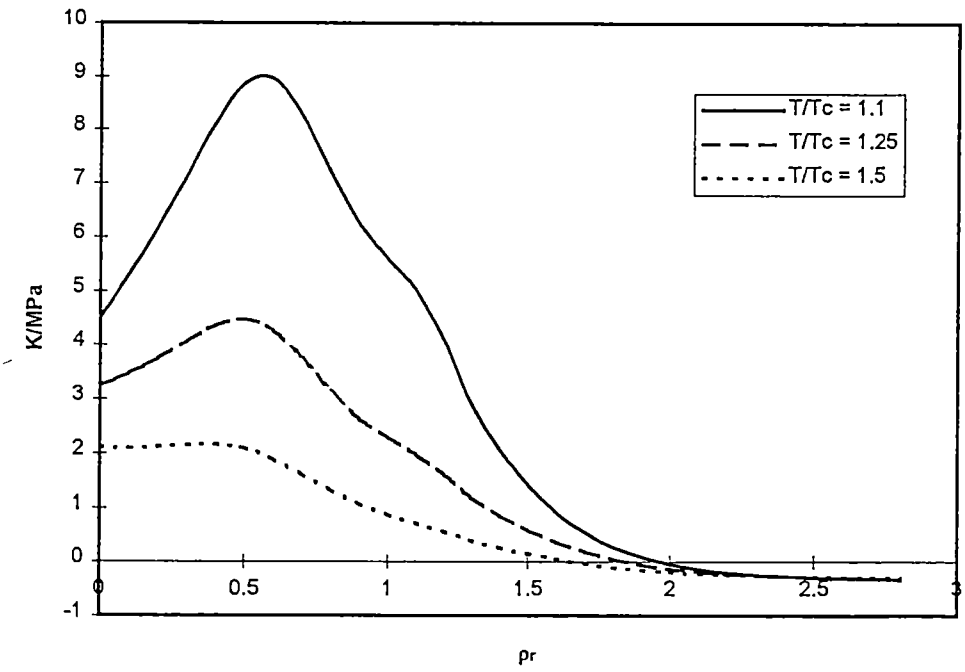

Appendix 7. Derivative properties R152a

C_v^r/R R152a with the 32-MBWR EOS

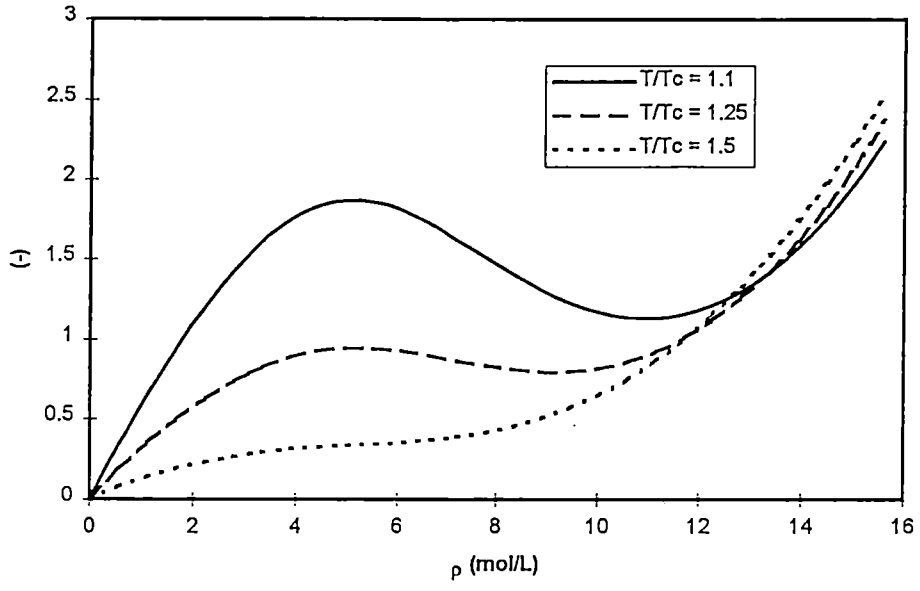

C_p R152a with the 32-MBWR EOS

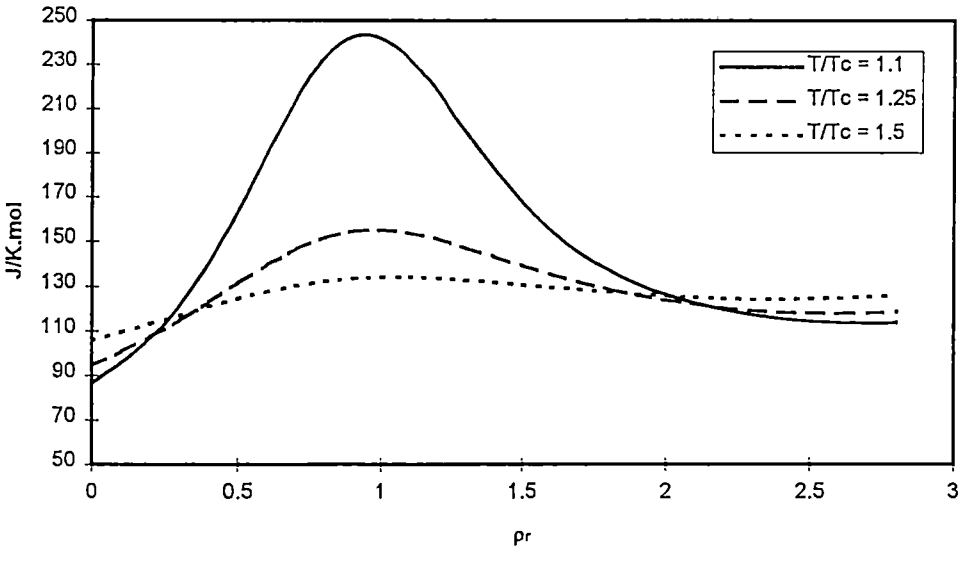

Speed of Sound R152a with the 32-MBWR EOS

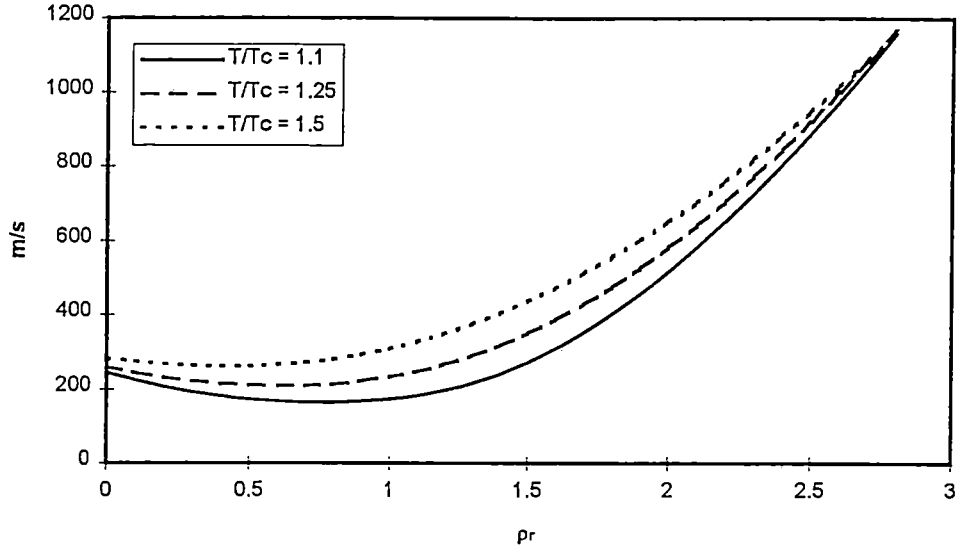

The Joule - Thomson coeff. R152a with the 32-MBWR EOS

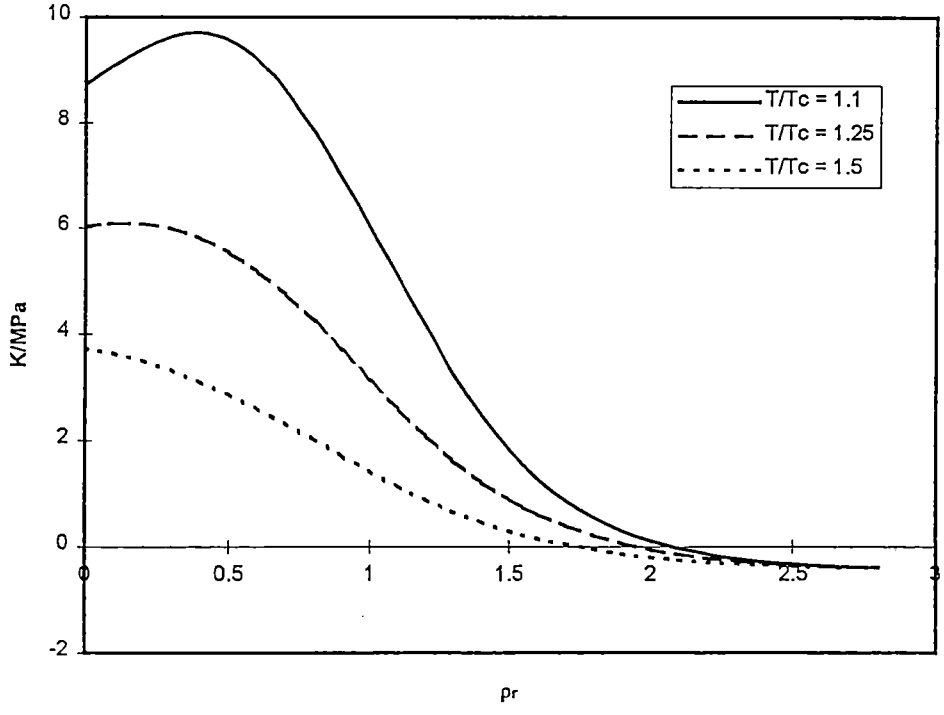

Appendix 8. Derivative properties sulfurhexafluoride

C_v^r/R sulphurhexafluoride with the Wagner EOS

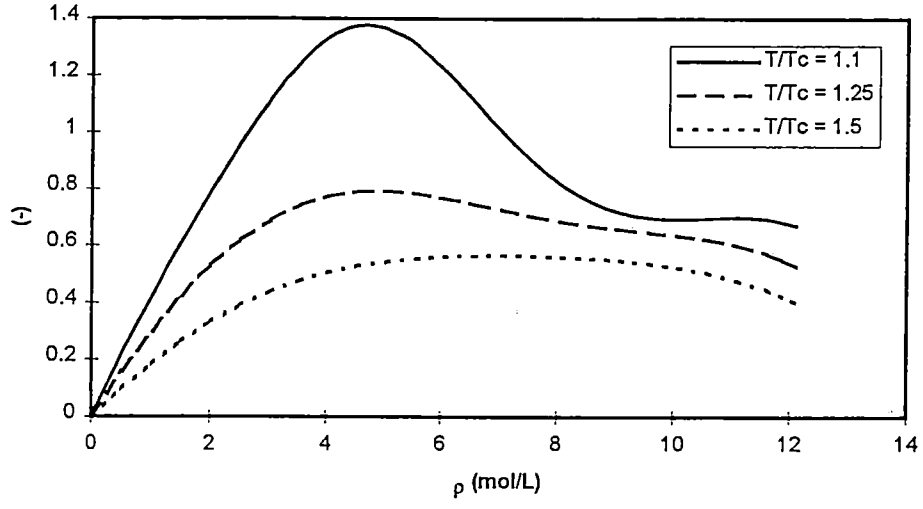

C_p F6S with the wagner EOS

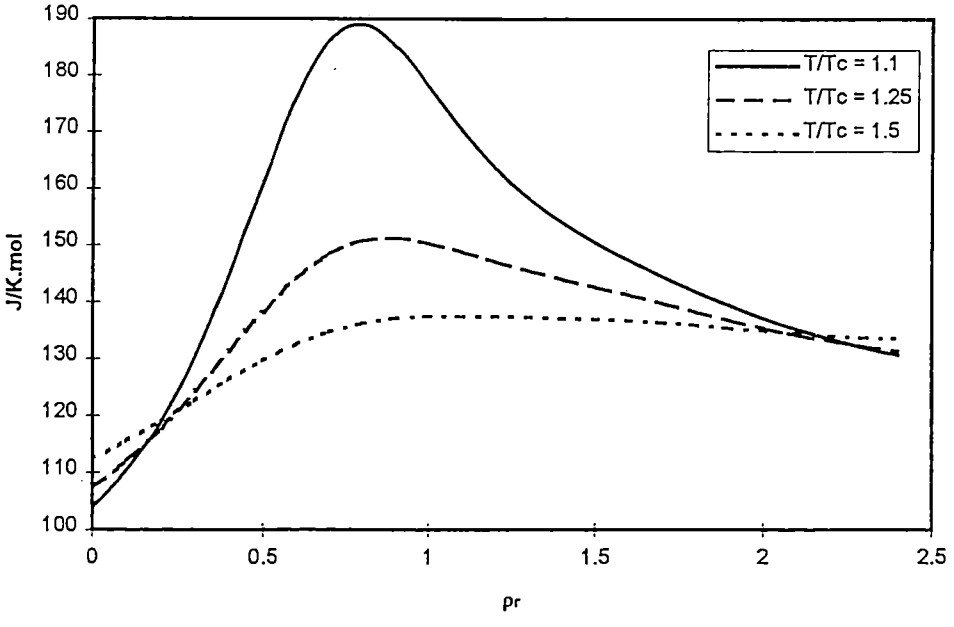

Speed of Sound F6S with the wagner EOS

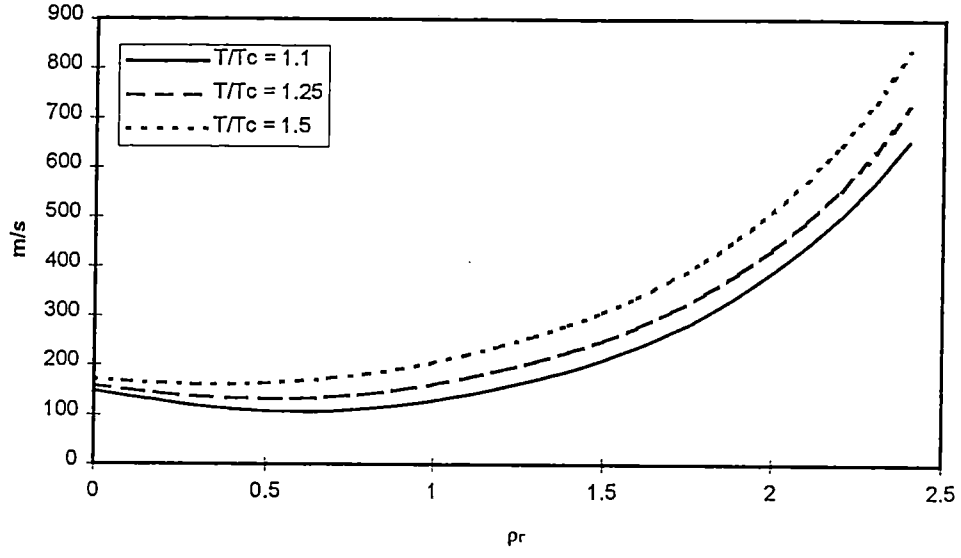

The Joule - Thomson coeff. F6S with the wagner EOS

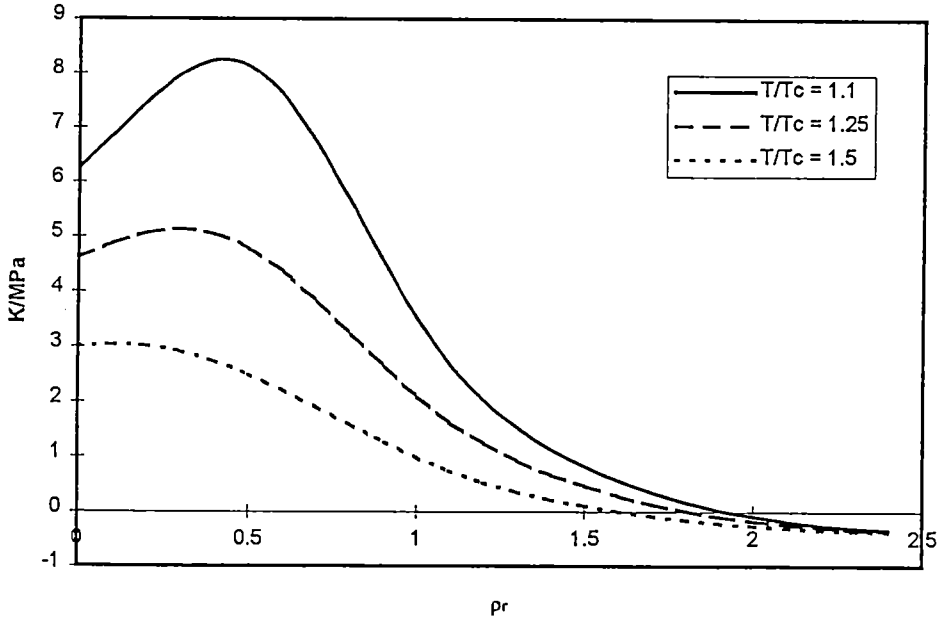

Appendix 9. Derivative properties methanol

C_v^r/R methanol with the Wagner EOS

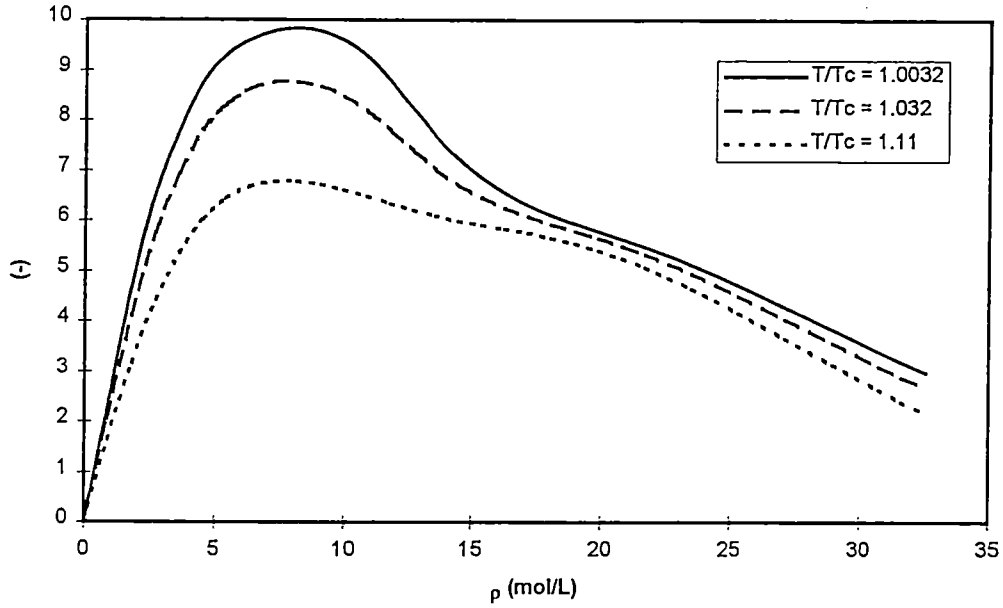

C_p methanol with the wagner EOS

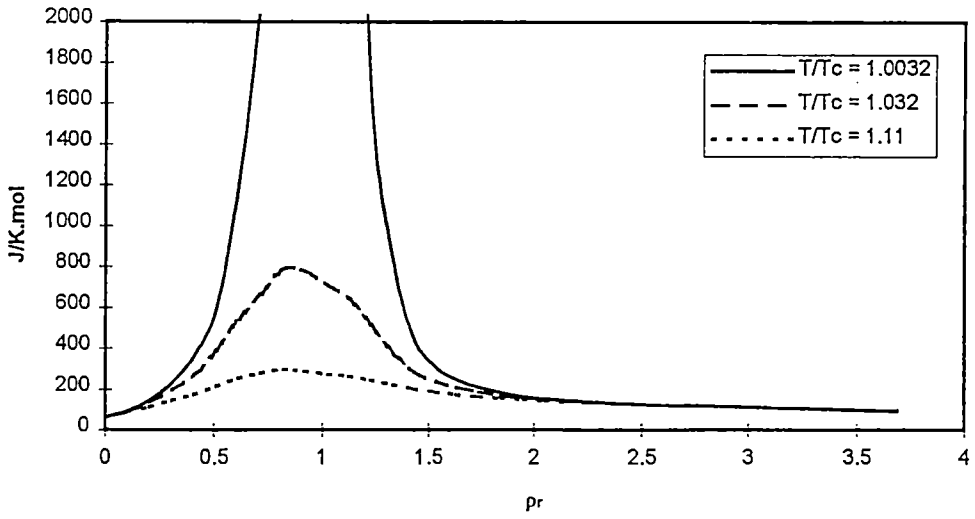

Speed of Sound methanol with the wagner EOS

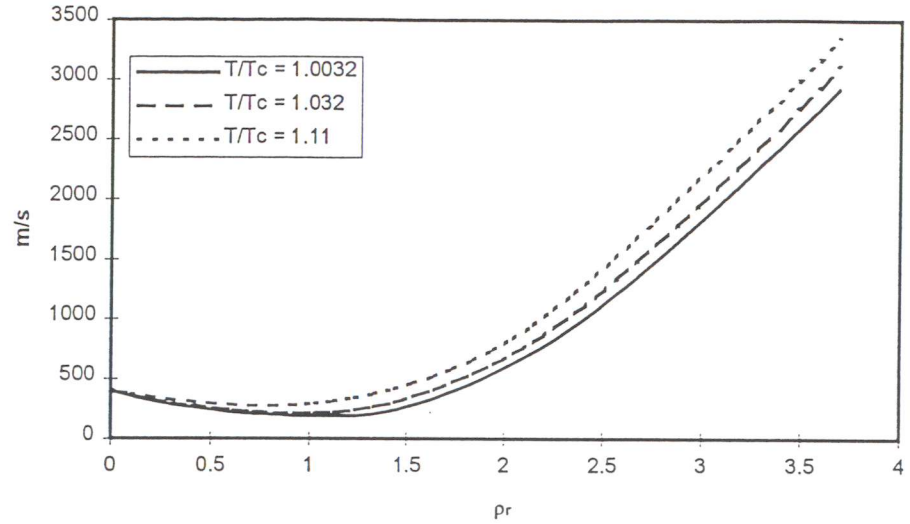

The Joule - Thomson coeff. methanol with the wagner EOS

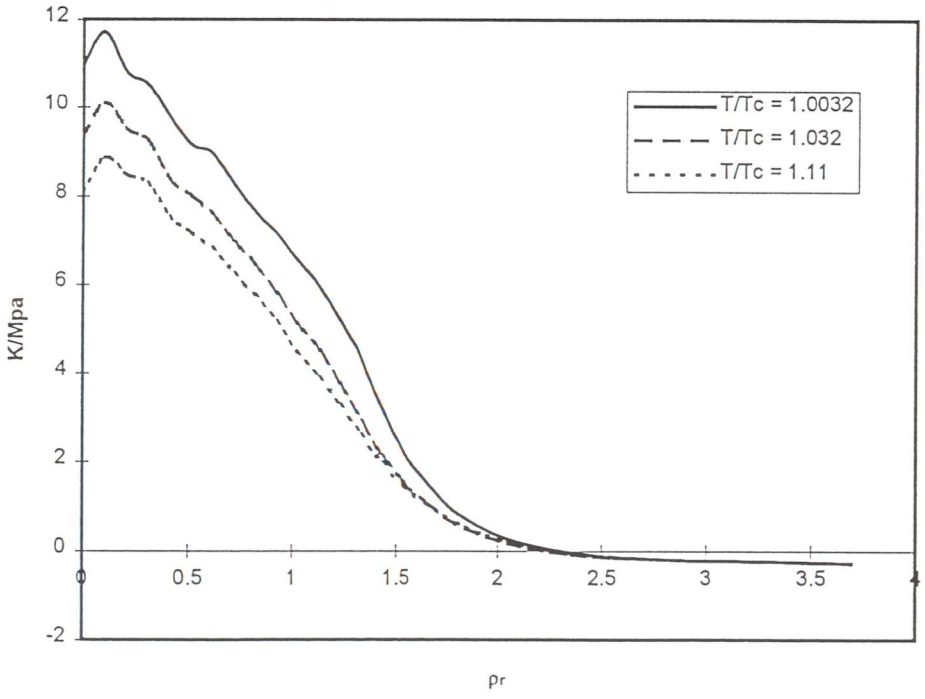

Appendix 10. Derivative properties water

C_v^r/R water with the Wagner EOS

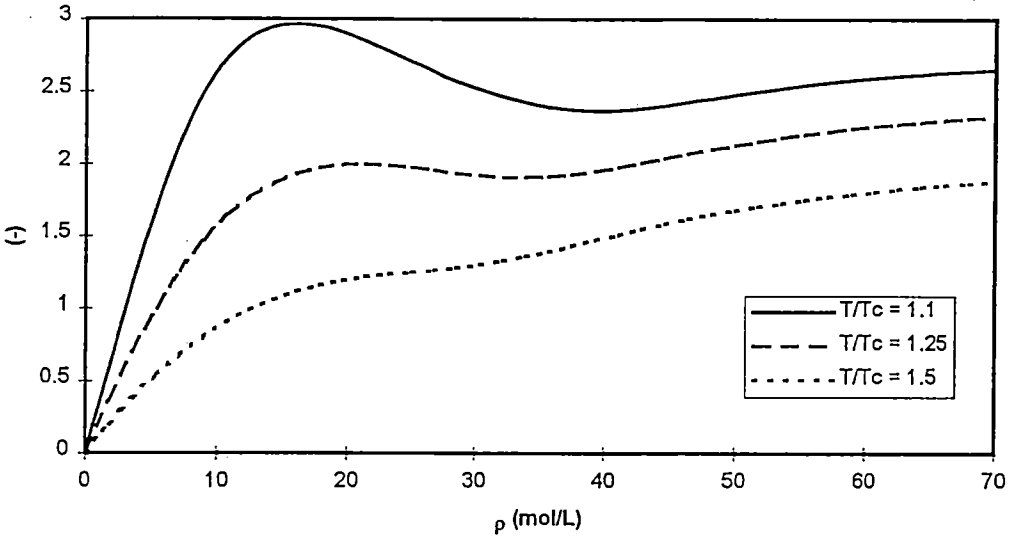

C_p water with the wagner EOS

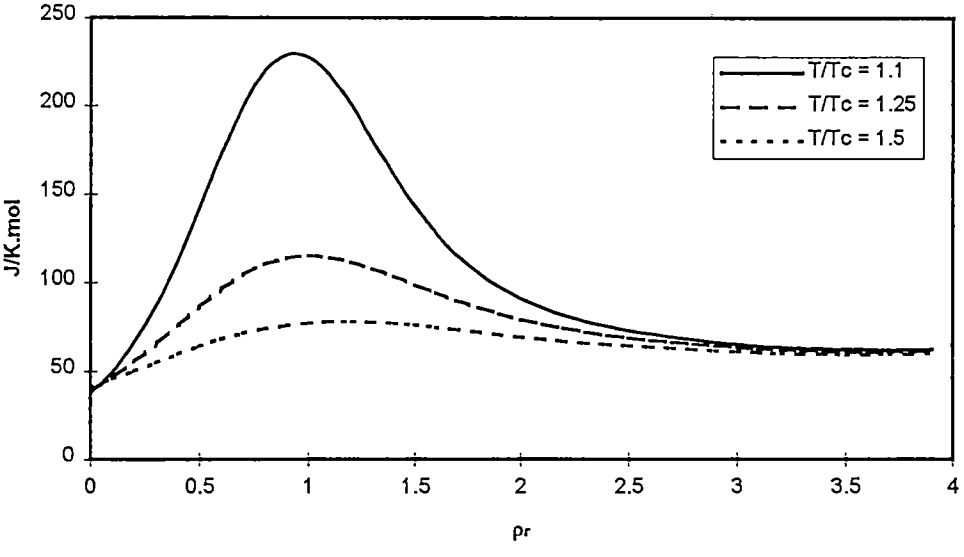

Speed of Sound water with the wagner EOS

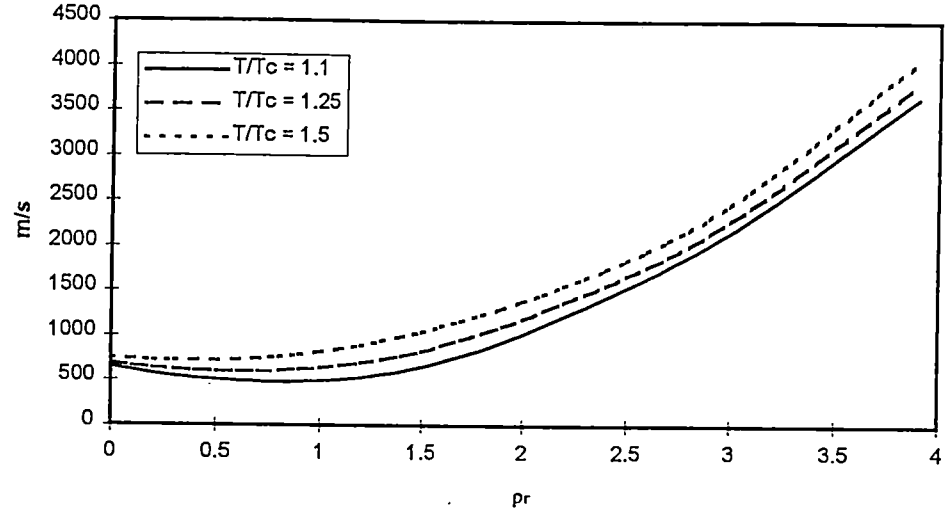

The Joule - Thomson coeff. water with the wagner EOS

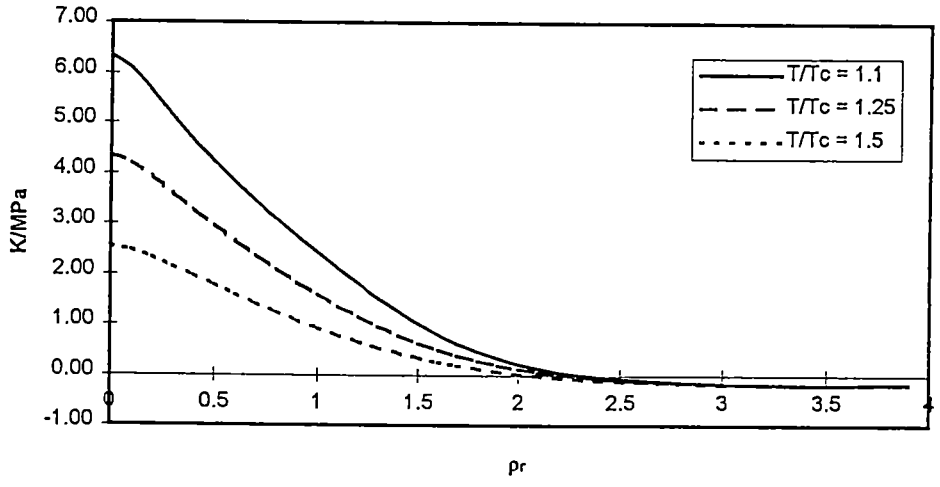

Appendix 11. Extreme points propane

Extreme points and the Joule - Thomson inversion curve
propane

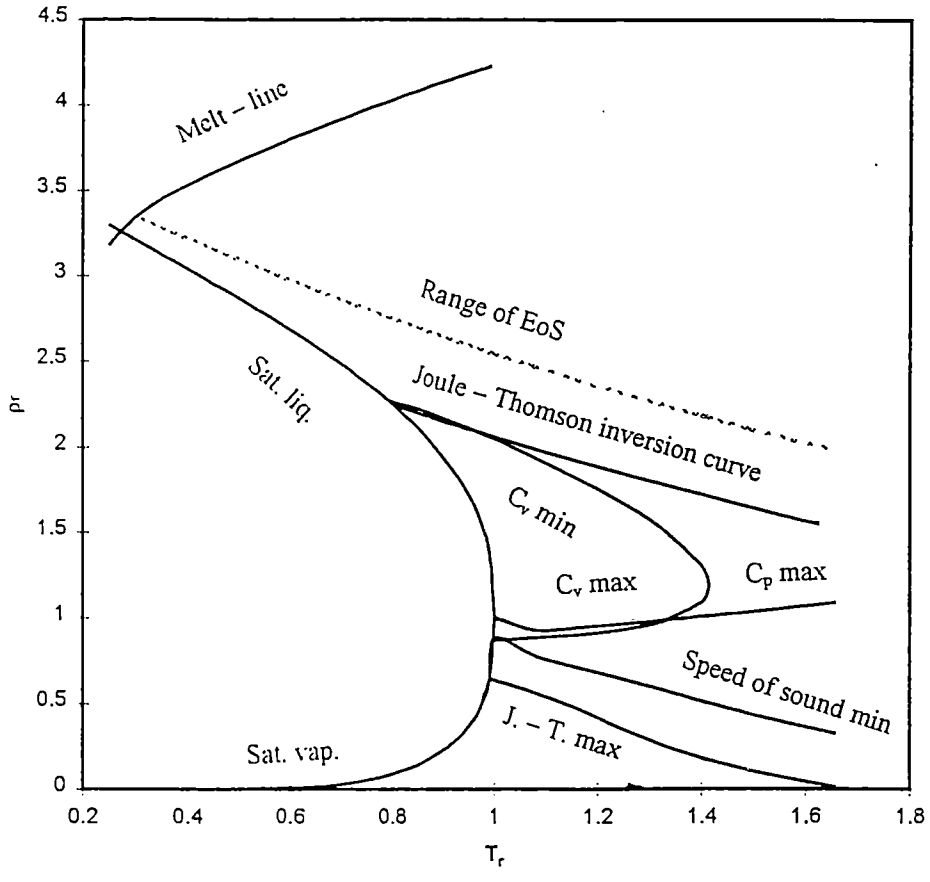

Appendix 12. Extreme points i-butane

Extreme points and the Joule - Thomson curve i-butane

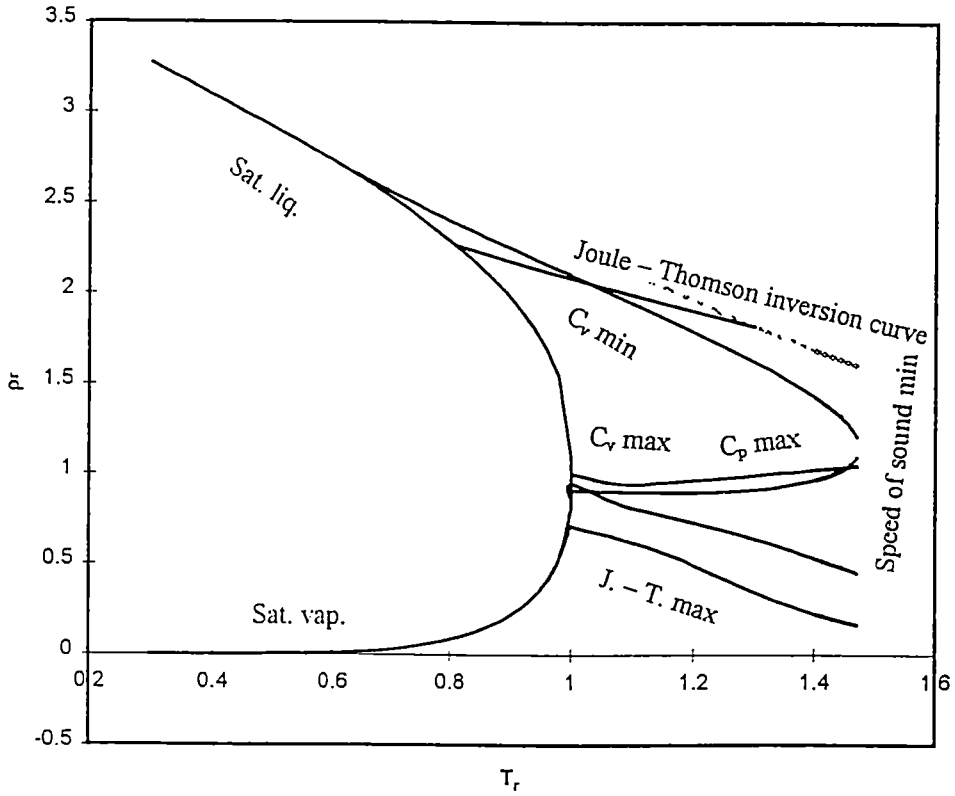

Appendix 13. Extreme points n-butane

Extreme points and the Joule - Thomson inversion curve n-butane

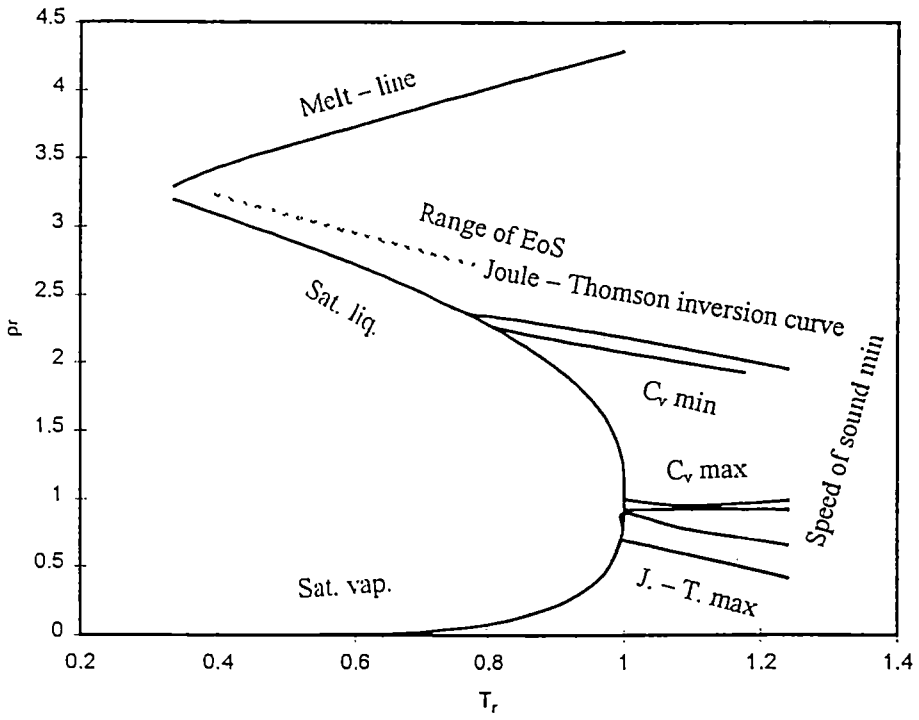

Appendix 14. Extreme points R152a

Extreme points and the Joule - Thomson inversion curve R152a